ADAPTATIONS IN *IN VIVO* CATECHOLAMINE SIGNALING IN MODELS OF STRESS AND ADDICTION

Megan Elizabeth Fox

A dissertation submitted to the faculty at the University of North Carolina at Chapel Hill in partial fulfillment of the requirements for the degree of Doctor of Philosophy in the Department of Chemistry.

Chapel Hill
2016

Approved by:

R. Mark Wightman

Eric Brustad

Dorothy Erie

Paul Manis

Donita Robinson

ABSTRACT

Megan Elizabeth Fox: Adaptations in *in* vivo catecholamine signaling in models of stress and addiction
(Under the direction of R. Mark Wightman)

Catecholamine neurotransmission plays a key role in regulating a variety of behavioral and physiological processes, and its dysregulation is implicated in both neurodegenerative and neuropsychiatric disorders. Understanding how catecholamine signaling is regulated *in vivo* may provide insight into its role in disease states ranging from anxiety and drug addiction to Parkinson's disease. This work combines rapid, selective, and spatially resolved voltammetric measurements with pharmacology and behavior. We used this approach in divergent animal models to investigate the dynamics of *in vivo* norepinephrine and dopamine signaling. Our initial investigations focused on norepinephrine release in the ventral bed nucleus of the stria terminalis (vBNST), where we found differential regulation in models of anxiety and depression. When animals were challenged with social-isolation stress and drug-dependence, adaptations in vBNST norepinephrine regulation varied with respect to both stressor and baseline stress-reactivity. We hypothesized that certain stressors elicited catecholamine efflux, and turned to real-time measurements in awake, freely moving

animals. To understand how release could produce plasticity in catecholamine regulation mechanisms after drug dependence, we focused on opiate exposure and withdrawal. We found opposing responses from dopamine and norepinephrine: whereas dopamine fluctuations in the nucleus accumbens (NAc) increased during morphine intoxication, they decreased during precipitated withdrawal. Conversely, increased norepinephrine overflow in the vBNST was found only during withdrawal, and was time locked to somatic withdrawal behaviors. While probing real-time catecholamine overflow, we also discovered hemispheric synchrony of NAc dopamine fluctuations, and revealed previously unappreciated cross-hemispheric projections in both the dopaminergic and noradrenergic systems. Our findings of opposing catecholamine responses, combined with genetic differences in response to stressors provide new insight into catecholamine regulation. Future work should continue to address how dopamine and norepinephrine signal *in vivo* and in real time and contribute to the development of a variety of neuropsychiatric conditions.

ACKNOWLEDGEMENTS

The work in this dissertation reflects the combined efforts of many individuals. First, I would like to acknowledge my advisor, Dr. Mark Wightman. My experience working with you has made me a better independent scientist. You let me ask interesting questions, even when you didn't see why anyone would want to ask them. Your confidence in me helped me grow as a problem solver, and when results were confusing, we worked together to better communicate them. Second, I would like to acknowledge Dr. Zoe McElligott, under whose tutelage I learned how to make norepinephrine measurements. Although some of the data we collected together verged on unpleasant (quantitative fecal boli, e.g.), I greatly appreciate the mentorship you provided during the first two years of my time here. Our work together is described in Chapter 2, and without this jumping off point, none of the subsequent work would have been possible. Third, I would like to acknowledge Dr. Elizabeth Bucher who taught me how to make measurements in freely moving animals, which was crucial for the work in Chapters 4 and 5. We worked together on many projects, and one of our joint efforts is described in Chapter 6. The work described in Chapter 5 was made possible with contributions from Masha Mikhailova and Dr. Evgeny Budygin at Wake Forrest, and Dr. Caroline Bass at SUNY Buffalo. It is exciting to uncover new properties of well-characterized systems, and I am glad to have had your assistance and support throughout that work.

I also had extensive help from several talented undergraduate students. Isaac Studebaker and Nathaniel Swofford contributed to the work in Chapter 3, and amazed me with their ability to manage their own experiments. In this way, we were able to "divide and conquer" and for that I am especially grateful. I also received help from Daniel Seebold and Nicholas Boustead with electrode fabrication, and Hannah Yoo with HPLC. I would also like to acknowledge several current and former members of the Wightman Lab. Lindsay Walton helped with HPLC troubleshooting. Nathan Rodeberg contributed to some of the dopamine measurements in Chapter 4, and performed a great deal of the principal component analysis. Dr. Elyse Dankoski provided editorial assistance on nearly every chapter, in addition to helpful discussions, both in and outside of lab. Dr. Nina Owesson-White helped me order drugs, change cages, and her friendship and support during difficult times was invaluable. Lastly, to all past and present members of the Wightman Lab who have lent a listening ear, a critical eye, or a cold beer, I am grateful.

I would also like to thank Dr. Jose Barreto and Patricia Barreto at Florida Gulf Coast University. You provided me with my first bench space and set of pipettes, and your feedback and support helped me to develop top-notch troubleshooting skills. Without this experience, I doubt I would have been able to push through my graduate work in the face of numerous obstacles. Finally, I would like to thank Jessica Finn for being my first science critic. Not only were you my greatest ally, both professionally and personally, but we can always talk about where our research is taking us despite divergent scientific interests.

TABLE OF CONTENTS

LIST OF TABLES

LIST OF FIGURES

.

LIST OF ABBREVIATIONS

4V	fourth ventricle
6-OHDA	6-hydroxydopamine
$[X]_{con}$	contralaterally evoked analyte X
$[X]_{con\text{-}max}$	maximal contralaterally evoked analyte X
$[X]_{ips}$	ipsilaterally evoked analyte X
$[X]_{max}$	maximum analyte X concentration
µA	microamperes
µg/g	microgram/gram
µL	microliters
µM	micromolar
µm	microns
AAV	adeno associated virus
ac	anterior commissure
aCSF	artificial cerebral spinal fluid
ADHD	attention deficit hyperactivity disorder
Ag/AgCl	silver/silver chloride
AMPH	amphetamine

ANOVA	analysis of variance
AP	anterior-posterior
AR	adrenergic receptor
AV	anteroventral thalamus
BNST	bed nucleus of the stria terminalis
BRL	BRL-44408
$CaCl_2$	calcium chloride
cc	central canal
ChR_2	channelrhodopsin 2
CO_2	carbon dioxide
COMT	catechol-o-methyl transferase
contra	contralateral
CRF	corticotropin releasing factor
CV	cyclic voltammogram
DA	Dopamine
DAB	diaminobenzadine
DAT	dopamine transporter
dBNST	dorsal bed nucleus of the stria terminalis

DBS	deep brain stimulation
DIA	diarrhea
dlBNST	dorsolateral bed nucleus of the stria terminalis
dmBNST	dorsomedial bed nucleus of the stria terminalis
DMS	dorsomedial striatum
DNB	dorsal noradrenergic bundle
DS	dorsal Striatum
DSP-4	N-(2-chloroethyl)-N-ethyl-2-bromobenzylamine
DV	dorsal-ventral
E_{app}	applied potential
EB	excessive eye-blinks
EDTA	ethylenediaminetetraacetic acid
EEP	spontaneous erection, ejaculation, penile-grooming
EPM	elevated plus maze
FG	fluorogold
FITC	fluorescein isothiocyanate
FSCV	fast-scan cyclic voltammetry
g/kg	grams/kilogram

GABAA	gamma-aminobutyric acid A
GBR	GBR-12909
GFC	guanfacine
GFP	green fluorescent protein
GRK	G-protein receptor kinase
HClO4	perchloric acid
HDCV	high definition cyclic voltammetry
HEPES	2-[4-(2-hydroxyethyl)piperazin-1-yl]ethanesulfonic acid
HPA	hypothalamic-pituitary-adrenal
HPLC	high performance liquid chromatography
HSD	honestly significant difference
i.p.	intraperitoneal
i.v.	intravenous
IBA	ibotenic acid
ICSS	intra-cranial self-stimulation
IDA	idazoxan
IgG	immunoglobulin G
ipsi	ipsilateral

JP	JP-1302
KCl	potassium chloride
K_m	Michaelis constant
L	Lewis
LC	locus coeruleus
L-DOPA	L-3,4-dihydroxyphenylalanine
LIDO	lidocaine
LV	lateral ventricle
MAO-A	monoamine oxidase A
MFB	medial forebrain bundle
mg/kg	milligram/kilogram
$MgCl_2$	magnesium chloride
ML	medial-lateral
mL	milliliters
mm	millimeters
mM	millimolar
M-N	morphine-naloxone
morph	morphine

mPFC	medial prefrontal cortex
MRP	morphine
ms	millisecond
nA	nanoamps
NAc	nucleus accumbens
NAcc	nucleus accumbens core
NaCl	sodium chloride
NAcsh	nucleus accumbens shell
NaH_2PO_4	monosodium phosphate
$NaHCO_3$	sodium bicarbonate
NAL	naloxone
NE	norepinephrine
NET	norepinephrine transporter
NGS	normal goat serum
nM	nanomolar
NMDAR	N-methyl D-aspartate receptor
NO	nitrous oxide
NTS	nucleus of the solitary tract

O_2	molecular oxygen
OCT	organic cation transporter
OT	olfactory tubercle
P	pair housed
PAG	periaqueductal gray
PBS	phosphate buffered saline
PBST	phosphate buffered saline-tween 20
PCA	principal component analysis
PFC	prefrontal cortex
PGi	nucleus paragigantocellularis
pM	picomolar
PPtg	penducolopontine tegmental nucleus
PT	ptosis
PTSD	post-traumatic stress disorder
r^2	coefficient of determination
Rac	raclopride
RM-ANOVA	repeated measures analysis of variance
ROI	region of interest

RT	room temperature
S	single housed
s.c.	subcutaneous
SD	Sprague-Dawley
SEM	standard error of the mean
SM	swallowing-movements
SN	substantia nigra
S-N	saline-naloxone
SNc	substantia nigra pars compacta
SNr	substantia nigra pars reticulata
$t_{1/2}$	clearance half-life
TC	teeth-chattering
TH	tyrosine hydroxylase
TrisHCl	trizma hydrochloride
UBE3A	ubiquitin protein ligase E3A
V	volts
vBNST	ventral bed nucleus of the stria terminalis
VEH	vehicle

Vmax	maximum velocity of uptake
VNB	ventral noradrenergic bundle
VP	ventral pallidum
VTA	ventral tegmental area
WDS	wet dog shakes
WKY	Wistar-Kyoto
YFP	yellow fluorescent protein

CHAPTER 1: CONTRASTING REGULATION OF CATECHOLAMINE NEUROTRANSMISSION IN THE BEHAVING BRAIN

Introduction

The catecholamine neurotransmitters dopamine and norepinephrine modulate a variety of behavioral and physiological processes through their actions on post-synaptic receptors, and their dysregulation underlies the pathophysiology of many disease states. Deficits in dopamine and norepinephrine are a hallmark of neurodegenerative disorders such as Alzheimer's (Weinshenker, 2008) and Parkinson's disease (Schapira, 2009), and maladaptive catecholamine signaling promotes the development of psychiatric disorders such as depression and drug addiction (Chaudhury *et al*, 2015; Koob and Volkow, 2010). Despite making up a relatively small proportion of synapses within the brain (Brady, 2005), catecholamine neurons can signal through volume transmission (Cragg *et al*, 2001; Garris *et al*, 1994a) to affect a wide variety of downstream targets and influence communication throughout the entire brain. Over 40 years ago, Ralph Adams envisioned using electrochemistry *in vivo* to measure oxidizable neurotransmitters (Kissinger *et al*, 1973). This technique has enabled researchers to measure neurotransmitter release and uptake in brain slices, anesthetized and freely behaving animals to more precisely determine their actions on neural communication and behavior. Although several electrochemical techniques have been applied to the challenge, fast-scan cyclic voltammetry (FSCV) has been more widely applied due to its fast time resolution and chemical selectivity over other

measurements.

It is impossible to cover the last four decades of *in vivo* electrochemistry in a single review. Therefore this introduction has three goals. First, we will provide a general overview of fast-scan cyclic voltammetry and the pioneering work in brain slices that led to measurements in intact animals. Second, we will focus on the use of anesthetized animals combined with pharmacology to reveal differences in regulation of dopamine and norepinephrine. Third, we will highlight studies in freely moving animals that reveal contrasting roles for these catecholamines in modulating behavior.

1. Building the foundation for *in vivo* recordings

Fast-scan cyclic voltammetry

In fast-scan cyclic voltammetry (FSCV), a potential sweep is applied to an electrode at a rapid scan rate (100-1000V/s) to oxidize and reduce electroactive species. The resultant current from this potential sweep can be converted into concentration estimates for the species of interest through the use of *in vitro* calibration factors and multivariate analysis techniques (Keithley *et al*, 2009; Rodeberg *et al*, 2015). FSCV measurements are typically conducted at glass-encased, carbon-fiber microelectrodes where the sensor is 5-10 microns in diameter, and with an active length of 50-150 microns. The small size of the sensor allows for minimal tissue damage, as well as excellent spatial selectivity (Peters *et al*, 2004). Voltammetric measurements are typically conducted at fast sampling frequencies by repeating the potential sweep every 20-200 ms. A commonly used waveform for detection of catecholamines sweeps from -0.4 to +1.3V at 400 V/s, applied every 100-ms (Figure 1.1). This rapid sampling allows for the detection of single release and uptake events.

Regulation of extracellular catecholamines in brain slices

In brain slices, or "*ex vivo"* recordings, a carbon-fiber electrode is positioned ~100 µm into the tissue near a stimulating electrode. The release and subsequent uptake of neurotransmitters is measured while directly depolarizing nearby terminals. Early studies focused on dopamine, and FSCV in brain slices allowed researchers to determine that extracellular concentrations were a balance of release and uptake, with metabolism operating on a slower time scale (Near *et al*, 1988). In contrast to striatal dopamine, norepinephrine release in slices containing the bed nucleus of the stria terminalis (BNST) requires delivery of longer pulse trains and follows different release kinetics (Miles *et al*, 2002) which may be due to the differences in vesicular release rate between norepinephrine and dopamine (Chiti and Teschemacher, 2007) or differential dependence on N-time calcium channel activity (Mitchell and Adams, 1993). Additionally, maximal norepinephrine efflux only weakly depends on stimulation current above 250 µA, unlike striatal dopamine, which does not approach saturation even with stimulation currents of 450 µA (Kennedy *et al*, 1992). Despite evidence that both catecholamines are released from similar sized vesicles (Bergquist and Ludwig, 2008; Papke *et al*, 2012), the mechanism underlying differential release kinetics is unknown.

After catecholamines are released they are cleared from the extracellular space by neuronal transporters. The primary clearance mechanism for dopamine is the dopamine transporter (DAT) which obeys Michaelis-Menten kinetics (Wightman *et al*, 1988) and genetic deletion of DAT prolongs the life of extracellular dopamine by three hundred-fold (Jones *et al*, 1998). Release and uptake rates are heterogeneous in sub-

regions of the striatum (Salinas *et al*, 2016; Trout and Kruk, 1992) which might be attributed differences in striosome and matrix compartments (Salinas *et al*, 2016). The primary clearance mechanism for norepinephrine is the norepinephrine transporter (NET), but non-NET mechanisms may play a larger role in norepinephrine clearance, as the lifetime of vBNST clearance is only prolonged six-fold in NET knockout mice (Miles *et al*, 2002; Xu *et al*, 2000). DAT is also expressed in the vBNST, and there is some evidence that DAT may help clear norepinephrine from the extracellular space in mice lacking NET. Although DAT has a higher affinity for dopamine over norepinephrine, catecholamine transporters are notoriously promiscuous (Daws, 2009), and mice lacking DAT exhibit a slight reduction in norepinephrine clearance rate (Miles *et al*, 2002). However, DAT is not likely a major contributor to norepinephrine clearance in animals with normal transporter function, because pharmacological blockade of DAT in rats does not affect norepinephrine clearance rate (Palij and Stamford, 1992). However, in cases of prolonged signaling, DAT may serve as an additional mechanism for norepinephrine clearance.

Extracellular catecholamine concentrations are also governed by autoreceptor control of release. Circuitry is mostly severed in a slice preparation, which serves as an advantage when examining regulation of release at catecholamine terminals. Any effects on release exerted by receptor agonists/antagonists can thus be attributed to direct actions on terminals. The principal autoreceptor for dopamine is the D2 (Beaulieu and Gainetdinov, 2011). D2 receptors maximally inhibit dopamine release within 500-1000ms, and the time course varies between dorsal and ventral striatum (Phillips *et al*, 2002). D2 receptors become markedly desensitized after knockout of DAT due to

persistent elevation of extracellular dopamine concentrations (Jones *et al*, 1999). The principle autoreceptor controlling norepinephrine efflux is the α_2, and it operates on a similar time course as D2 receptors (Palij and Stamford, 1993; Trendelenburg *et al*, 2001). Despite having similar mechanisms in place to control extracellular concentrations, the fundamental differences in dopamine and norepinephrine release and uptake position them to influence neuronal communication in diverse ways.

Catecholaminergic Plasticity

A number of studies have used brain slice preparations to investigate adaptations to release and uptake mechanisms. In animals trained to self-administer high levels of cocaine, both electrically stimulated and cocaine-potentiated dopamine release is attenuated (Calipari *et al*, 2014a; Ferris *et al*, 2012; Ferris *et al*, 2011; Mateo *et al*, 2005). This effect is reversed by a single amphetamine infusion in cocaine self-administering animals (Ferris *et al*, 2015). Similar to the persistent elevated dopamine concentrations in DAT knock-outs, chronic amphetamine self-administration produces increases in evoked dopamine and attenuates D2 receptor function (Calipari *et al*, 2014b). Catecholamine receptors are also regulated by G protein-coupled receptor kinases and deletion of G protein-coupled receptor kinase 2 (GRK2) from D1 or D2 containing neurons produces contrasting effects on dopamine regulation. GRK2 deletion in D2-containing neurons enhances D2 activity and depresses baseline dopamine release, whereas GRK2 deletion from D1-containing neurons enhances dopamine release and uptake. These adaptations are paralleled by bidirectional sensitivity to cocaine: in D1 containing neurons, GRK2 deletion increases cocaine sensitivity, whereas lack of GRK2 in D2 neurons reduces sensitivity (Daigle *et al*, 2014).

Dopamine regulation can also become dysregulated in rats reared in social isolation. These animals exhibit enhanced dopamine release and uptake as compared with group-reared rats. Interestingly, social isolation amplifies psychostimulant, but not cocaine inhibition of DAT (Yorgason *et al*, 2016). Because methamphetamine and cocaine both inhibit dopamine uptake, these findings suggest other adaptations outside of DAT play a role in the plasticity. The stress of social-isolation likely facilitates release of corticosterone, which has a profound impact on other transport mechanisms, such as organic cation transporters (Gasser *et al*, 2006).

Although fewer studies have used slice voltammetry to assay changes in noradrenergic function, work from the Stamford lab demonstrated adaptations in somatodendritic norepinephrine release in the locus coeruleus (LC). Bath application of the analgesic tramadol reduces norepinephrine clearance (Halfpenny *et al*, 1999), but chronic treatment does not affect uptake mechanisms. Instead, chronic tramadol appears to sensitize α_2 function (Hopwood *et al*, 2001). In mice lacking the metabolic enzyme monoamine oxidase A (MAO-A), presynaptic control mechanisms become dysregulated. Peak LC norepinephrine efflux is higher, and accompanied by decreased clearance rates and α_2 control over release (Owesson *et al*, 2002; Owesson *et al*, 2003). Similar adaptations to vBNST norepinephrine were found in anesthetized rats following stressors as discussed below in section 2.

Other modulators of catecholamine release

Terminal catecholamine release can be modulated by other signaling molecules. For example, optogenetic activation of cholinergic interneurons is sufficient to elicit dopamine release in the striatum (Cachope *et al*, 2012; Threlfell *et al*, 2012). In the

striatum, insulin also activates cholinergic interneurons to enhance dopamine release (Stouffer *et al*, 2015), however in the ventral tegmental area (VTA), it suppresses somatodendritic release and enhances dopamine reuptake (Mebel *et al*, 2012). Nitric oxide (NO) donors also modulate dopamine in a manner dependent on cholinergic activity. Under reduced acetylcholine, NO modulates dopamine release in a frequency-independent manner and acts directly on dopamine terminals, in contrast to its frequency-dependent modulations in the presence of nicotinic receptor activity (Hartung *et al*, 2011). We could find no reports detailing how norepinephrine release is influenced by other signaling molecules in slices. Since infusion of NO donors into the BNST produces anxiety (Faria *et al*, 2016), and norepinephrine in the BNST regulates the stress axis (Forray and Gysling, 2004), NO donors may potentiate norepinephrine release in the BNST to produce elevated stress/anxiety, but this has not yet been shown. Additionally, a host of neuropeptides are known to regulate BNST activity (Kash *et al*, 2015) and may, in turn, regulate norepinephrine release. By combining slice voltammetry with the diverse tool-box of genetic manipulations, specific cell-type activation, and selective pharmacology, new modulators of catecholamine release will be identified that will contribute to a better understanding of how these neurotransmitters are regulated, and aid in the development of more effective pharmacotherapies.

2. *In vivo* recordings in anesthetized animals

Voltammetric measurements in anesthetized animals allow for precise measurements of release and uptake in the intact brain. Since neural activity is suppressed in anesthetized animals, neurotransmitter release is typically elicited by

stimulating neurons or their axon bundles directly. Early studies used direct electrical stimulation, although recent optogenetic strategies provide an opportunity to excite or inhibit discrete cell-types (McCutcheon *et al*, 2014; Witten *et al*, 2011). Dopamine and norepinephrine differ structurally by only one hydroxyl group and their voltammograms *in vivo* are indistinguishable (Park *et al*, 2009). Thus, we have turned to a multi-step approach to validate the origin of the signal at the electrode. First, we limit our measurements to regions containing predominately dopamine or norepinephrine. Tissue homogenate studies have confirmed that norepinephrine is the primary catecholamine in the ventral bed nucleus of the stria terminalis (vBNST) and the anteroventral thalamus (AV), thus our first *in vivo* norepinephrine measurements were restricted to those regions (Park *et al*, 2009). Many dopamine rich regions lie adjacent to the vBNST and without the visual confirmation of electrode placement afforded by a slice preparation, we turned to a pharmacological approach to rule out contributions by dopamine (Figure 1.2). Voltammetric signals are only considered noradrenergic if they respond to norepinephrine drugs (e.g., α_2 antagonist idazoxan) but not dopamine drugs (e.g., D2 antagonist raclopride). Finally, a constant current is applied to the carbon-fiber electrode to make a lesion in the brain for subsequent histological validation of electrode placement in the target region.

Differential release of catecholamines in anesthetized animals

Dopamine release is typically evoked by stimulating neurons in the ventral tegmental area (VTA)/ substantia nigra (SN) or the medial forebrain bundle (MFB). By carefully lowering the carbon-fiber and stimulating electrodes, it is possible to generate a “functional map” of the neurons and terminals that support catecholamine release.

The excellent spatial selectivity afforded by microelectrodes enables the characterization of regulation mechanisms in discrete structures or microdomains of a given region. Early studies used voltammetry in anesthetized rats to reveal an apparent heterogeneity of release and uptake in compartments of the striatum and basolateral amygdala (Garris and Wightman, 1994b; May and Wightman, 1989). Dopamine regulation also differs between the NAc and the olfactory tubercle (OT). Dopamine release reaches smaller concentrations in the OT as compared with the NAc, and DAT inhibition produces smaller increases in OT dopamine compared with NAc (Wakabayashi *et al*, 2016). Recent work in our lab has used this classical mapping approach combined with multiple electrodes and pharmacology to reveal an unexpected population of dopamine neurons that release dopamine into the contralateral striatum. Whereas NAc dopamine release is ~20x higher as elicited by ipsilateral vs contralateral VTA stimulations, dopamine release in the contralateral dorsomedial striatum is hemispherically equivalent with SN or pendunculopontine tegmental nucleus (PPTg) stimulations. The contralaterally projecting dopamine neurons originating from the VTA are also differentially regulated by D2 receptors, as they are more sensitive to the D2 antagonist raclopride than ipsilateral VTA projections (Fox *et al*, 2016a). The high spatial resolution afforded by microelectrodes combined with pharmacological approaches will continue to enable functional characterization of dopaminergic circuits in intact animals.

In anesthetized animals, norepinephrine release is typically measured in the vBNST with stimulation of neurons in the nucleus of the solitary tract, or its axon bundles. Using a multi-electrode approach, Park and colleagues measured dopamine

and norepinephrine release simultaneously in the NAc and vBNST with a stimulation that targeted both noradrenergic axons and the VTA/SN. As previously demonstrated in slices, release and uptake of norepinephrine in the vBNST is slower as compared with dopamine in the NAc, even with identical stimulation location. The two catecholamines are also differentially regulated. Basal levels of dopamine increase when D2 receptors are antagonized and uptake is blocked with amphetamine (Park *et al*, 2011). In the vBNST, α_2 autoreceptor antagonism with amphetamine does not elevate basal norepinephrine (Park *et al*, 2011). Additionally, tyrosine hydroxylase inhibition depletes dopamine release faster than norepinephrine (Park *et al*, 2011). This contrasting regulation is further corroborated in studies using more selective uptake inhibition. When dopamine regulating mechanisms are blocked in anesthetized animals (i.e., D2 and DAT), dopamine concentrations fluctuate spontaneously in the striatum (Venton and Wightman, 2007). However, similar blockade of noradrenergic regulation (i.e., α_2 and NET) does not elicit spontaneous norepinephrine fluctuations in the vBNST (Park *et al*, 2015). Although norepinephrine and dopamine have similar regulation mechanisms, they signal in distinct ways when control mechanisms are blocked. These findings hint at uncovered mechanisms controlling norepinephrine release. Moreover, the larger stimulations required to elicit norepinephrine suggest that norepinephrine is only released endogenously under extreme physiological conditions.

A few studies have made measurements in regions with mixed catecholamines, despite their indistinguishable voltammograms. The prefrontal cortex (PFC) receives both dopaminergic and noradrenergic innervation, and early work shows dopamine is the predominant catecholamine released in the medial PFC following VTA stimulations

(Garris *et al*, 1993). This finding was confirmed in a recent report; however, D2 receptor antagonism paradoxically attenuates dopamine release in this region (Shnitko and Robinson, 2014b). Pharmacology in cortical regions must thus be selected carefully for signal validation, particularly because NET takes up dopamine in the PFC (Moron *et al*, 2002). Both the dorsal BNST and the NAc shell receive some norepinephrine innervation in addition to dopamine. Selective pharmacology indicates norepinephrine in the NAc is restricted to the more caudal portion of the shell, (Park *et al*, 2010) and norepinephrine in the dorsal BNST is contained to the medial portion. One study found dmBNST norepinephrine is ~50% of vBNST release and is accompanied by slower clearance and reduced α_2 and NET function compared to vBNST regulation (Herr *et al*, 2012). These studies highlight that voltammetry, combined with anatomical and pharmacological validation enables characterization of release and uptake mechanisms in an intact brain. Moreover, this basic understanding provides a basis for comparison following manipulations such as stress or drug exposure.

Adaptations in catecholamine function

Voltammetric measurements in anesthetized animals allow for researchers to identify how different manipulations interact with intact circuitry to produce functional adaptations in catecholamine release. For example, selective genetic inactivation of NMDA receptors in dopamine neurons disrupts evoked dopamine release in a stimulation-site dependent manner. Whereas dopamine release is unchanged in NMDAR knock-out mice following MFB stimulations, dopamine release elicited by the PPTg is blunted compared with controls (Zweifel *et al*, 2009). In mice overexpressing catechol-o-methyl transferase (COMT), striatal dopamine release capacity is increased

despite unchanged levels of tyrosine hydroxylase or DAT (Simpson *et al*, 2014). Without the intact circuitry afforded by an anesthetized preparation, these differences in release may not have been discovered. Recent work in our lab has examined how baseline genetic differences impact catecholamine regulation mechanisms. Norepinephrine in the vBNST of Sprague-Dawley (SD) rats was compared with Lewis and Wistar-Kyoto (WKY) rats. Whereas release and uptake were similar between SD and WKY rats (Fox *et al*, 2015), there were marked differences in release, uptake, and autoreceptor control in Lewis rats, without differential α_2 or NET expression (McElligott *et al*, 2013). Additionally, depletion of LC norepinephrine with DSP-4 produced adaptations to α_2 receptors and uptake in SD, but not WKY rats without changing norepinephrine release magnitude (Fox *et al*, 2015). These findings underscore the importance of voltammetric catecholamine measurements in intact systems, because differential release and uptake likely contribute to the phenotypic variations observed in genetically diverse animal models.

Dysregulations in catecholamine signaling are implicated in the development of addiction and numerous neuropsychiatric conditions (Koob *et al*, 2010). Several studies have used anesthetized preparations to uncover adaptations to catecholamine circuits following drugs of abuse, particularly cocaine. Chronic administration of cocaine, heroin, or a “speedball” cocktail of the two produces variable adaptations to NAc dopamine in rats. In animals with a history of chronic self-administration, evoked dopamine is reduced compared with animals receiving a single drug dose. Dopamine reuptake rate is also greater in speedball administering animals compared with animals administering cocaine or heroin alone. Furthermore, evoked dopamine is increased following an

injection of either cocaine or speedball in animals with self-administration history (Pattison *et al*, 2012). In another study, one day pre-treatment with cocaine does not alter dopamine response to a subsequent cocaine challenge. However, 7 days of cocaine exposure potentiates the effect of a cocaine challenge on dopamine signaling in the NAc and is accompanied by an increase in apparent K_m of DAT (Addy *et al*, 2010). There is some evidence that kappa opioid receptors mediate cocaine-potentiated dopamine release in the NAc. The endogenous ligand for kappa opioid receptors is dynorphin, which is released during stress and promotes dysphoria (Chavkin, 2013). Kappa activation alone inhibits evoked dopamine in the NAc, and on a short-time scale, pre-treatment with a kappa agonist attenuates dopamine response to cocaine in the NAc. However, on a longer time-scale, pre-treatment with a kappa agonist increases the cocaine-induced increase in NAc dopamine (Ehrich *et al*, 2014).This is an interesting finding in the context of stress-induced cocaine use. It is possible that dynorphin released by stress promotes a dysphoric state that drives drug administration. On a short time-scale, this stress decreases cocaine's actions on mesolimbic dopamine, resulting in escalation of drug-intake to compensate for cocaine's attenuated effect. However, on a longer time-scale, kappa activation potentiates cocaine's effects on dopamine, further driving its reinforcing properties. Although cocaine clearly increases extracellular dopamine concentrations, there are other signaling mechanisms outside of elevated dopamine that drive persistent drug use.

Adaptations to dopamine signaling have also been studied after other drugs of abuse. Large doses of methamphetamine reduce evoked striatal dopamine and decrease DAT uptake rates (Howard *et al*, 2011). This effect is exacerbated when

methamphetamine is administered in the presence of reward-associated cues, but can be attenuated with cannabinoid receptor antagonism (Loewinger *et al*, 2012). This disruption in normal dopamine function likely drives increased methamphetamine use. Similar to methamphetamine in the striatum, a high dose of ethanol decreases evoked dopamine and slows clearance in the mPFC. However, when the same dose is given to adult animals with a history of intermittent alcohol exposure in adolescence, dopamine clearance is slowed, but ethanol does not suppress dopamine release (Shnitko *et al*, 2014a; Shnitko *et al*, 2015b). In the NAc, adolescent alcohol use reduces tonic levels of dopamine in adulthood. However PPTg, but not MFB evoked dopamine release is increased in these animals. The administration of an allosteric $GABA_A$ agonist attenuates increased dopamine release and decreases risk-taking behavior of animals with adolescent alcohol exposure (Schindler *et al*, 2016). These findings suggest that there is increased inhibitory tone after alcohol exposure that drives changes in dopaminergic signaling through a disinhibitory mechanism. Dopamine modulated learning signals are disrupted in humans with a long history of alcohol-intake (Deserno *et al*, 2015), which may increase craving and contribute to the increased risk-taking behavior found in both humans and animal models. Although ethanol does not exert direct actions on dopamine neurons, its disruption of normal dopamine signaling contributes to alcohol abuse.

Work investigating adaptations to norepinephrine signaling have been limited, but two recent studies from our lab examined the effects of stress and drug-exposure on norepinephrine release and regulation. Three days of morphine paired with naloxone precipitated withdrawal produces exacerbated norepinephrine in the vBNST. In SD

rats, both α_2 and uptake are blunted, whereas only α_2 function is attenuated in WKY. The treatment did not impact regulation mechanisms in Lewis rats, highlighting the importance of genetic factors in susceptibility to catecholamine dysregulation after drug exposure (Fox *et al*, 2015; McElligott *et al*, 2013). Furthermore, when SD and WKY rats were exposed to 2-weeks of social isolation, SD rat noradrenergic function resembles that of a morphine-addict, whereas WKY norepinephrine is unchanged (Fox *et al*, 2015). Similar to drug exposure, Lewis rats also did not alter noradrenergic synaptic function following social isolation, suggesting their regulation mechanisms are maximally disrupted (Fox and Wightman, unpublished observations). Researchers have also used anesthetized animals to investigate the mechanisms of non-abused drugs on catecholamine regulation. For example, the dopamine precursor, L-DOPA, enhances dopamine release in both dorsal and ventral striatum, but causes a delayed inhibition of dopamine release in the dorsal striatum. L-DOPA also reduces uptake rates by decreasing V_{max} of DAT (Harun *et al*, 2015). Since dopamine is the metabolic precursor to norepinephrine, L-DOPA may also affect norepinephrine concentrations, but this area is currently unexplored. Noradrenergic deficits are also a key component in the development of Alzheimer's disease, and the way pharmacotherapies alter catecholaminergic function should be a topic of ongoing investigation. Electrochemical measurements in anesthetized animals allow researchers to examine discrete circuits and how they become functionally altered after a variety of treatments. Continued efforts should focus on changes in norepinephrine function in addition to dopamine due to their distinctly different patterns of release and uptake *in vivo*.

3. Catecholamines function in awake animals

The first awake-animal FSCV dopamine measurements were conducted nearly 20 years ago and the signals researchers found were closely associated with a novel stimulus or environment (Garris *et al*, 1997; Rebec *et al*, 1997; Robinson *et al*, 2001). However, dopamine concentrations were also found to fluctuate in the absence of any external stimuli in awake animals at rest (Robinson *et al*, 2002). Spontaneous dopamine fluctuations, or "transients" have been measured in the dorsal striatum, nucleus accumbens, and olfactory tubercle (Robinson *et al*, 2002), and they display heterogeneity in their frequency, amplitude, and duration in subregions of the NAc (Wightman *et al*, 2007). Dopamine transients in the NAc originate from cell-firing in the VTA (Sombers *et al*, 2009), are increased by cannabinoid receptor activation (Cheer *et al*, 2004), and are the main source of average extracellular NAc dopamine levels (Owesson-White *et al*, 2012). DAT blockade with nomifensine increases spontaneous and stimuli-related dopamine transients (Robinson and Wightman, 2004), and acute phenylalanine/tyrosine depletion reduces the frequency, but not amplitude of spontaneous transients (Shnitko et al., 2016). Recent work employing a dual-electrode approach has revealed that at rest, spontaneous dopamine transients in the NAc shell synchronize ~75% of the time (Fox *et al*, 2016a). Importantly, FSCV measurements of dopamine transients provide a clearer picture of dopaminergic activity, and the time course of dopamine transients as measured by FSCV is more closely linked with uptake-inhibition induced stereotypy than microdialysis measurements (Budygin *et al*, 2000). In contrast to striatal dopamine, norepinephrine concentrations are not known to

fluctuate spontaneously in the vBNST of animals at rest, further illustrating the differences in endogenous catecholamine signaling.

ICSS

Intracranial self-stimulation (ICSS) was first described by Olds and Milner (Olds and Milner, 1954), and through extensive mapping studies, it was determined that sites that supported the best self-stimulation were centered around the medial forebrain bundle, implicating catecholamine signaling as a principle mediator of the behavior. In this paradigm, an animal is trained to respond instrumentally (e.g. lever-press) to deliver an electrical stimulation to its brain. The presentation of the lever is traditionally preceded by a cue that predicts reward availability. Dopamine is released following direct electrical stimulation of the VTA/SN or MFB, but as animals become well trained, the NAc dopamine release moves to the cue in a time-locked fashion and is accompanied by decreases in stimulation-evoked dopamine (Owesson-White *et al*, 2008). To this end, the dopamine response elicited by a reward-predicting cue, but not the reward, provides strong support for dopamine's involvement in reward prediction error (Schultz, 2013). Disruption of endocannabinoid signaling reduces cue-evoked dopamine, whereas increases in cannabinoid receptor 1 signaling increase cue-evoked dopamine and reward seeking (Oleson *et al*, 2012). Recent work employing a multimodal sensor has uncovered how dopamine interacts with specific post-synaptic receptors in the NAc to drive ICSS (Owesson-White *et al*, 2016). The combination of voltammetric dopamine measurements with single unit activity allows for real-time measurement of dopaminergic modulation of cell firing in awake animals (Takmakov *et al*, 2011). As before in non-behaving animals, iontophoresis barrels lying adjacent to the

multimodal sensor enable localized drug delivery to chemotype nearby cells (Belle *et al*, 2013); i.e., unit activity is selectively altered by either D1 or D2 drug delivery and the functional receptor activity of individual neurons is identified in real time. In this recent report, rats were trained to press a lever for electrical stimulation of the VTA. As before, dopamine is elicited by the lever-predicting cue, but cue-associated dopamine acts directly on identified D2-containing neurons. Dopamine responses associated with the lever press are instead mediated by both D1 and D2-containing neurons (Owesson-White *et al*, 2016). In agreement with this, intra-NAC shell infusions of D1 antagonists block lever-press behavior and alter lever-press associated firing (Cheer *et al*, 2007a). The coupling of iontophoresis with electrochemical and electrophysiological recordings provide a technical advantage over previous drug delivery techniques, since large volumes of drugs can disrupt animal behavior. Future work employing this discrete drug delivery technique will allow for receptor-level mechanisms to be uncovered in real time, without necessitating the use of transgenic animals. Furthermore, this technique may be extended into regions containing mixed catecholamines for signal validation prior to making measurements during behavior.

Typical ICSS stimulations also target noradrenergic axons, and in one study, norepinephrine and dopamine responses were recorded in subterritories of the BNST during ICSS. Both norepinephrine and dopamine are evoked by the electrical stimulation delivered following the lever press. Similar to the NAc, cues that predict lever presentation elicit dopamine release in the dorsolateral BNST, however cues do not elicit norepinephrine in the vBNST even during NET inhibition. When animals undergo extinction, i.e. a lever-press no longer results in electrical stimulation,

norepinephrine and dopamine overflow switch. Whereas norepinephrine is released in the vBNST at the time of stimulation anticipation, dopamine concentrations in both NAc and dlBNST decrease (Park *et al*, 2013). It is tempting to speculate that vBNST norepinephrine is acting to suppress dopamine release through its actions on VTA projecting neurons in the BNST. Norepinephrine is not elicited by cues predicting ICSS, but its release during extinction may serve as a signal to guide action selection. When effort no longer results in reward or positive outcome, norepinephrine may shape dopamine's response in order to facilitate learning about the negative outcome. Indeed, animals lacking LC norepinephrine lever-press longer and with more vigor during ICSS extinction (Mason and Iversen, 1979), and LC lesions impair attention (Selden *et al*, 1990). Future work should address the involvement of norepinephrine in extinction from other reward paradigms, which may provide insight into how action selection is shaped in the context of negative or unanticipated outcomes.

Natural Rewards and Aversion

A number of studies have measured dopamine release in response to natural rewards, such as food pellets or sucrose. Oral infusion of sucrose elicits dopamine in the NAc (Roitman *et al*, 2008) and is potentiated by infusions of ghrelin into the lateral ventricle or intra VTA orexin-A. Moreover, the magnitude of dopamine release is greater in animals previously food-restricted (Cone *et al*, 2014), and dopamine response to an unexpected food reward is blunted in mice lacking NMDARs in dopamine neurons (Parker *et al*, 2010). Additionally, prolonged high-fat diet alters dopamine release by reducing uptake in the absence of DAT gene expression adaptations (Cone *et al*, 2013). "Food addiction" has been recently added to the DSM-5 (APA, 2013), thus uncovering

the effects of high calorie food and insulin on dopamine signaling is an important area of investigation (Stouffer *et al*, 2015). Stressful life experience dysregulates dopaminergic signaling (Yorgason *et al*, 2016), and may contribute to the development of eating disorders through its actions on the dopamine system.

In contrast to dopamine, little is known regarding norepinephrine signaling during caloric rewards or changes to diet, which is of particular interest given norepinephrine's involvement in anorexia (Janhunen *et al*, 2013; Nedelescu *et al*, 2016). One study showed unexpected sucrose delivery does not elicit release in the vBNST (Park *et al*, 2012), however norepinephrine may be released during prolonged omission of food as it is during omission of ICSS reward. Moreover, norepinephrine influences the HPA axis (Forray *et al*, 2004) and by engaging the brain's stress centers, it may suppress feeding behavior and promote anorexia. Recording norepinephrine overflow in awake animals after delivery/omission of high-calorie foods may reveal its modulation of dopamine signaling and contribute to dysregulated patterns of food consumption.

Food-predictive cues also elicit dopamine in the NAc (Roitman *et al*, 2004), and sucrose-predictive cues evoke greater dopamine release than those that predict saccharin (McCutcheon *et al*, 2012). Inactivation of the basolateral amygdala with baclofen/muscimol attenuates NAc dopamine evoked by sucrose paired cues without blunting VTA-stimulated release in the NAc (Jones *et al*, 2010). Dopamine release can also time-lock to sucrose-predictive cues in the dorsolateral, but not dorsomedial striatum (Shnitko and Robinson, 2015a). NAc dopamine selectively modulates excitatory responses of NAc neurons during sucrose-seeking behavior, and cue-evoked dopamine is observed in both NAc core, and shell, although it is of greater magnitude

and duration in the shell as compared with the core (Cacciapaglia *et al*, 2012; Cacciapaglia *et al*, 2011). When rats must press one lever to extend a second lever for sucrose delivery, dopamine responses vary between the NAc core and shell. In the core, dopamine release is greatest after presentation of the first lever, or the "seeking lever", and less for subsequent presentation of the "taking lever" and reward delivery. In the shell, dopamine release is robust to both levers as well as reward delivery (Saddoris *et al*, 2015a). When animals are asked to choose between immediate and delayed reward, dopamine responses in the shell scale with the interval between cue and reward delivery (Day *et al*, 2010), and with an animals' preferred reward (Day *et al*, 2010; Sugam *et al*, 2012). Enhancing dopamine release in the NAc during cues with optogenetics alters the decisions rats make regarding which lever to press to get which magnitude of reward, and they alter choice based on delay, but not magnitude of reward (Saddoris *et al*, 2015b). Norepinephrine may be released in the vBNST during presentation of a lesser-magnitude reward than anticipated by the animal, but no studies have investigated norepinephrine signaling in paradigms involving different food reward magnitude.

Dopamine is also elicited during delivery of a non-caloric reward. When animals are sodium-depleted, NAc dopamine signaling increases when animals are given a salt solution, and over time, dopamine responses move to the salt-predictive cue in sodium-depleted rats (Cone *et al*, 2016). Delivery of aversive stimuli suppress dopamine transmission in the NAc (Fortin *et al*, 2016) and fear-cues decrease NAc core signaling but increase NAc shell signaling (Badrinarayan *et al*, 2012). Corticosterone treatment acutely decreases NAc dopamine uptake, possibly via uptake-2 inhibition, and the

suppression of NAc dopamine signaling after the aversive tastant quinine depends on corticotropin releasing factor-VTA interactions (Graf *et al*, 2013; Twining *et al*, 2015). During delivery of an aversive tastant, decreased dopamine in the NAc is accompanied by increased vBNST norepinephrine (Park *et al*, 2012; Roitman *et al*, 2008). The reciprocal signaling of dopamine and norepinephrine during rewarding and aversive stimuli is corroborated in studies investigating the response of these catecholamines during delivery of a noxious stimulus (Park *et al*, 2015). Dopamine responses vary after cessation of a tail pinch, although the predominant effect is suppression of dopamine overflow during the noxious stimulus. A tail pinch increases norepinephrine in the vBNST, and although these studies were conducted in anesthetized animals, one might suspect that norepinephrine in the vBNST would also increase in awake animals during a noxious stimulation, such as a foot-shock. Indeed, markers of noradrenergic activity increase following foot-shock (Passerin *et al*, 2000; Rassnick *et al*, 1998). How norepinephrine is released during a variety of noxious stimuli should be investigated, as there may be an important role of norepinephrine to suppress dopamine responses to support learning about aversive or negative outcomes.

Social interactions also elicit phasic dopamine responses, and presentation of a conspecific increases the frequency of dopamine transients, although habituation decreases this response (Robinson *et al*, 2002). Dopamine is also released in the NAc in response to prosocial ultrasonic vocalizations, and like conspecific presentation, decline rapidly upon subsequent playbacks (Willuhn *et al*, 2014). NAc dopamine is also modulated by reward delivery to a conspecific, as stronger dopamine release is measured during conspecific reward receipt vs. an empty box. Similar to other pro-

social interactions, this response attenuates, and even becomes reversed in repeated trials, with reductions in dopamine during conspecific reward delivery (Kashtelyan *et al*, 2014). Interaction with an aggressive, and unfamiliar rat also elicits dopamine release in the accumbens (Anstrom *et al*, 2009); however, how unconditioned aggression interacts with norepinephrine signaling has not been explored. Interestingly, aggressive Lewis rats have higher norepinephrine content in the amygdala (Patki *et al*, 2015), and social defeat stress increases norepinephrine synthesis and NET expression in the LC (Chen *et al*, 2012; Fan *et al*, 2013). Given that norepinephrine influences the HPA axis, it is tempting to hypothesize norepinephrine is released during an animal's decision to fight or flee during aggressive social interactions, and this should be a topic of future investigation.

Drugs of Abuse

Drugs of abuse have variable actions on catecholamine neurons, and those that interfere with reuptake (e.g. cocaine, psychostimulants) have been recently reviewed (Covey *et al*, 2014). Emerging evidence supports cannabinoid modulation of dopamine signaling and drug-reward (Cheer *et al,* 2007b; Hernandez *et al,* 2014) and has been reviewed in detail elsewhere (Covey *et al*, 2015). Despite reports that cannabinoids increase LC norepinephrine activity (Oropeza *et al*, 2005; Page *et al*, 2007), how cannabinoid receptor activation influences phasic norepinephrine release has not been investigated.

Electrophysiological data show that ethanol stimulates dopaminergic transmission (Brodie *et al*, 1999), and tonic activation of VTA dopamine neurons suppresses voluntary alcohol drinking by elevating basal dopamine efflux (Bass *et al*,

2013). However, there is disparity in alcohol's effects on neurochemistry. Microdialysis data support a biphasic dopaminergic response, where low doses produce increases in NAc dopamine (Yoshimoto *et al*, 1992) and decreases at higher doses (Blanchard *et al*, 1993). As measured by FSCV, acute ethanol dose-dependently decreases evoked dopamine in the dorsal striatum (Budygin *et al*, 2001), but there is an apparent heterogeneity of dopamine response in the NAc. In some recording locations, ethanol increases dopamine transient frequency, whereas in some the frequency is decreased or even unaffected (Robinson *et al*, 2009). Interestingly, cues that predict ethanol reward are time locked to dopamine release in the dorsolateral striatum and NAc, but not in the dorsomedial striatum (Shnitko *et al*, 2015a). This apparent heterogeneity in dopamine response to ethanol should be addressed, because alcohol exposure has circuit specific effects on dopaminergic transmission (Schindler *et al*, 2016). Furthermore, information regarding the effect of phasic norepinephrine signaling after alcohol is lacking, despite microdialysis work demonstrating a sensitization to norepinephrine response to alcohol after early life stress (Karkhanis *et al*, 2014). Polymorphisms in vesicular monoamine transporter 2 are associated with increased risk for alcoholism (Fehr *et al*, 2013), and how alcohol impacts catecholaminergic signaling in these individuals would be an interesting area of exploration.

In addition to alcohol, recent work has examined the effect of an acute intravenous delivery of opiates on catecholamine release. In one study, researchers delivered the opiates oxycodone and morphine to freely moving rats. Intravenous oxycodone evokes a lasting effect on dopamine transient frequency and magnitude in the NAc; however, i.v. morphine produces a much shorter (~1 min) increase in phasic

dopamine transmission (Vander Weele *et al*, 2014). In our laboratory, we extended this work to determine the impact of drug withdrawal in addition to drug exposure on dopamine release. In contrast to the previous report, subcutaneous administration of morphine produces a persistent (>1 hr) increase in dopamine transient frequency, which may reflect the differential time course of drug delivery between the two studies. When animals underwent naloxone-precipitated withdrawal, dopaminergic transmission decreased in the NAc. Although naloxone decreased the frequency of dopamine transients regardless of prior drug-exposure, only in animals undergoing withdrawal were dopamine transient concentrations suppressed. We also measured norepinephrine in the vBNST, and found that morphine-exposure did not elicit norepinephrine responses, but robust norepinephrine release events occurred during precipitated withdrawal that coincided with specific somatic withdrawal behaviors (Fox *et al*, 2016b). Similar the opposing responses highlighted above, contrasting dopamine and norepinephrine signaling under drug exposure and withdrawal confirm their reciprocal signaling during appetitive and aversive stimuli. These findings are interesting in the context of the allostasis model, which suggests that during the development of addiction, positively reinforced behaviors dominate early on, with negatively reinforced behaviors emerging later in the addiction cycle (Koob *et al*, 2010). It is tempting to speculate that the noradrenergic response during withdrawal acts to suppress transient dopamine concentrations through its actions on VTA projecting vBNST neurons. Since glutamatergic inputs from the vBNST exert an excitatory influence over VTA dopamine neurons (Georges and Aston-Jones, 2002), and norepinephrine's actions through α_{2A} receptors decrease excitatory transmission in the vBNST (Egli *et al*, 2004),

norepinephrine release during withdrawal/aversion may act through α_2 receptors in the vBNST to suppress VTA activity and decrease dopaminergic output as a consequence. This hypothesis is corroborated by the suppression of NAc dopamine concentrations after α_2 receptor activation with clonidine (Murai *et al*, 1998). Furthermore, norepinephrine causes $GABA_A$ inhibition of VTA-projecting BNST neurons (Dumont and Williams, 2004), which may serve as an additional source of reduced dopaminergic output via VTA inhibition. Thus noradrenergic suppression of dopamine may attenuate drug-potentiated dopamine signaling, causing escalation of intake per the allostasis model. Indeed noradrenergic signaling is exacerbated in Lewis rats, a model of increased drug consumption (McElligott *et al*, 2013), which may contribute to their increased drug self-administration (Picetti *et al*, 2012). Future work should address how this progresses longitudinally, as well as how exposure and withdrawal from other drugs of abuse might produce opposing responses from catecholamines to contribute to the addiction cycle.

4. Clinical Implications

Voltammetric catecholamine measurements in models of human disease have provided new insights into their pathogenesis. To model Parkinson's disease, researchers have turned to animals that express the mutant proteins found in human patients to uncover how these mutations lead to catecholaminergic deficits. For example, researchers expressed mutant human leucine-rich repeat kinase 2 in rats, and found impaired striatal dopamine release. The adaptations to circuit function appear in the absence of neurodegeneration, and suggest that dopaminergic dysfunction might precede measureable markers of neurodegeneration and cell-death (Sloan *et al*, 2016).

In another study, expression of mutant α-synuclein in tyrosine-hydroxylase neurons produces differential catecholamine deficits that are regionally specific: evoked dopamine is reduced in the dorsal striatum, but not in the NAc, and vBNST norepinephrine release is unchanged (Taylor *et al*, 2014). These genetic manipulations afford ways to test early circuit function, and might become a useful preclinical model for testing Parkinson's therapeutics. Researchers have also used voltammetry to investigate aberrant dopamine signaling in a model of the neurodevelopmental disorder, Angelman's syndrome. Mice lacking maternal ubiquitin ligase E3A (UBE3A) exhibit increased mesolimbic dopamine and attenuated nigrostriatal dopamine in the absence of adaptations to the number of dopaminergic cells (Riday *et al*, 2012). Although dopamine replacement therapies such as L-DOPA may have some therapeutic potential, due to the pathway-specific adaptations in these mice, such global elevation of extracellular dopamine may instead lead to more dysfunction. In apparent contrast to this, a recent report found optogenetically evoked NAc dopamine in brain slices did not differ between mice lacking UBE3A and their controls (Berrios *et al*, 2016). It is important to note that different cell populations are activated by electrical vs. optical stimulations which may contribute to the differences in dopamine release. However in both studies, animals lacking UBE3A were more sensitive to VTA self-stimulation; i.e., they delivered more optical stimulations, and also acquired robust self-stimulation behavior to lower electrical stimulation currents. This brings up two important points. First, direct depolarization of dopamine terminals in a brain slice is not necessarily indicative of the magnitude of dopamine release in an intact brain. Second, adaptations in non-catecholamine neurons may facilitate dysregulated signaling that are not readily

apparently in a slice preparation with selective terminal depolarization. Moving forward, we need to consider the evidence from both preparations to integrate how circuit function becomes disrupted in disease models.

Recent advances have enabled researchers to also conduct electrochemical measurements in humans in parallel with deep brain stimulation (DBS) probes. Human recordings typically employ a fused-silica microelectrode assembly that house reference and recording electrodes and are positioned within or nearby DBS probes. In the first human recordings, striatal dopamine fluctuations were measured during a decision-making task (Kishida *et al*, 2011). Separate work at the Mayo clinic has made voltammetric measurements of adenosine during implantation of DBS probes for treatment of essential tremor using a wireless system (Chang *et al*, 2012a; Kasasbeh *et al*, 2013). More recent work asked how dopamine encodes reward prediction errors in Parkinson's patients (Kishida *et al*, 2016). Although this study found dopamine integrates reward prediction error with counterfactual prediction error, it is difficult to determine if this is a normal property of dopamine neurons, given the relatively low dopamine concentrations and possible adaptations following pharmacological intervention in Parkinson's patients. Human measurements are further complicated by the calibration methodology often employed. Although standardized training sets for principle component analysis may predict the identity of a given analyte (e.g. dopamine), they are notoriously poor at concentration prediction, which may lead to inappropriate interpretation of the data (Johnson *et al*, 2016). Nevertheless, information gleaned from preclinical disease models with recordings in humans will provide new mechanistic insight for the progression and treatment of neurodegenerative diseases.

5. Summary

Over the last four decades, electrochemical methods for measuring catecholamine dynamics and circuit function have been employed in brain slices, anesthetized, and freely behaving animals. Despite the progress in understanding the fundamentals of catecholamine release and uptake, and how they become dysregulated in disease models, lingering questions still remain. Contrasting signaling mechanisms between norepinephrine and dopamine have been described at the *ex vivo* level, and the two catecholamines are similarly divergent in anaesthetized and freely behaving animals. An ideal approach to correct the relative dearth in norepinephrine recordings, while maintaining the high spatiotemporal resolution of FSCV at microelectrodes, would be to employ a waveform that differentiates between the two catecholamines. This would further facilitate recordings in brain regions containing mixed catecholamines, such as the PFC. However, due to their structural similarity, the development of a waveform that differentiates the catecholamines electrochemically has proven difficult if not impossible. For the time being, future work should address norepinephrine signaling using selective pharmacology for signal validation. The seemingly opposing nature of these catecholamines during rewarding/aversive stimuli may not hold true in all behavioral paradigms, and should be a topic of future investigation.

Table 1.1: Opposing Catecholamine Responses		
Stimulus	**NAc Dopamine**	**vBNST Norepinephrine**
At rest	↑↓	-
ICSS		
Stimulation	↑	↑
ICSS-predictive cue	↑	-
ICSS-extinction	↓	↑
Food reward		
Unexpected Food	↑	-
Food-predictive cue	↑	?
Food-omission	↓	?
Drugs of abuse		
Drug exposure	↑	-, ?
Drug Withdrawal	↓	↑, ?
Noxious/Aversive		
Quinine	↓	↑
Fear cues	↑↓	?
Tail pinch	↑↓	↑

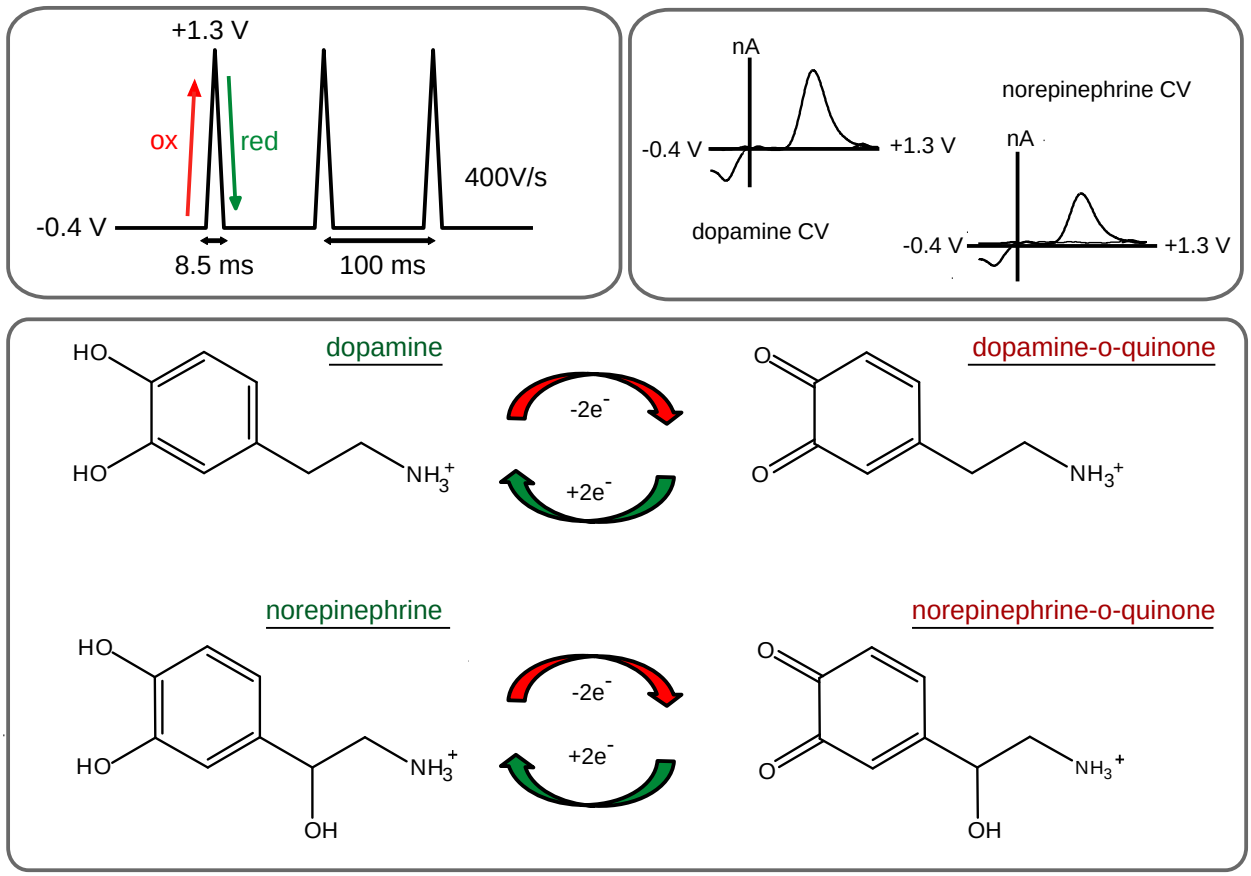

Figure 1.1: Fast-scan cyclic voltammetry for the detection of catecholamines. The most commonly used waveform sweeps from -0.4 to +1.3 V at a scan rate of 400 V/s. The positive-going scan oxidizes dopamine and norepinephrine to their ortho-quinone form, and the negative going scan reduces them back to dopamine or norepinephrine. Plotting the resultant current vs potential results in identical characteristic cyclic voltammograms (CVs) for both dopamine and norepinephrine.

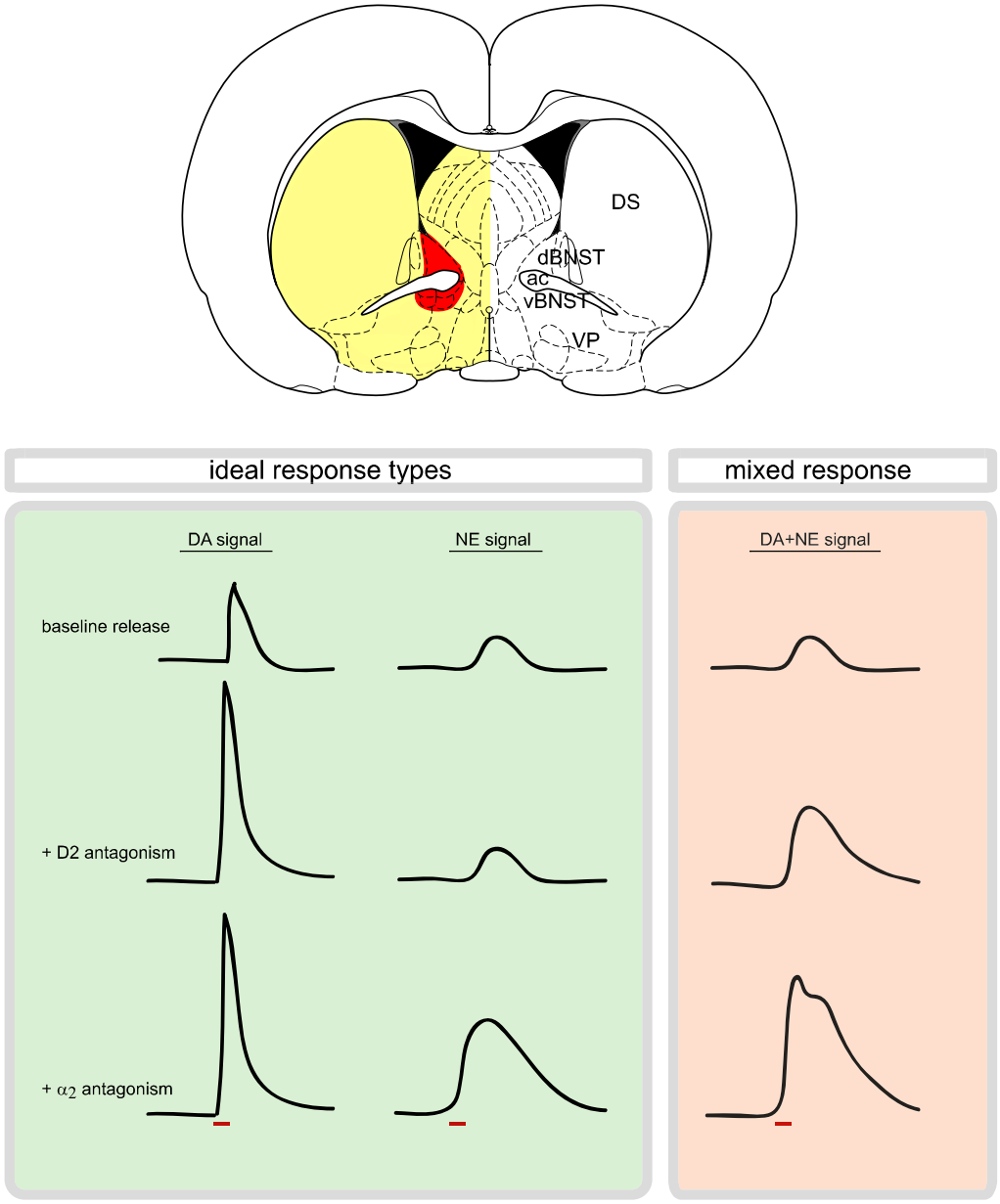

Figure 1.2: Spatially resolved measurements combined with pharmacology ensure selective dopamine or norepinephrine measurements. Brain slice, adapted from the atlas of Paxinos and Watson showing norepinephrine terminals (red) surrounded by dopamine terminals (yellow), highlighting the need for a small sensor. Boxes show mock electrically stimulated response types to different drugs. Red bar denotes stimulation. In the green box, a pure dopamine signal increases with D2 antagonism, and remains elevated with α_2 antagonism; a pure norepinephrine signal does not increase following D2 antagonism and only responds to α_2 antagonism. In the red box, a mixed dopamine / norepinephrine signal responds to both D2 and α_2 antagonists. Abbreviations: DS, dorsal striatum; ac, anterior commissure; dBNST, dorsal bed nucleus of the stria terminalis; vBNST, ventral bed nucleus of the stria terminalis; VP, ventral pallidum

CHAPTER 2: NORADRENERGIC SYNAPTIC FUNCTION IN THE BED NUCLEUS OF THE STRIA TERMINALIS VARIES IN ANIMAL MODELS OF ANXIETY AND ADDICTION[1]

Introduction

In drug-dependent individuals, researchers have highlighted the development of a persistent 'negative emotional state' when access to drugs is terminated (Koob, 2009). Substance abuse is often co-morbid with anxiety disorders and impacted by stressful life experiences (Hyman *et al*, 2009; Sinha, 2008). The risk for developing an addiction, however, varies considerably between individuals, and different people can have very different responses to drug or stress exposure. One means for addressing this issue is examining animals with divergent behavioral phenotypes in appropriate neuronal structures. Akin to human addicts, inbred Lewis (L) rats self-administer opiates at high levels (George and Goldberg, 1989), and show escalation of drug-taking behavior (Picetti *et al*, 2012). Additionally, L rats display several anxiety-like phenotypes as compared with outbred Sprague-Dawley (SD) rats, as well as hypocortisolemia; thus, they have been suggested to be a good model of post-traumatic stress disorder (PTSD)

[1] This chapter originally appeared as an article in *Neuropsychopharmacology*. The original citation is as follows : McElligott ZA, Fox ME, Walsh PL, Urban DJ, Ferrel MS, Roth BL, Wightman RM (2013). "Noradrenergic Synaptic Function in the Bed Nucleus of the Stria Terminalis Varies in Animal Models of Anxiety and Addiction." *Neuropsychopharm* **38**(9): 1665-1673.

(Cohen *et al*, 2006). The bed nucleus of the stria terminalis (BNST) is a forebrain nucleus in the extended amygdala positioned to relay between cortical, hippocampal

and amygdalar inputs, and stress and reward centers (Drolet, 2009). The BNST is densely innervated by noradrenergic fibers arising from the A1, A2 (via the ventral noradrenergic bundle or VNB), and A6 (via the dorsal noradrenergic bundle) cell bodies (Forray *et al*, 2004). Norepinephrine signaling within the BNST modulates anxiety-like behavior and influences induction of the hypothalamic–pituitary–adrenal (HPA) axis (Cecchi *et al*, 2002), affects expression of learned and physical opiate withdrawal behaviors (Delfs *et al*, 2000) and contributes to stress-induced reinstatement of drug seeking (Erb *et al*, 2000; Leri *et al*, 2002; Wang *et al*, 2001). Furthermore, norepinephrine impacts both excitatory (McElligott and Winder, 2009) and inhibitory synaptic transmission (Dumont *et al*, 2004), induces synaptic plasticity (McElligott and Winder, 2008), and releases corticotropin-releasing factor (CRF) in the BNST (McElligott *et al*, 2010; Nobis *et al*, 2011). The Morilak lab found that extracellular norepinephrine in the BNST was the same in non-manipulated L and SD rats; however, when restrained for 30 min, extracellular norepinephrine was elevated in L rats compared with SD rats (Pardon *et al*, 2002) . Furthermore, L rats exhibit fear generalization and anxiety-like behaviors that are BNST dependent (Duvarci *et al*, 2009).

Here, we hypothesized that the noradrenergic system projecting to the BNST may be differently regulated in these two rat strains. Furthermore, we tested whether the noradrenergic system is differentially modulated in a model of morphine addiction. Previously, we demonstrated that norepinephrine dynamics and their regulation can be examined in the BNST with fast-scan cyclic voltammetry (Herr *et al*, 2012; Park *et al*, 2009). We used this technique in the ventral BNST (vBNST) to investigate the

mechanisms underlying differences in norepinephrine overflow in L rats as compared with SD rats, and to test the hypothesis that morphine dependence alters regulatory mechanisms at noradrenergic neurons. We found that non-manipulated L rats had a reduced rate of clearance and decreased sensitivity at their α_2-adrenergic receptors (ARs) as compared with SD rats. Furthermore, using high-performance liquid chromatography (HPLC), we found that non-manipulated L rats had higher norepinephrine tissue content. When SD rats were made physically dependent on morphine (Schulteis *et al*, 1999), modeling the condition of a human addict, there was a significant reduction in their norepinephrine uptake rate and in their response to a challenge with an α_2-AR antagonist as compared with controls. In contrast, neither clearance rate nor α_2-AR sensitivity were different in morphine-dependent L rats as compared with control or non-manipulated animals. Correlated to these alterations at norepinephrine synapses in the BNST, morphine-dependent SD rats, but not L rats, showed heightened anxiety-like behavior as compared with controls. The changes that occurred in morphine-dependent SD rats were profound: they exhibited indistinguishable norepinephrine uptake rates and similar responses to an α_2-AR antagonist as non-manipulated L rats. Thus, noradrenergic synapses underwent a remarkable adaptation when SD rats were made physically dependent on morphine. Furthermore, the data revealed that the vBNST norepinephrine system of the non-manipulated L rat resembled a ‘morphine-dependent state’.

Materials and Methods

Animal care

All experiments were performed in accordance with the University of North Carolina at Chapel Hill (UNC) Institutional Animal Care and Use Committee's guidelines. SD and L rats (males; 350–450 g; L rats total *n*=70, SD total *n*=85; Charles River, Wilmington, MA) were housed within UNC animal facilities and given food and water *ad libitum*. Electrochemical, biochemical, and behavioral experiments were performed as follows: voltammetry, SD *n*=34, L *n*=26; HPLC, SD *n*=22, L *n*=15; autoradiography, SD *n*=14, L *n*=13; elevated plus maze, SD *n*=15, L *n*=16.

Evoked norepinephrine release

Norepinephrine release in the vBNST was evoked from stimulation of the VNB as previously described (Park *et al*, 2009). Briefly, animals were anesthetized with urethane (1.5 g/kg *i.p.*) and placed in a stereotaxic frame (Kopf, Tujunga, CA). Holes were drilled in the skull for the carbon-fiber and stimulating electrodes at coordinates from a rat brain atlas(Paxinos and Watson, 2007). A Ag/AgCl reference electrode was placed in the contralateral hemisphere. A carbon-fiber microelectrode was placed in the vBNST (+1.2 mm ML, 0 mm AP, 7.2–7.8 mm DV). An untwisted bipolar stimulating electrode (Plastics One, Roanoke, VA) was placed in the VNB (+1.0 mm ML, −5.2 mm A-P, 8.0–8.5 mm DV from bregma). Both the carbon-fiber and stimulating electrodes were adjusted in the dorsal-ventral axis to obtain optimum norepinephrine release.

The electrical stimulation was delivered with a pair of constant-current stimulus isolators (model NL800, NeuroLog System, Digitimer). The stimulations consisted of

biphasic pulses (±300 μA, 2 ms/phase) applied at 60 Hz and 60 pulses unless otherwise noted. Stimulation pulses were computer generated and applied between cyclic voltammograms.

To measure evoked norepinephrine release, a triangular scan (−0.4 to +1.3 V, 400 V/sec) was repeated every 100 ms to generate cyclic voltammograms. Data were digitized with a computer employing Tar Heel CV software written in LABVIEW (National Instruments, Austin, Texas). Three-dimensional color plots were used to examine the voltammetric data with the abscissa as voltage, the ordinate as acquisition time, and the current in false color. The average of 10 cyclic voltammograms collected before the electrical stimulation was used for background subtraction. Digital smoothing was accomplished under software control after data collection. Data were evaluated with principal component analysis to resolve individual analytes as described previously (Keithley *et al*, 2010; Keithley *et al*, 2009). An average calibration factor (6 nA/1 μM NE/100 μm carbon fiber) was used to convert current to concentration.

Electrode placement was verified by making electrolytic lesions with the carbon-fiber microelectrode as previously described (Park *et al*, 2009). Animals were euthanized with urethane before a constant current (20 μA for 10 s) was applied to the electrode in the recording site. Brains were subsequently removed from the skull, and stored for at least three days in 10% formaldehyde. Coronal sections (45 μm thick) were made with a cryostat (Leica, Germany), and slices were mounted on slides and coverslipped before viewing under a light microscope.

Determination of norepinephrine and dopamine content in tissue slices

Brains were rapidly removed from anesthetized rats (urethane 1.5 mg/kg). Coronal sections (300 µm thick) were prepared using a Lancer Vibratome (World Precision Instruments, Sarasota, FL) in 4 °C artificial cerebral spinal fluid (aCSF). The aCSF (in mM: 126 NaCl, 25 $NaHCO_3$, 2.45 KCl, 12 NaH_2PO_4, 1.2 $MgCl_2$, 2.4 $CaCl_2$, 20 HEPES, and 11 glucose) was adjusted to pH 7.4 and oxygenated (95% O_2/5% CO_2). Tissue containing the vBNST or nucleus accumbens (NAc) was excised with a 1-mm punch, and homogenized in 0.1 N $HClO_4$ containing 1 µM hydroquinone. Tissue processing and HPLC were performed as previously described (Park *et al*, 2009). The tissue was homogenized with a sonic dismembrator (Fisher Scientific, Model 60, Pittsburgh, PA), and the homogenate was spun down at 6000 rpm for 10 minutes. The supernatant was removed and filtered using a 0.2 µm syringe filter (Millex-LG). HPLC employed published procedures (Lahdesmaki *et al*, 2002; Mefford, 1981). Briefly, 20 µL injections were made onto a reverse-phase column (5 µm, 4.6 x 5 mm, Waters Atlantis). The mobile phase consisted of 0.1 M citric acid, 1 mM sodium hexylsulfate, and 0.1 mM EDTA (pH = 3), with 5% or 10% methanol as an organic modifier. The flow rate was 1.0 mL/min. Catecholamines were detected with a thin layer radial electrochemical cell (BASi, West Lafayette, IN) at constant potential vs Ag/AgCl. Data were collected at 60 Hz using a LabVIEW stripchart recorder program (Jorgenson Lab, UNC) and homebuilt electronics. Standards were prepared fresh in 0.1 N $HClO_4$ and the ratio of analyte peak area to hydroquinone peak area was used to calculate tissue concentrations.

Autoradiography

Norepinephrine transporter (NET) and α_2-adrenergic receptor (α_2-AR) receptor autoradiography methods were adapted from autoradiography methods previously described (Allen *et al*, 2011). Briefly, brains were quickly removed, frozen on dry ice, and stored at -80°C until processing. Coronal brain sections (16 µm) (Bregma: 0 mm to Bregma -0.1 mm) were cut on a cryostat and thaw-mounted onto slides (Fisher Scientific Tissue Path Superfrost Plus Gold Slides, #15-188-48) and vacuum desiccated at 4°C overnight. For α_2-AR receptor autoradiography, sections were incubated with ^{125}iodoclonidine (200 pM; α_2-AR receptor agonist) for 1 hour at RT in binding buffer (170 mM TrisHCl, pH 7.6; 20 mM $MgCl_2$) to determine total binding. Rauwolscine (10 µM; adrenergic antagonist) was added to the incubation mixture to determine non-specific binding. Sections were washed (2X5 min) in ice-cold binding buffer (170 mM TrisHCl, pH 7.6; 20 mM $MgCl_2$), rinsed in ice-cold water (to remove residual salts), then air-dried and exposed to hyperfilm (GE Healthscience) for 48 hours. For NET autoradiography, sections were incubated with ^{125} Nisoxetine ((R)-N-methyl-(2-[(125)I]iodo-phenoxy)-3-phenylpropylamine; 60 pM) for 90 minutes at RT in transporter buffer (50 mM TrisHCl, pH 7.4; 120 mM NaCl; 5 mM $CaCl_2$) to determine total binding. Nisoxetine (1 µM; adrenergic antagonist) was added to the incubation mixture to determine non-specific binding. Sections were washed (2X5 min) in ice-cold buffer (50 mM TrisHCl, pH 7.4; 120 mM NaCl; 5 mM $CaCl_2$), rinsed in ice-cold water (to remove residual salts), then air-dried and exposed to hyperfilm (GE Healthscience) for 48 hours.

Films were developed and photographed with a digital camera system (Metaview). Image analysis was performed using ImageJ software to define regions of

interest (ROI) in the ventral bed nucleus of the stria terminalis and this ROI was transposed onto the non-specific binding images. Average pixel intensities of the nonspecific ROI was subtracted from the total ROI to obtain qualitative specific binding data.

Acute morphine dependence

The morphine-dependence protocol was modified from (Schulteis *et al*, 1999). Briefly, over the course of 3 days rats were injected once daily with 10 mg/kg morphine s.c., followed 4 h later by 1 mg/kg naloxone s.c. Behavioral, electrochemical, and autoradiography experiments were performed on the fourth day.

Elevated plus maze

The elevated plus maze (EPM) was used to assay anxiety-like behavior. Animals were isolated in a novel cage for 5 min before running the maze. Animals explored the maze for 5 min and their movement and time spent in each section (open arms, center, enclosed arms) was measured and recorded using Ethovision software (Noldus, Netherlands).

Chemicals and drugs

All chemicals and drugs were purchased from Sigma-Aldrich (St Louis, MO), with the exception of naloxone (Tocris Bioscience, Ellisville, MO), and used as received. Drugs were dissolved in sterile saline (0.9%).

Statistics

Results are average values ± SEM. Mainly unpaired Student's *t*-tests and 2-way analysis of variance (ANOVA) with *post-hoc* Bonferroni tests were used to determine statistical significance. Morphine withdrawal scores, pre-withdrawal weight, and fecal boli weight were compared using a 3-way ANOVA with a *post-hoc* Tukey's Honestly Significant Difference (HSD) Test. Linear regression analysis was used to examine the relationship between stimulation intensity and $[NE]_{max}$. Differences were considered significant when $*P<0.05$, $**P<0.01$, $***P<0.0001$.

Results

L rats had greater norepinephrine tissue content

Owing to the phenotypes discussed above, we investigated the catecholamine tissue content in the nucleus accumbens (NAc) and the vBNST in L rats compared with SD rats. We did not see significant differences between the strains in the levels of dopamine in the NAc (SD: 5.25±0.96 µg/g *n*=5, L: 6.06±0.32 µg/g *n*=5); however, in the vBNST, L rats had significantly more dopamine and norepinephrine tissue content (SD NE: 4.55±0.84 µg/g *n*=5 *vs* L NE: 10.9±1.52 µg/g *n*=5; SD DA: 1.06±0.32 *vs* 3.15±0.46 *n*=5; Figure 2.1 a–c). We presumed the dopamine in the vBNST was mainly localized in norepinephrine neurons because dopamine is the metabolic precursor to norepinephrine, and dopaminergic projections are mainly to the dorsal lateral BNST (Meloni *et al*, 2006; Park *et al*, 2012).

L rats had altered noradrenergic neurotransmission compared with SD rats

Next, we examined regulation of noradrenergic synaptic function using electrically-evoked release measured with fast-scan cyclic voltammetry in anesthetized rats. This method has been used extensively to characterize regulation of dopamine and serotonin neurotransmission (John *et al*, 2006), and we recently demonstrated its use to measure norepinephrine dynamics *in vivo* in the vBNST(Herr *et al*, 2012; Park *et al*, 2009). With the carbon-fiber microelectrode positioned directly beneath the anterior commissure, norepinephrine release was evoked by electrical stimulation of the VNB (example electrode placement shown in Figure 2.1d). Norepinephrine release (shown in color plots encoding voltammetric recordings over a 15-s interval) occurred upon stimulation, and its concentration fell to its original value after stimulation. Consistent with our previous report (Park *et al*, 2009), norepinephrine evoked release was unaffected by raclopride (2 mg/kg), a D2 receptor antagonist. In contrast, idazoxan (5 mg/kg, IDA), an α_2–AR antagonist, increased norepinephrine evoked release (examples in Figure 2.1f).

We compared stimulated release of norepinephrine in the vBNST in L and SD rats. The maximal amplitude of stimulated release ($[NE]_{max}$) was evaluated as a function of pulse number in the stimulus train (at 60 Hz) and fit with a linear regression. Both strains responded to stimulation linearly, although the slope of the line was greater in the L rats (L *vs* SD, respectively, r^2=0.98 *vs* 0.99, slope: 4.93±0.11 *vs* 3.11±0.21, P<0.05; Figure 2.2b). The clearance half-life ($t_{1/2}$ or time from the $[NE]_{max}$ to half the maximal concentration) following 60 Hz 60 pulse stimulations was significantly greater in

L rats than in SD rats (2.6±0.2 s, n=6 *vs* 1.9±0.1 s, n=11 respectively, P<0.05; Figure 2.2c). Additionally, when a saturating dose of the α_2-AR antagonist IDA (5 mg/kg i.p.; see Figure 2.3 for dose response curve) was administered under the same stimulation conditions to L rats, the increase in $[NE]_{max}$ was significantly reduced compared with SD rats (163±11% of pre-drug baseline, n=8 *vs* 217±14% of pre-drug baseline n=10, respectively, P<0.05; Figure 2.3c), further suggesting that norepinephrine dynamics are different in these strains. Autoradiography for α_2-AR and the norepinephrine transporter (NET), however, showed no differences between the strains (SD n=4, L n=4, Figure 2.4), suggesting total protein levels are the same.

Following this characterization, we probed the effect of an acute morphine injection (5 mg/kg i.p.) on norepinephrine dynamics. Surprisingly, the acute morphine slightly but significantly increased $[NE]_{max}$ in L rats but not in SD rats (116±9% of pre-drug baseline, n=5, P<0.05 *vs* 91±5% of pre-drug baseline, n=5; Figure 2.3e). There was no change in $t_{1/2}$ in either strain following acute morphine (L rats: 118±15% of pre-drug baseline, n=5; SD rats: 120±12% of pre-drug baseline, n=9; Figure 2.3f). Furthermore, when the response to IDA was compared in acutely treated and non-manipulated animals, there was a main effect of strain (2-way ANOVA, F=9.41, P<0.01; SD rats: 191±12.8% *vs* 217±14% of pre-drug baseline, n=5 and 10, with and without morphine, respectively; L rats: 158.6±5.4% *vs* 163±11% of pre-drug baseline, n=5 and 8, with and without morphine, respectively) but not of drug treatment. Therefore, acute morphine alone did not alter IDA response in either strain.

Morphine-dependent SD rats had increased anxiety-like behavior

Next, we assayed animals that had experienced morphine withdrawal using a dependence paradigm that modeled the negative affect experienced by human addicts (Amitai *et al*, 2006; Koob, 2009; Schulteis *et al*, 1999). Once daily, we administered 10 mg/kg morphine s.c., followed by 1 mg/kg naloxone s.c. 4 h later (denoted MN), for a total of 3 days (SD n=27, L n=22). Control animals received a saline injection s.c. followed by 1 mg/kg naloxone 4 h later (denoted SN) once daily for a total of 3 days (SD n=26, L n=23). For 10 min following the injection of naloxone, animals were assayed for withdrawal behaviors and assigned a global withdrawal score (Figure 2.5a). There was a significant effect of drug and day on the global withdrawal score, but not of strain (3-way ANOVA, F=25.34, P<0.0001; Figure 2.5b). Thus, SD and L rats that received morphine had significantly greater withdrawal symptoms than their saline control counterparts. By the third day, both strains that received morphine showed withdrawal scores that were significantly different from the first day, while saline controls did not (Tukey's HSD Test, P<0.0001). Furthermore, there was an effect of day and treatment, but not strain, with regard to pre-withdrawal body weight (F=15.99, P<0.001). Both strains that received morphine had significant decreases in pre-withdrawal body weight (day 3 *vs* day 1, Tukey's HSD Test, P<0.01 SD, P<0.05 L; Figure 2.5c). As a quantitative measure of withdrawal-induced gut motility, we weighed the fecal boli produced during the 60 min following naloxone administration. Again, we found a significant effect of treatment but not strain (F=59.08, P<0.0001) and a significant increase in day 3 *vs* day 1 fecal boli weight (Tukey's HSD Test, P<0.001 SD, P<0.01 L; Figure 2.5d). The similarity in responses to the morphine/naloxone challenge shows that

morphine dependence was induced in both strains. Owing to the short half-lives of morphine and naloxone (Trescot *et al*, 2008), both drugs were eliminated by experimentation time on day 4.

We next examined MN and SN animals of both strains on the EPM. Both center and enclosed arm time showed an interaction (2-way ANOVA, center: F=5.78, P<0.05; enclosed: F=5.49, P<0.05) and a main effect of strain (2-way ANOVA, center: F=15.2, P<0.001; enclosed: F=14.0, P<0.001). *Post-hoc* analysis revealed significant differences between SD-MN and SD-SN time spent in the center (62±11 s *vs* 106±6 s, n=8 and 7, respectively, P<0.01) and the enclosed arms (222±15 s *vs* 175±9 s respectively, P<0.05). L-MN rats, however, failed to show any differences in time spent in the center or enclosed arms when compared with L-SN rats (center: 47±12 s *vs* 44±8 s, enclosed: 239±13 s *vs* 250±11 s, respectively, n=8; Figure 2.5 e–g). No significant differences were noted in number of entries or open arm time between groups.

Norepinephrine dynamics were altered in morphine-dependent SD rats but not L rats

After establishing morphine dependence, animals were anesthetized on day 4 and norepinephrine overflow was measured in the vBNST using fast-scan cyclic voltammetry. We found that the $t_{1/2}$ in SD-MN rats was significantly longer than in SD-SN rats (2.6±0.4 s *vs* 1.6±0.2 s, n=5 and 6, respectively, P<0.05; Figure 2.6a). Additionally the increase in $[NE]_{max}$, following IDA was significantly blunted in the SD-MN rats as compared with SD-SN rats (147±9% *vs* 186±8%, n=5 and 6, respectively, P<0.05; Figure 2.6b). Interestingly, neither $t_{1/2}$ nor the response to IDA was altered by

morphine dependence in the L rats ($t_{1/2}$: L-MN 2.3±0.3 s *vs* L-SN 2.6±0.3 s, IDA: L-MN 163±25% of pre-drug baseline *vs* L-SN 157±10% of pre-drug baseline, *n*=5; Figure 2.6c and d). Neither SD-MN, L-MN, nor L-SN groups were significantly different from the non-manipulated L group with respect to either $t_{1/2}$ or response to the IDA challenge. Similar to non-manipulated animals, we did not observe changes in α_2-AR or NET binding in the vBNST of either strain or condition (SD-MN *n*=5, SD-SN *n*=5, L-MN *n*=4, L-SN *n*=5, Figure 2.4).

Catecholamine tissue content in morphine-dependent and control Rats

Finally, we compared the catecholamine tissue content in the BNST and NAc of MN animals and their controls (Table 2.1). Contrary to naïve animals, when norepinephrine tissue content was examined there was no significant interaction between MN and SN animals of each strain (2-way ANOVA, SD-MN: 1.97±0.49 µg/g, *n*=9; SD-SN 3.23±0.72 µg/g, *n*=8; L-MN: 4.36±0.70 µg/g, *n*=5; L-SN: 3.12±0.65 µg/g, *n*=5 *P*>0.05). When BNST dopamine levels were examined, however, there was a main effect of both strain and drug treatment (2-way ANOVA, SD-MN: 1.32±0.22 µg/g, *n*=9; SD-SN 0.71±0.17 µg/g *n*=8; L-MN: 2.69±1.02 µg/g, *n*=5; L-SN: 1.55±0.59 µg/g, *n*=5, *P*<0.05 for each factor). Interestingly, when dopamine levels in the NAc were measured, there was a significant interaction (2-way ANOVA, SD-MN: 5.21±0.91 µg/g, *n*=9; SD-SN 4.85±0.75 µg/g *n*=8; L-MN: 7.25±1.31 µg/g, *n*=5; L-SN: 2.37+0.46 µg/g, *n*=5 *P*<0.05). *Post-hoc* analysis revealed that L-MN rats had significantly higher dopamine in the NAc than their L-SN controls (*P*<0.05), whereas SD animals showed no difference.

Discussion

Previous studies have shown that L rats have anxiety and PTSD-like phenotypes (Cohen *et al*, 2006) and elevated extracellular norepinephrine in the BNST in response to a stressor (Pardon *et al*, 2002). They are also predisposed to substance abuse (Picetti *et al*, 2012; Sánchez-Cardoso *et al*, 2007). Here, we found that the tissue content of norepinephrine and dopamine in the vBNST, but not dopamine in the NAc, was elevated in L rats as compared with SD rats. Furthermore, using fast-scan cyclic voltammetry, we uncovered profound differences in the regulation of norepinephrine synaptic function in the vBNST in the two strains. Norepinephrine is less regulated in L rats when compared with SD rats because they have a reduced norepinephrine uptake rate and less sensitivity to an α_2-AR antagonist. When SD rats were made dependent on morphine the two key regulators of norepinephrine overflow, uptake, and autoreceptor regulation, were both reduced such that norepinephrine neurotransmission resembled that of a non-manipulated L rat. In L rats, however, norepinephrine clearance and autoreceptor regulation were unaffected by morphine dependence. This physiological phenomenon correlated to an increase in anxiety-like behavior in SD-MN rats but not L-MN rats, as compared with their controls. The results demonstrate a robust plasticity within an organism's noradrenergic system that may be influenced by genetic factors as well as environmental insults.

L rats exhibited poor control over norepinephrine release and clearance

Neurotransmitter levels in the extracellular space are determined by the balance between release and uptake (Wightman *et al*, 1988). Release is a function of the rate of

impulse flow (action potentials), the relative amount of norepinephrine in the releasable pool, and regulation by autoreceptors. The principal inhibitory autoreceptor in noradrenergic neurons is the α_2 -AR (Trendelenburg *et al*, 2001). NET is primarily responsible for norepinephrine clearance by uptake (Xu *et al*, 2000), and it follows Michaelis–Menten kinetics (Park *et al*, 2009). Electrical stimulation of norepinephrine neurons provides a convenient way to monitor release and uptake. Stimulation at supraphysiological frequencies allows release to predominate over uptake, enabling its nature to be examined. The maximum concentration achieved ($[NE]_{max}$), measured at the end of the stimulation, is thus predominantly a function of release. Recently the Jones lab has shown that the $t_{1/2}$ after the stimulation provides a measure of the rate of uptake that agrees with more complex Michaelis–Menten modeling (Yorgason *et al*, 2011). Thus, the electrical stimulations used here allowed quantification of several basic parameters that control extracellular norepinephrine.

Our studies showed that $[NE]_{max}$ is similar in the two strains with shorter stimulation trains. This is surprising because the vBNST norepinephrine content is twice as large in naïve L rats compared with SD rats. While release is linear in both strains, the slope of the regression line in the SD rats was significantly less than L rats, indicating that L rats have a larger releasable pool (Montague *et al*, 2004). Microdialysis studies have shown that extracellular norepinephrine increases during restraint stress in L rats relative to SD rats (Pardon *et al*, 2002), possibly arising from the larger releasable pool revealed in this work. Additionally, our experiments that probed the efficacy of the autoreceptor revealed that it exerts greater inhibition of release in SD rats. Although urethane anesthesia has been shown to stimulate α_2-ARs in the periphery (Armstrong *et*

al, 1982), our results in anesthetized animals mimicked the IDA effects observed in awake rats (Park *et al*, 2012). Taken together, our results suggest that L rats appear optimized for maximal norepinephrine neurotransmission. The combination of high content, low uptake rate, and low autoreceptor regulation ensures enhanced norepinephrine tone.

Norepinephrine signaling in the BNST has been implicated in mediating control over the HPA axis and in anxiety-like behavior (Cecchi *et al*, 2002) and can release CRF within the BNST (McElligott *et al*, 2010; Nobis *et al*, 2011). Furthermore, prolonged norepinephrine signaling in the BNST induces synaptic plasticity that is modulated by stress (McElligott *et al*, 2010; McElligott *et al*, 2008). The altered mechanisms in L rats that allow enhanced norepineprhine signaling may result in their anxiety-like phenotypes observed by others (Cohen *et al*, 2006), and could translate to anxiety-susceptible human populations. Indeed, recent data show that targeting noradrenergic signaling mechanisms may alleviate symptoms of substance abuse and PTSD (Raskind *et al*, 2000; Simpson *et al*, 2009).

Morphine dependence enhanced anxiety-like behavior, increased norepinephrine clearance half-life and reduced autoreceptor function in SD but not L rats

It is hypothesized in the allostasis model that the progression to addiction requires the engagement of neuronal stress/anxiety systems, including the release of norepinephrine in the BNST (Delfs *et al*, 2000; Koob, 2009). Therefore, a predisposition to the negative emotional state associated with engagement of these neuronal substrates might explain the co-morbidity that is associated with anxiety disorders and addiction. L rats have a high anxiety/PTSD phenotype that is at least partially due to

BNST function (Cohen *et al*, 2006; Duvarci *et al*, 2009) and a propensity to self-administer and escalate opiate intake (Picetti *et al*, 2012; Sánchez-Cardoso *et al*, 2007). Interestingly, following withdrawal from morphine, but not acute morphine, SD rats showed profound plasticity in both autoreceptor regulation and uptake rates, as well as enhanced anxiety-like behavior. Moreover, the SD-MN rats had uptake rates and autoreceptor profiles indistinguishable from non-manipulated L rats. Surprisingly, L-MN rats exhibited neither this plasticity nor further increases in anxiety-like behavior, suggesting that autoreceptors and uptake rates in the L rats may be in a maximally depressed state. The correlation between vBNST norepinephrine and increased anxiety revealed in this work implicate plasticity at noradrenergic synapses as one mechanism for the development of anxiety and addiction phenotypes.

Interestingly, our autoradiography experiments demonstrated that neither naïve, MN, nor SN rats of either strain showed alterations in α_2-AR or NET levels in the vBNST. This may be due to several reasons. First, this technique probes targets that are on the cell surface and in internal pools; therefore, it does not exclusively examine functional receptors and transporters. Second, it is possible that the functional changes we observed are not due to alterations in protein level, but due to a post-translational modification. Finally, the BNST has strong expression of nonspecific organic cation transporters, which also may have a role in the clearance of NE (Gasser *et al*, 2009) and could be manipulated by the gene–environment interactions we probed here. Nevertheless, the functional results clearly showed that the synaptic dynamics are dramatically different between SD and L rats, and that they were greatly altered in SD-MN rats.

Examining catecholamine tissue content in MN and control rats showed interesting changes in our treatment groups. Our data demonstrated that naloxone treatment lowered norepinephrine levels in the BNST in both strains regardless of pretreatment with morphine, and the effect was long lasting. These data are intriguing because naloxone and other μ-opioid antagonists are prescribed to humans for opiate and alcohol dependence (Heilig and Egli, 2006). Further, we found that L-MN rats had elevated dopamine in their NAc as compared with their controls, which may also contribute to their self-administration escalation phenotype (Picetti *et al*, 2012).

We have shown that norepinephrine synapses in a genetic model of anxiety and addiction (L rats) permit exacerbated noradrenergic signaling due to reduced uptake and autoreceptor function. Furthermore, we showed that vBNST norepinephrine synapses in a relatively non-anxious SD rat resemble L rat norepinephrine synapses when SD rats are made morphine dependent. These data suggest that noradrenergic synapses undergo a plasticity event where increased norepinephrine signaling (here stemming from precipitated withdrawal) results in a biophysical/biochemical change within the presynaptic cell to permit prolongation of future norepinephrine signaling on post synaptic cells. Furthermore, these alterations correlated to enhanced anxiety-like behavior in the SD rats. Additionally, the data support the allostasis model (Koob *et al*, 2010) and the idea that genetic factors contributing to negative affect could in turn increase susceptibility to developing substance abuse issues.

Support

The authors thank Dr Michael Saddoris for advice on statistical methods, Dr Ryan Vetrano and Dr Fulton Crews for behavioral advice and assistance, and Dr Elyse Dankoski and Dr Thomas Kash for comments on an earlier version of the manuscript. This work was supported by an NIH grant (NS15841) to RMW and the NIMH Psychoactive Drug Screening Program Contract to BLR

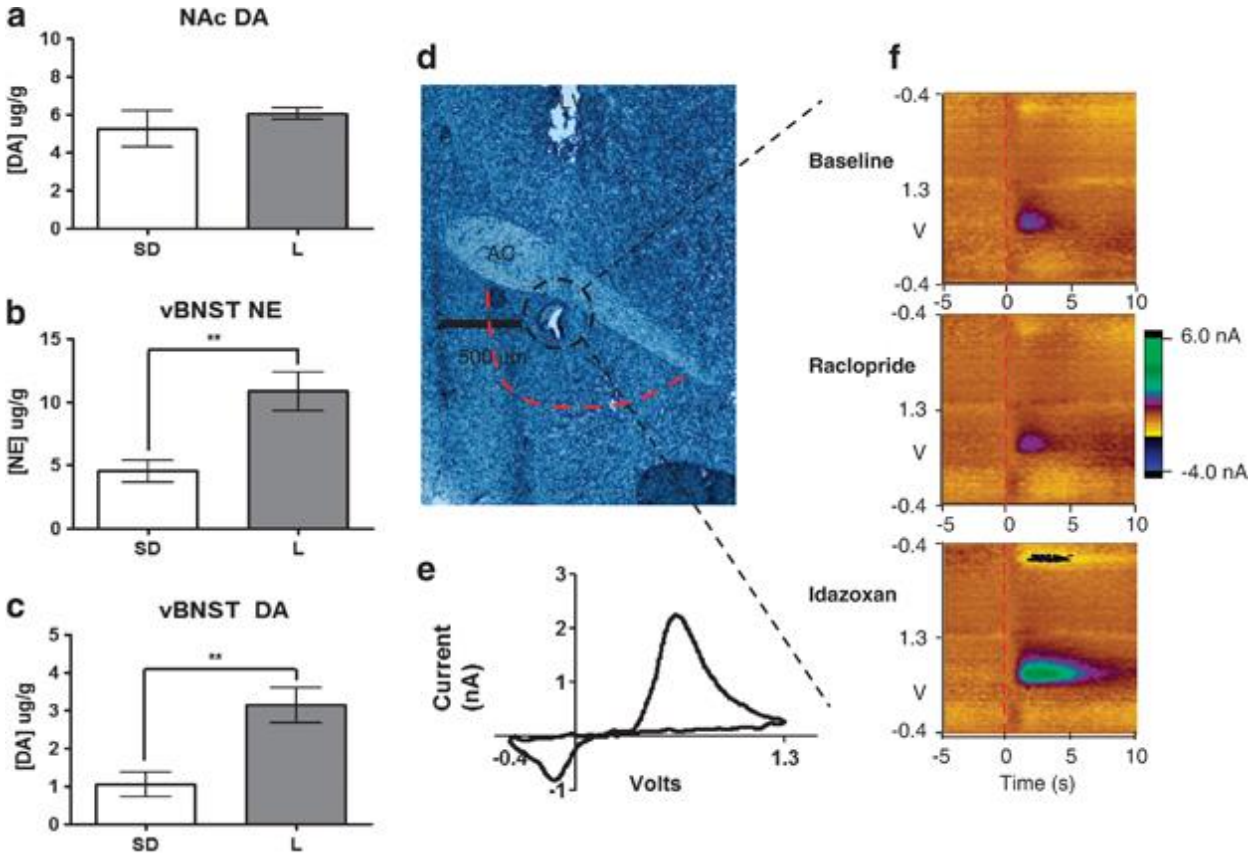

Figure 2.1: Fast-Scan Cyclic Voltammetry of norepinephrine (NE) in the bed nucleus of the stria terminalis (BNST). (a–c) Tissue content analysis of catecholamines in the BNST and nucleus accumbens (NAc). (d) Representative histology of recording electrode placement in the ventral BNST (vBNST) (black dashed circle) and area excised for tissue content analysis (red dashed line; LV, lateral ventricle; AC, anterior commissure). (e) Representative cyclic voltammogram of NE at $[NE]_{max}$. (f) Representative color plots demonstrating NE release and uptake in baseline conditions, following 2 mg/kg raclopride, or 5 mg/kg idazoxan.

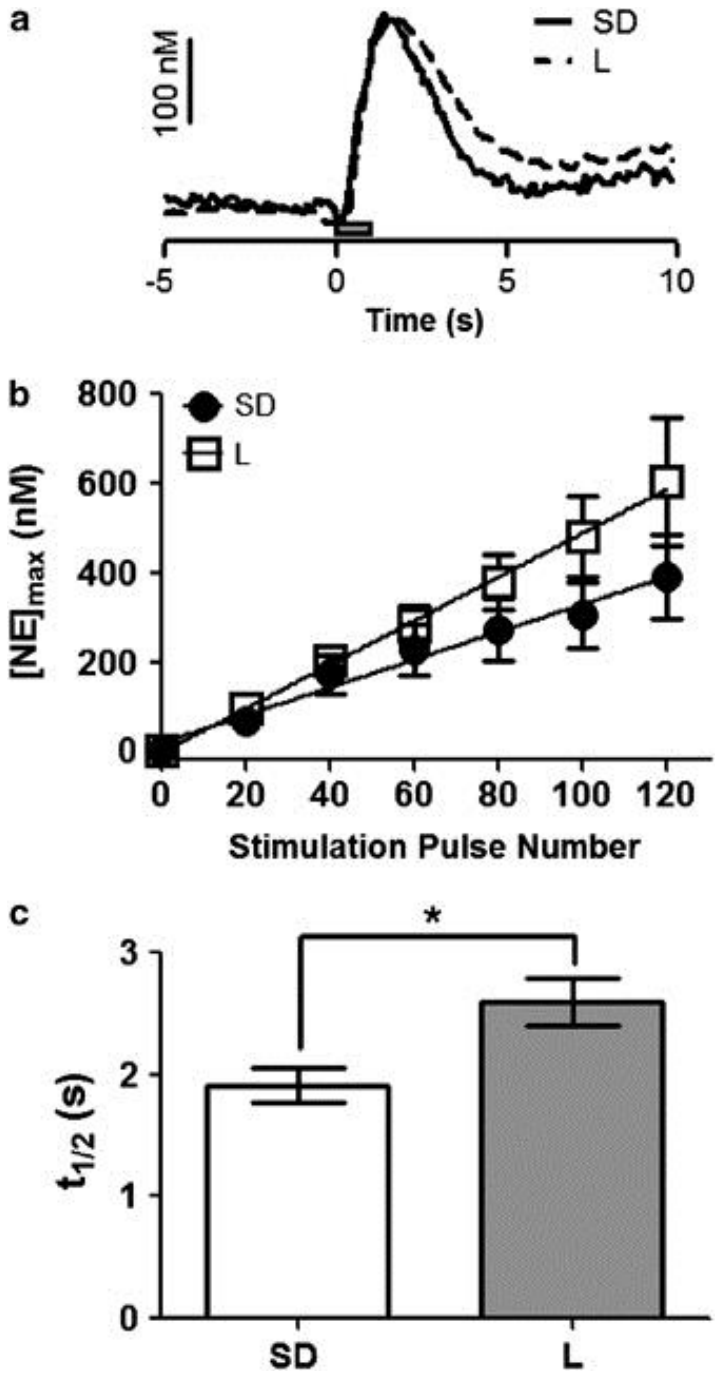

Figure 2.2: Comparison of norepinephrine (NE) dynamics in naïve Lewis (L) and Sprague-Dawley (SD) rats. (a) Representative concentration traces demonstrating NE release and uptake in the ventral bed nucleus of the stria terminalis (vBNST) of both SD and L rats (scale bar, 100 nM; gray box =stimulation, 60 pulses, 60 Hz). (b) Input–output curve of [NE]max at 20, 40, 60, 80, 100 and 120 pulses in SD and L rats. (c) Histogram of mean clearance half-life of NE following 60 Hz, 60 pulse stimulation in both SD and L rats.

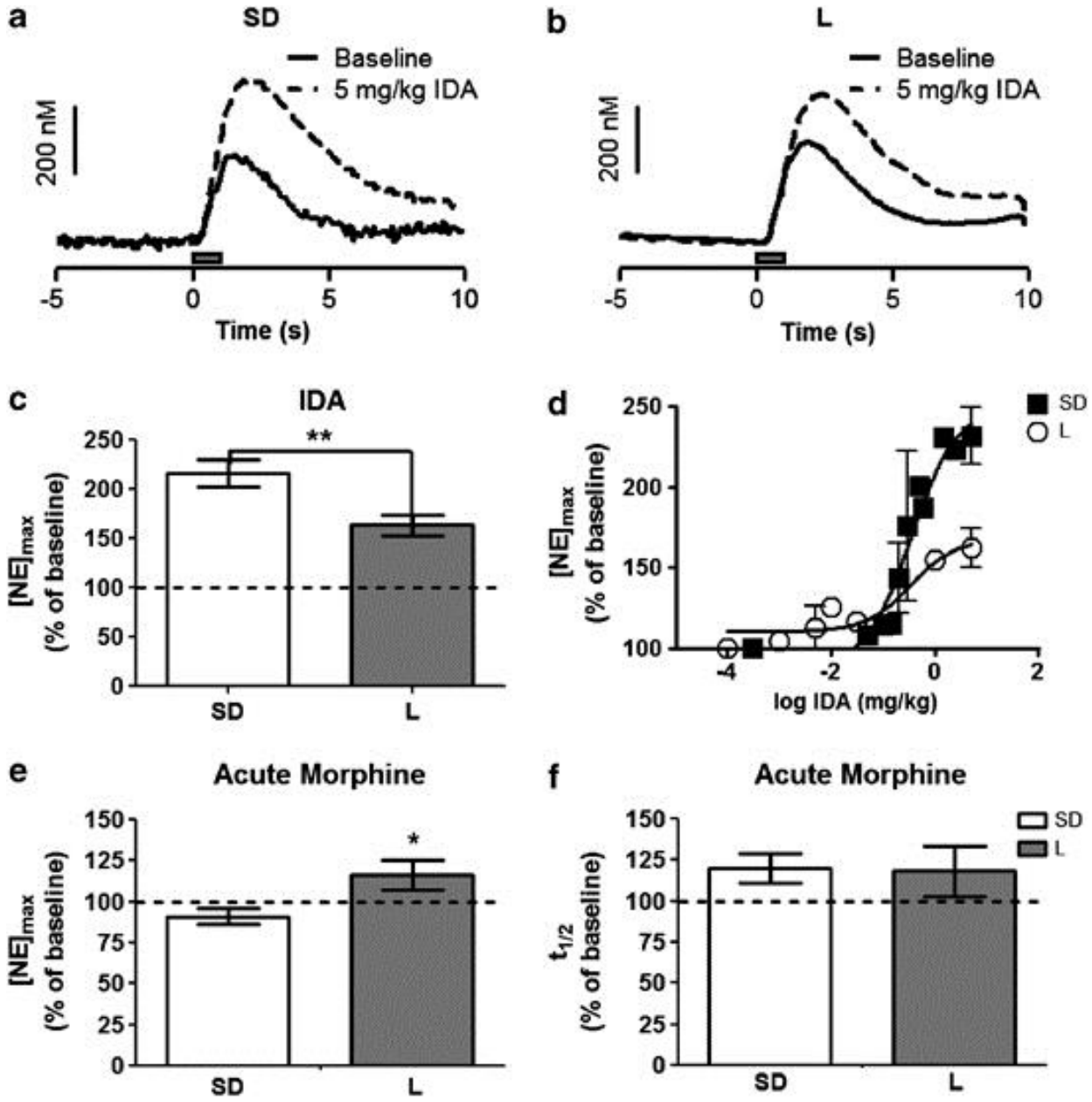

Figure 2.3: Effect of idazoxan (IDA) and morphine on norepinephrine release in the ventral bed nucleus of the stria terminalis (vBNST). (a and b) Representative concentration traces of Sprague-Dawley (SD) and Lewis (L) rats, respectively. Solid line—evoked norepinephrine (NE) concentration with 60 Hz, 60 pulses stimulation; dashed line—evoked NE concentration following 5 mg/kg IDA with the same electrical stimulus. (c) Average [NE]max following 5 mg/kg IDA relative to pre-drug stimulated release. (d) Change in [NE]max as percent of pre-drug baseline in both Sprague-Dawley (closed squares) and Lewis (open circles) rats, plotted vs log concentration of IDA (n=3 each strain). (e) Average [NE]max to acute 5 mg/kg morphine relative to pre-drug stimulated release. (f) Average clearance half-life following acute 5 mg/kg morphine relative to pre-drug stimulated release.

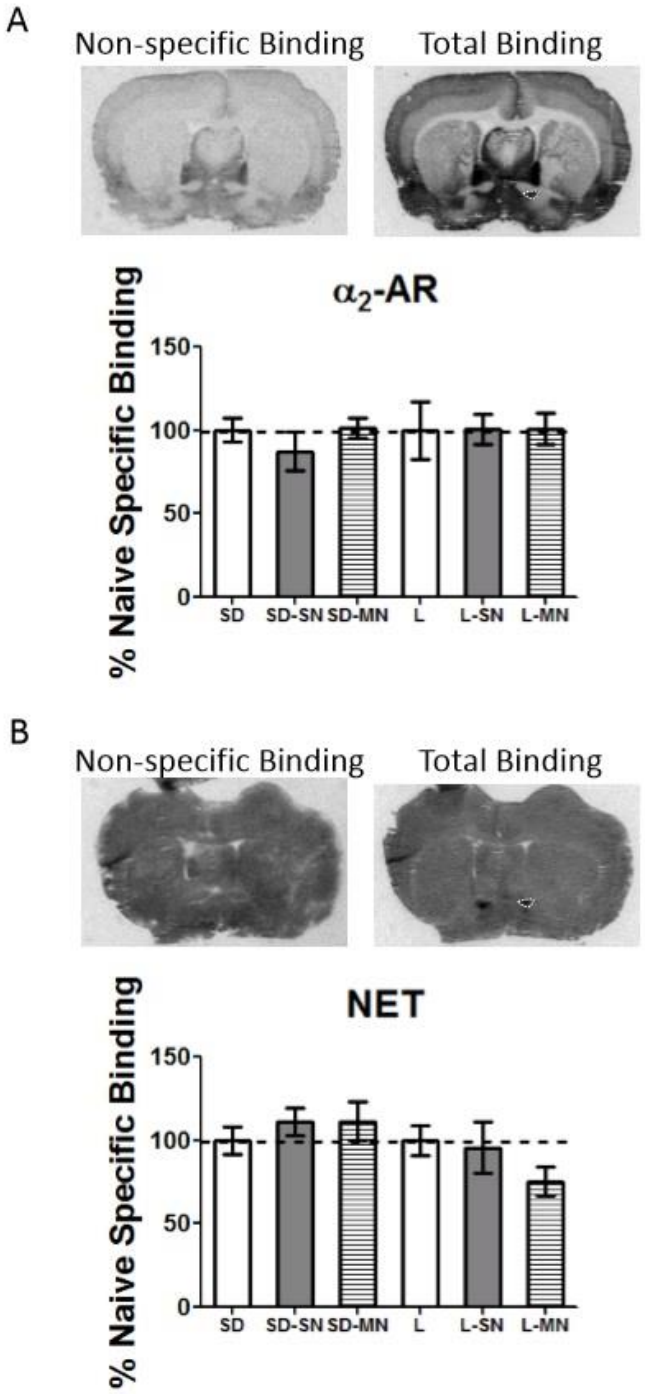

Figure 2.4: Autoradiography for α2AR and NET in naïve, MN, and SN animals. Representative non-specific, total binding, and autoradiography totals for A. α2-AR with 125iodoclonidine and B. NET with 125 Nisoxetine in SD-MN, SD-SN, L-MN and L-SN rats.

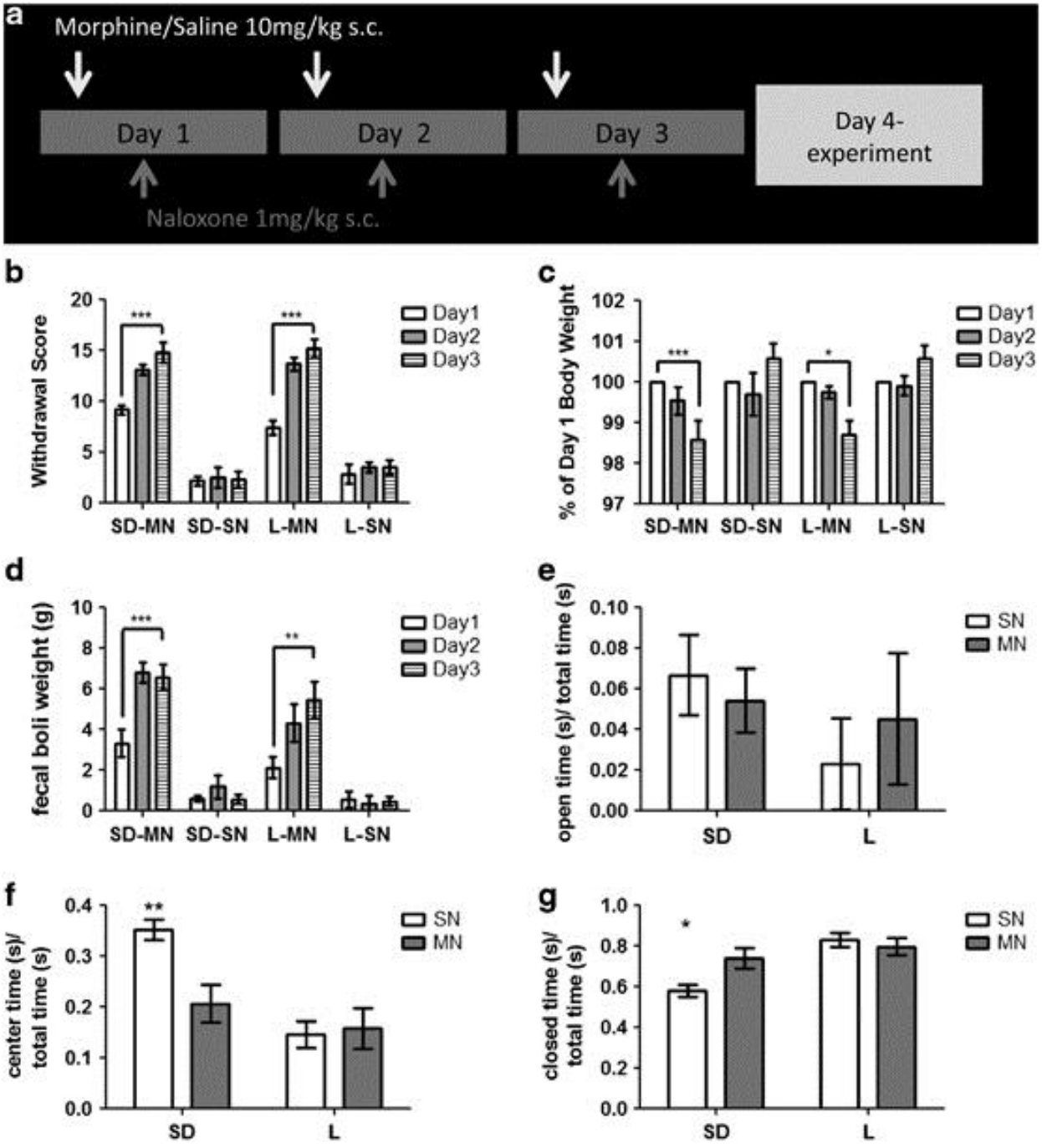

Figure 2.5: Morphine dependence in Sprague-Dawley (SD) and Lewis (L) rats. (a) Model of drug administration paradigm. (b) Global withdrawal scores, (c) pre-withdrawal body weight (as % of day 1), and (d) fecal boli weight in SD morphine/naloxone (SD-MN) and L-MN rats following withdrawal, compared with control SD saline/naloxone (SD-SN) and L-SN rats. Time spent in (e) open arms (f), center or (g) closed arms of the elevated plus maze as a fraction of total time in the maze in SD-MN, SD-SN, L-MN, and L-SN rats.

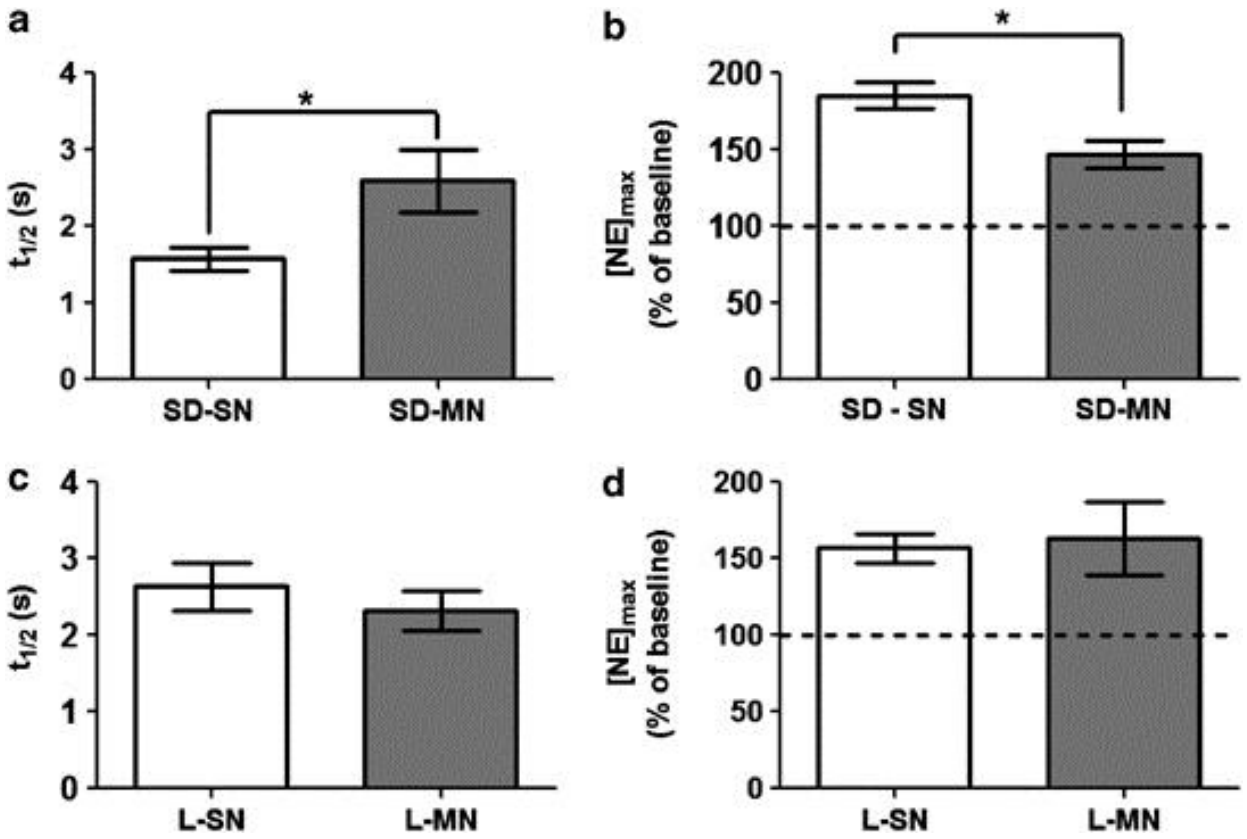

Figure 2.6: Clearance half-life and change in response following idazoxan (IDA) administration in morphine/naloxone (MN) animals vs saline controls. (a) t1/2 and (b) change in [NE]max as percent of pre-drug baseline in MN Sprague-Dawley (SD) rats vs saline controls ($P<0.05$). (c) t1/2 and (d) change in [NE]max as percent of pre-drug baseline in MN Lewis (L) rats vs saline controls (n.s.). SN, saline/naloxone.

Table 2.1 Catecholamine Tissue Content Analysis (µg/g) in the Nucleus Accumbens and Ventral Bed Nucleus of the Stria Terminalis of Control (Saline/Naloxone) and Morphine-Dependent (Morphine/Naloxone) Rats by HPLC.

	DA NAc (µg/g)	NE vBNST (µg/g)	DA vBNST (µg/g)
Sprague-Dawley			
Saline/naloxone (*n*=8)	4.85±0.75	3.23±0.72	0.71±0.17
Morphine/naloxone (*n*=9)	5.21±0.91	1.97±0.49	1.32±0.22
Lewis			
Saline/naloxone (*n*=5)	2.37±0.46*	3.12±0.65	1.23±0.37
Morphine/naloxone (*n*=5)	7.25±1.31*	4.36±0.70	2.69±1.02

*$P<0.05$.

CHAPTER 3: STRESS AND DRUG DEPENDENCE DIFFERENTIALLY MODULATE NOREPINEPHRINE SIGNALING IN ANIMALS WITH VARIED HPA AXIS FUNCTION [2]

Introduction

Researchers have demonstrated the importance of central noradrenergic activation in regulating behavioral and physiological responses to stress (Cecchi *et al*, 2002; Fendt *et al*, 2005). In part, this is because norepinephrine can engage the hypothalamic-pituitary-adrenal (HPA) axis. Through such actions, norepinephrine has been identified as an important neural substrate associated with the aversive components of morphine withdrawal (Delfs *et al*, 2000). Such evidence has given support to the view that the negative affect experienced during drug withdrawal is mediated in part by norepinephrine, and can contribute to the addiction cycle (Koob *et al*, 2010). Interestingly, a number of psychological disorders and addictions are comorbid with stress and involve noradrenergic dysregulation (eg, post-traumatic stress disorder) (Hyman *et al*, 2006; Sinha, 2008). For example, exposing rats to intruder stress evokes an opiate-dependent like state and alters firing of norepinephrine neurons (Chaijale *et al*, 2013). Therefore, investigation of noradrenergic systems and their role in the initiation/termination of stress is important for understanding the pathophysiology of diseases that co-express with addiction.

[2] This chapter originally appeared as an article in *Neuropsychopharmacology.* The original citation is as follows: Fox ME, Studebaker RI, Swofford NJ, Wightman RM (2015) "Stress and drug dependence differentially modulate norepinephrine signaling in animals with varied HPA axis function." *Neuropsychopharm* **40**(7):1752-61

The ventral bed nucleus of the stria terminalis (vBNST) is a major target of norepinephrine innervation within the brain (Kilts and Anderson, 1986). Here, forebrain, limbic, and brainstem inputs converge to relay information about both physical and psychological stressors. The BNST receives small noradrenergic input from the locus coeruleus (LC), and major noradrenergic innervation from the A1 and A2 (via the ventral noradrenergic bundle) cell groups, and projects to stress and reward centers (Drolet, 2009; Forray *et al*, 2004). The BNST has neurons containing corticotropin-releasing factor (McElligott *et al*, 2010), excitatory and inhibitory projections to the paraventricular nucleus of the hypothalamus (Choi *et al*, 2007), and activates the HPA axis (Forray *et al*, 2004). Norepinephrine is released in the BNST during restraint stress, oral administration of an aversive tastant, and during morphine withdrawal (Fuentealba *et al*, 2000; Pardon *et al*, 2002; Park *et al*, 2012). Thus, norepinephrine release in the BNST can integrate stressful and aversive stimuli to generate an appropriate physiological response.

Previously, we showed that two different rat strains, Sprague-Dawley and Lewis, markedly differed in the response of their noradrenergic system to morphine withdrawal (McElligott *et al*, 2013). Sprague-Dawley rats demonstrated profound plasticity of uptake and autoreceptor function, whereas control mechanisms were unchanged in Lewis rats. To better understand how genetic differences interact with drug withdrawal and stressors, we chose to compare the stress responses of Sprague-Dawley (SD) and Wistar-Kyoto (WKY) rats. WKY rats exhibit increased depressive phenotypes and HPA axis function relative to Sprague-Dawley rats (Carr and Lucki, 2010; Cohen *et al*, 2006), and under restraint-stress, extracellular norepinephrine varies between the two (Pardon

et al, 2002). Here, we used fast-scan cyclic voltammetry to evaluate differences in norepinephrine overflow and regulation between SD and WKY rats in response to stress. We subjected animals to acute morphine-dependence, 2 weeks of social-isolation, and DSP-4 lesioning. In response to these stressors, we found robust neurochemical changes that differed between strains and corresponded with anxiety-like behavior.

Materials and Methods

Animal Care

Experiments were performed in accordance with University of North Carolina at Chapel Hill (UNC) Institutional Animal Care and Use Committee's guidelines. Subjects were Sprague-Dawley and Wistar-Kyoto rats (males, 250–350 g on arrival from Charles River, Wilmington, MA) pair-housed in UNC animal facilities on a 12-hour day/light cycle. Animals were given *ad libitum* access to food and water, and their health was monitored daily during treatments. For social isolation, after 1-week of acclimation, subjects were randomly split into single or pair-housing for 2 weeks. Care was taken to reduce the number of animals used. For anesthetized voltammetry experiments, 108 Sprague-Dawley and 103 Wistar-Kyoto rats were used. A separate group of 32 Sprague-Dawley and 48 Wistar-Kyoto rats was used for anxiety measures on the Elevated Plus Maze (EPM).

Chemicals and Drugs

Drugs were purchased from Sigma-Aldrich (St Louis, MO), with the exception of α_{2C} antagonist JP-1302 dihydrochloride (Tocris Bioscience, Ellisville, MO), dissolved in sterile saline (0.9%), and used as received. JP-1302 and α_{2A} antagonist BRL-44408 maleate were administered to naïve animals in a range from 0.2 to 5 mg/kg i.p. to build a dose–response curve. Treated and control animals were given either 2 mg/kg BRL-44408 i.p. or 2 mg/kg α_{2A} agonist Guanfacine HCl i.p. to assay α_{2A} function. At the end of the experiment, animals were given 2 mg/kg dopamine D2 antagonist raclopride tartrate i.p., followed by 5 mg/kg α_2 antagonist idazoxan i.p. to validate signal per (Park *et al*, 2009).

Measurement of Norepinephrine Release

Norepinephrine release in the vBNST was measured in anesthetized animals as described previously (Park *et al*, 2009) Briefly, rats were anesthetized with urethane (1.5 g/kg), affixed in a stereotaxic instrument (Kopf instruments) and the scalp removed. Holes were drilled for the BNST (0.0 A-P, +1.2 M-L) and VNB (-5.2 A-P, +1.0 M-L) referenced from bregma and based on the atlas of Paxinos and Watson(Paxinos *et al*, 2007). A Ag/AgCl reference electrode was placed contralaterally and secured with a screw. A carbon-fiber microelectrode (~100 um long) was lowered into the vBNST (7.0-7.6 mm D-V), and a bipolar stimulating electrode into the VNB (8-8.5 mm D-V). Dorsal-Ventral coordinates were optimized to achieve maximal measured norepinephrine release. The maximum amplitude of evoked release ([NE]max) was taken as a measure of the combined processes of release and uptake (Yorgason *et al*, 2011). The

half-life (t1/2) for norepinephrine to return to baseline after stimulation was taken as a quantitative measure of uptake rate(McElligott *et al*, 2013; Yorgason *et al*, 2011). Drug effects were measured as a percentage of pre-drug stimulated release.

Electrical stimulations were delivered with two constant-current stimulus isolators (model NL800, NeuroLog System, Digitimer). The stimulations consisted of biphasic pulses (±300 μA, 2 ms/phase) applied at 60 Hz and 60 pulses unless otherwise noted. Stimulation pulses were computer generated and applied between cyclic voltammograms.

For norepinephrine measurements, a triangular scan (−0.4 to +1.3 V, 400 V/sec) was repeated every 100 msec to generate cyclic voltammograms. Data were digitized with a computer employing HDCV software(Bucher *et al*, 2013). Color plots were used to examine the voltammetric data with the y-axis as voltage, the x-axis as acquisition time, and the current in false color. The average of 10 cyclic voltammograms collected before the electrical stimulation was used for background subtraction. Digital smoothing was accomplished under software control after data collection. Data were evaluated with principal component analysis to resolve individual analytes as described previously (Keithley *et al*, 2009). An average calibration factor (6 nA/1 μM NE/100 μm carbon fiber) was used to convert current to concentration.

Elevated Plus Maze

Anxiety-like behavior was measured as described previously (McElligott *et al*, 2013). Briefly, the number of entries and time spent in each section of the maze was measured over 5 min. Preference for the open arms was determined in each animal and

was expressed as a ratio of open-arm time over closed-arm time. The maze consisted of a cross-shaped platform elevated 1 m from the floor with two open and two closed arms. Each arm was 50 cm long and 10 cm wide and the closed arms were surrounded on three sides by 40 cm tall opaque walls. Arms of the same type were located across from each other. Rats were isolated in a novel chamber for 5 minutes prior to maze exposure, then placed in the center of the maze facing an open arm, and allowed to explore for 5 minutes. Time and entries spent in each section was recorded using Ethovision software (Noldus, Netherlands).

Morphine Dependence

For 3 days, rats were administered 10 mg/kg morphine sulfate s.c. once daily, followed 4 h later by 1 mg/kg naloxone HCl to induce withdrawal. Somatic indices of withdrawal (eg, teeth chattering) were scored each day per (Schulteis *et al*, 1999). Control animals received 3 days of 0.5 ml saline s.c., followed 4 h later by 1 mg/kg naloxone. On day 4, drug-free rats were assayed on the EPM or underwent surgery for norepinephrine measurements.

DSP-4 Lesioning

Wistar-Kyoto and Sprague-Dawley rats (150–200 g on arrival) were pair-housed, and administered two i.p., 50 mg/kg N-(2-chloroethyl)-N-ethyl-2-bromobenzylamine (DSP-4) injections in 1 ml/kg saline 3 days apart. Control animals were given two 1 ml/kg i.p. saline injections 3 days apart. Animals were allowed to recover for >10 days after the last injection.

Statistics

Results are presented as average values ± SEM. Two-way analysis of variance (ANOVA) with *post hoc* Bonferroni tests were used to determine statistical significance. An unpaired *t*-test was used to determine differences in anxiety between morphine-dependent and control WKY rats. Differences were considered significant when $*P<0.05$, $**P<0.01$, $***P<0.005$.

Results

First, we chose to extend prior work demonstrating strain-dependent differences in norepinephrine regulation during stress (McElligott *et al*, 2013; Pardon *et al*, 2002). We characterized vBNST norepinephrine synaptic function in anesthetized WKY rats with electrical stimulations of the ventral noradrenergic bundle, and measured subsequent norepinephrine overflow with fast-scan cyclic voltammetry (Herr *et al*, 2012; Park *et al*, 2009). This technique allows characterization of release and uptake of biogenic amines (John *et al*, 2006). We measured norepinephrine by placing the carbon-fiber microelectrode directly beneath the anterior commissure (electrode placement shown in Figure 3.1a, sample color plot encoding voltammetric recordings in Figure 3.1b). Release increased linearly with increasing stimulation duration in WKY rats (60 Hz stimulations, r^2=0.99, slope: 3.71±0.24; Figure 3.1c) similar to our findings in SD rats (slope: 3.11±0.21, (McElligott *et al*, 2013). Despite known phenotypic variations (Carr *et al*, 2010), we found no differences in norepinephrine clearance ($t_{1/2}$) between WKY and SD rats in a baseline state (1.6±0.12 s *vs* 1.7±0.10 s, *n*=22 and 26, respectively).

The adrenergic α_2 receptor serves as the inhibitory autoreceptor for norepinephrine, and two differentially regulated subtypes are present in the BNST (Scheinin *et al*, 1994). We assayed autoreceptor influence on release with α_2 antagonist idazoxan in WKY and SD rats. After drug administration (5 mg/kg), the amplitude in evoked norepinephrine ($[NE]_{max}$) was increased similarly in both strains (WKY: 205±10.3% *vs* SD: 216±21.1%, *n*=6 and 5, respectively). To examine α_2 subtype-specific effects, we employed α_{2A} and α_{2C} selective antagonists BRL-44408 and JP-1302, respectively. We found increased evoked norepinephrine in WKY rats following 2 mg/kg BRL-44408, but not 2 mg/kg JP-1302 (examples in Figure 3.1e and f, BRL: 140±6.9% *vs* JP: 95±4.5%, *n*=5). Similar effects were found in SD rats: (BRL: 157±15.4%. *vs* JP: 102±7.3%, *n*=5 and 6, respectively). The selected doses (2 mg/kg) approach saturation (Figure 3.2) and are sufficient to produce robust behavioral effects *in vivo* (Sallinen *et al*, 2007). Thus, our findings indicate the α_{2A} subtype is the principle noradrenergic autoreceptor in the vBNST of both WKY and SD rats, and it exerts similar control over norepinephrine release in both strains.

Norepinephrine Dynamics were Differentially Altered in Morphine-Dependent SD and WKY Rats

We hypothesized that SD and WKY rats would not differ in their response to morphine-dependence, owing to their noradrenergic similarity in a baseline state. To compare noradrenergic plasticity, we established morphine-dependence in SD and WKY rats as before (McElligott *et al*, 2013; Schulteis *et al*, 1999). Briefly, rats received 10 mg/kg morphine followed 4 h later by 1 mg/kg naloxone once daily for 3 days. Consistent with our prior work, withdrawal was behaviorally evident in both strains by

day 3 (Figure 3.3). On day 4, rats were anesthetized and electrically evoked norepinephrine was recorded. First, we examined the effects on norepinephrine clearance and found clearance half-life showed a main effect of strain ($F=5.8$, $P<0.05$) and treatment ($F=5.8$, $P<0.05$). There was also a significant treatment × strain interaction (two-way ANOVA, $F=10.35$, $P<0.01$). In agreement with our previous work, morphine-dependent SD rats showed impaired uptake relative to controls (2.2±0.16 s *vs* 1.5±0.06 s, $n=12$ and 11, respectively, $P<0.001$). To our surprise, uptake was unaltered in WKY rats (1.5±0.14 s *vs* 1.6±0.10 s, $n=9$ and 10, respectively, $P>0.05$, Figure 3.4a). As before, the protocol we employed allows time for clearance of morphine and naloxone (Trescot *et al*, 2008), thus altered uptake in SD rats is a consequence of morphine withdrawal.

To assay the effects of morphine withdrawal on α_{2A} function in these two strains, we administered 2 mg/kg of selective antagonist BRL-44408, or agonist guanfacine (2 mg/kg, GFC) and determined the effects on release. The doses were selected based on dose–response analysis in Figure 3.2 and 3.5. Response to autoreceptor drugs showed a main effect of morphine treatment (two-way ANOVA, BRL: $F=26$, $P<0.0005$; GFC: $F=18.2$, $P<0.005$) and strain (two-way ANOVA, GFC: $F=4.7$ $P<0.05$). *Post hoc* analysis revealed a significant decrease in response to BRL between morphine-dependent animals and their saline-naloxone controls (SD: 102±3.5% for morphine withdrawal *vs* 167±9.1% for control, $n=7$, respectively, $P<0.001$; WKY: 104±6.5% for morphine withdrawal *vs* 147±6.4% for control, $n=7$, respectively, $P<0.001$, Figure 3.4b). Additionally, the α_{2A} agonist, GFC, was less effective at inhibiting evoked norepinephrine release in both strains (SD: 87±3.6% for morphine withdrawal *vs*

65±4.9% for control, *n*=7, respectively, *P*<0.05; WKY: 102±8.9% for morphine withdrawal *vs* 75±3.8% for control, *n*=7, respectively, *P*<0.01, Figure 3.4c). Thus, following morphine withdrawal, α_{2A} function is desensitized in both SD and WKY rats.

WKY and SD Rats Exhibited Increased Anxiety-Like Behavior following Morphine-Dependence

We previously showed that morphine withdrawal increases anxiety-like behavior in SD rats (McElligott *et al*, 2013). To examine its impact on WKY rats, we assayed their behavior on the EPM. Withdrawal caused WKY rats to become more anxious, as they had reduced preference for the open arms compared with their saline-naloxone controls (unpaired *t*-test, Open/Closed time: 0.05±0.03 *vs* 0.39±0.12, *n*=8, respectively, *P*<0.01, Table 3.1). WKY rats treated with saline-naloxone did not demonstrate a change in open-arm preference relative to naïve animals (Table 3.2, pair-housed).

Social-Isolation Altered Norepinephrine Signaling in SD, but not WKY Rats

To further investigate differences between SD and WKY norepinephrine responses, we treated rats with chronic social isolation. This is a passive stressor that removes injection/handling stress, and is suggested to generate depression in rodents (Butler *et al*, 2014; Nestler and Hyman, 2010). Following 2 weeks of single-housing, rats were anesthetized and evoked norepinephrine was recorded. When comparing norepinephrine uptake between single (S) and pair (P)-housed animals, we found significantly slower uptake in SD-S rats compared with SD-P (2.3±0.09 s *vs* 1.7±0.10 s, *n*=20 and 26, respectively, *P*<0.001). However, WKY-S did not slow uptake relative to

pair-housed controls (1.6±0.06 s *vs* 1.6±0.12 s, *n*=21 and 22, respectively, *P*>0.05, Figure 3.6a).

We next compared α_{2A} drug effects between single and pair-housed animals, and found a main effect of housing (two-way ANOVA, BRL: F=24.12, *P*<0.0001; GFC: F=7.2, *P*<0.05) and a housing × strain interaction (BRL: F=8.2, *P*<0.01; GFC: F=5.4, *P*<0.05). *Post hoc* analysis revealed that BRL was less effective in increasing norepinephrine in SD-S animals as compared with SD-P (97±1.4% *vs* 158±11.9%, *n*=7, respectively, *P*<0.001, Figure 3.6b). Similarly, the decrease in release following GFC was attenuated in single-housed animals (91±3.2% *vs* 64±7.9%, *n*=7, respectively, *P*<0.01, Figure 3.3c). WKY-S failed to decrease drug response when compared with WKY-P rats (BRL: 124±8.9% *vs* 140±4.8%, *n*=7 respectively, *P*>0.05; GFC: 78±6.4% *vs* 76±2.2%, *n*=7, respectively, *P*>0.05).

Social Isolation Induces Anxiety-Like Behavior in SD Rats

We assayed anxiety-like behavior in singly housed animals on the EPM. Enclosed arm time showed a main effect of strain (two-way ANOVA, F=8.24, *P*<0.01) and a housing × strain interaction (F=4.89, *P*<0.05). Open arm time showed a main effect of housing (F=4.83, *P*<0.05). Total number of entries showed a main effect of strain (F=6.11, *P*<0.05), and the reduced number of WKY entries agrees with previous studies (Carr *et al*, 2010; Cohen *et al*, 2006). *Post hoc* analysis revealed a significant reduction in open arm preference in single-housed animals (Open time/Closed time: 0.33±0.09 *vs* 0.12±0.05, SD-S *vs* SD-P, *n*=8 and 7, respectively, *P*<0.05). WKY-S did not increase anxiety-like behavior relative to WKY-P rats (Table 3.2).

Coerulean Lesion Induced Noradrenergic Plasticity in SD Rats, but not WKY

As both morphine dependence and social stress can alter the firing rate of the LC (Chaijale *et al*, 2013; Van Bockstaele and Valentino, 2013), we wanted to mimic the effects of long-term LC inhibition on BNST norepinephrine and behavior. We lesioned coerulean norepinephrine terminals using the neurotoxin DSP-4, which reduces norepinephrine from LC but not medullary cells (Fritschy and Grzanna, 1989). The vBNST receives little LC input, and stimulation electrode placement in the ventral noradrenergic bundle targets axons primarily from A1/A2 cell groups. Not surprisingly, $[NE]_{max}$ was unchanged by DSP-4 treatment (SD: 219±37 nM *vs* 322±87 nM, *n*=7, and 6, respectively, *P*>0.05; WKY: 230±23 nM *vs* 239±19 nM, *n*=7 and 5, respectively, *P*>0.05). However, differences in synaptic function were found between vehicle and DSP-4-treated SD rats. Clearance half-life showed a strain × treatment interaction (F=9.5, *P*<0.01) and main effect of strain (F=13.2, *P*<0.005). DSP-4-treated SD rats had slower uptake than their controls (2.6±0.27 s *vs*1.6±0.15 s, *n*=7 and 8, respectively, *P*<0.01). WKY rats were unchanged (1.1±0.23 s *vs* 1.5±0.22 s, *n*=5 and 8, respectively, *P*>0.05, Figure 3.7a). Response to both BRL and GFC showed a strain × treatment interaction (two-way ANOVA, BRL: F=6.7, *P*<0.05; GFC: F=4.5, *P*<0.05), and main effect of treatment (BRL: F=11.9, *P*<0.01; GFC: F=5.8, *P*<0.05). *Post hoc* analysis revealed the response to BRL and GFC was blunted in DSP-4 treated SD rats (BRL: 100±5.3% *vs* 155±14.7%, *n*=5, respectively, *P*<0.05; GFC: 90±2.8% *vs* 64±7.9%, *n*=5 and 7, respectively, *P*<0.01) but not WKY rats (BRL: 130±6.4% *vs* 138±7.2% *n*=5, respectively, *P*>0.05; GFC: 80±3.8% *vs* 78±1.3% *n*=5, respectively, *P*>0.05, Figure 3.7c).

Coerulean Lesion Increased Anxiety-Like Behavior in SD Rats

The impact of DSP-4 lesioning on anxiety is dependent on dosage, recovery, and housing (Harro *et al*, 1995; Itoi *et al*, 2011; Lapiz *et al*, 2001). Our treatment increased anxiety-like behavior in SD rats, but not WKY rats as measured on the EPM. DSP-4-treated SD rats spent less time in the open arms, and more time in the enclosed arms (Open time/Closed time: 0.12±0.03 *vs* 0.26±0.01, n=8, DSP-4 *vs* saline, respectively, P<0.05. The number of entries was also reduced (6±2 *vs* 15±2, n=8, respectively, P<0.05). DSP-4-treated WKY rats did not show increased anxiety compared with controls (Table 3.2).

Discussion

Extracellular neurotransmitter concentrations are balanced by release and uptake processes (Wightman *et al*, 1988). Norepinephrine release is controlled by both cell firing and autoreceptor modulation, and the norepinephrine transporter is the primary clearance mechanism (Xu *et al*, 2000) with metabolism operating on a slower time scale (Near *et al*, 1988). Previously, we showed Lewis rats have hindered uptake, blunted autoreceptor function, and increased anxiety compared with SD rats (McElligott *et al*, 2013). When stressed with morphine withdrawal, Lewis rats showed no change in the regulation of BNST norepinephrine. This was in contrast to the dramatic alterations in norepinephrine clearance rate and autoreceptor function found in drug-dependent SD rats (McElligott *et al*, 2013). Here, we show that naïve SD and WKY rats are indistinguishable from each other with respect to evoked norepinephrine overflow, however, each strain diverges in their adaptations to stress. We found that following

morphine withdrawal, WKY rats were similar to SD rats with increased anxiety and attenuated autoreceptor function, however, norepinephrine uptake rate in WKY rats was unaltered. Additionally, BNST norepinephrine control mechanisms were unchanged in socially isolated WKY rats, whereas SD rats challenged with social isolation became more anxious and exhibited exacerbated norepinephrine signaling. Following lesions of norepinephrine in the LC, SD rats showed reduced norepinephrine control and increased anxiety, surprisingly similar to acute morphine dependence, but WKY rats were unaffected. Overall, we find WKY rats respond only to select stressors and that anxiety correlates with the degree of regulation of extracellular norepinephrine in the BNST.

The α_2 receptors are the primary adrenergic autoreceptors, and they show subtype-specific desensitization and phosphorylation by G-protein receptor kinases (Jewell-Motz and Liggett, 1996). As two subtypes of α_2 receptors are expressed in the BNST (Scheinin *et al*, 1994), we paired fast-scan cyclic voltammetry measurements with receptor-subtype-specific pharmacology to assay control over norepinephrine release by each subtype. Knock-out mice were used to determine that α_{2A} acts as the principle autoreceptor (Trendelenburg *et al*, 2001). In agreement with this, we found the inhibition of α_{2A} increased norepinephrine overflow in the vBNST to a similar extent in both rat strains. Although blockade of α_{2C} receptors did not increase norepinephrine overflow, α_{2C} inhibition generated a large alkaline flux following stimulated norepinephrine release, seen in Figure 3.1f as blue current just below norepinephrine peak oxidation potential. The α_{2C} receptors in the vBNST may therefore be positioned to regulate blood flow/metabolism in the vBNST (Bucher *et al*, 2014).

WKY rats exhibit reduced locomotion in an open field, limited exploration in the EPM, low baseline startle, and limited stress responsivity as compared with SD rats (Cohen *et al*, 2006; Pardon *et al*, 2002). Correspondingly, increases in extracellular norepinephrine in the BNST, evaluated by microdialysis, were greater in SD during restraint stress than WKY rats (Pardon *et al*, 2002). Following the stresses of both social isolation and morphine withdrawal, we found in SD rats that uptake and autoreceptor regulation are downregulated. The decreased noradrenergic control in SD rats could generate the comparatively larger increase in extracellular norepinephrine found with microdialysis. In WKY rats, morphine withdrawal produced only attenuated autoreceptor function, whereas social stress had no effect on norepinephrine control mechanisms. These limited adaptations would result in the smaller alteration in the level of extracellular norepinephrine induced by stress (Pardon *et al*, 2002). Importantly, cellular activation in the BNST during stress is similar between the two strains (Ma and Morilak, 2004). Thus, the greater norepinephrine overflow others have measured in stressed SD likely reflect the changes in uptake rate and desensitized autoreceptors revealed in this work.

Non-specific organic cation transporters (OCTs) are expressed throughout the BNST (Gasser *et al*, 2009). The high-capacity, low-affinity OCT3 is thought to act as a secondary means of norepinephrine clearance, and is inhibited by physiological levels of corticosterone (Gasser *et al*, 2006). The extent to which BNST norepinephrine is taken up by OCTs *in vivo* is not currently known, however, NET knockout mice still demonstrate catecholamine clearance in brain slices (Xu *et al*, 2000) relative to dopamine transporter knockouts (Giros *et al*, 1996), indicating this may be a significant

clearance mechanism for norepinephrine. Previously, we showed the altered norepinephrine clearance in SD rats following withdrawal was not due to decreased NET binding sites (McElligott *et al*, 2013). Instead, stress-induced corticosterone release may inhibit OCT3 and reduce clearance rate. WKY rats have elevated peak diurnal levels of corticosterone relative to SD rats (Rittenhouse *et al*, 2002), which may eliminate any OCT3 component of norepinephrine uptake because of chronic inhibition. In addition, WKY rats exhibit behavioral sensitivity to the NET inhibitor desipramine (López-Rubalcava and Lucki, 2000), highlighting the importance of NET in WKY rats. The unaltered norepinephrine uptake in WKY rats corresponds with their low stress responsivity, and is likely the result of HPA axis dysfunction.

Social stressors promote drug self-administration and escalation, generate a long-lasting tolerance to opiate analgesia, and are as efficacious as physical stress at reinstating morphine place preference (Butler *et al*, 2014; Miczek *et al*, 2004; Ribeiro Do Couto *et al*, 2006). Exposure to stressful life events and HPA axis dysfunction have been implicated in the development of several psychiatric disorders that are comorbid with addiction, however, stress alone is not sufficient for their development (Faravelli *et al*, 2012). It has been suggested that stress can interact with genetic vulnerabilities in predisposed individuals to create the psychopathology. Valentino and coworkers (Chaijale *et al*, 2013) found stress activation of the endogenous opioid system sufficient to generate a cellular opiate dependence in SD rats. Here, we used chronic social isolation, a passive stressor suggested to induce depression and anxiety in rodents (Butler *et al*, 2014; Nestler *et al*, 2010). Remarkably, after SD rats were socially isolated for 2 weeks, they resembled morphine-dependent SD rats, with increased anxiety and

enhanced noradrenergic signaling in the vBNST. Moreover, following social isolation, SD rats anxiety and norepinephrine regulation resembled that of our previous work in Lewis rats (McElligott *et al*, 2013) , a model of increased drug-intake and PTSD (Cohen *et al*, 2006; Picetti *et al*, 2012; Sánchez-Cardoso *et al*, 2007). In stark contrast, we found that WKY rats were unresponsive to social isolation, exhibiting no changes in anxiety-like behavior or norepinephrine signaling relative to their controls. These results support the idea that genetic differences can predispose individuals to psychological disorders or addictions, as their noradrenergic system may already resemble a drug-dependent or anxious state. Additionally, individuals with anxiety or depression may not be able to appropriately adapt to stress because of low responsivity of the noradrenergic system.

During stress, LC activity is tuned by a balance of CRF excitation, and endogenous opioid inhibition (Van Bockstaele *et al*, 2013), and chronic stress can decrease LC discharge rates (Chaijale *et al*, 2013). The BNST receives a small input from the LC (Forray *et al*, 2004), and its activation may be influenced by altered coerulean discharge rates following stress. Thus, we chose to mimic stress-induced LC inhibition by lesioning it with the potent and selective neurotoxin DSP-4. DSP-4 induces degradation of norepinephrine axons arising from the LC, while leaving brainstem norepinephrine innervation intact (Fritschy *et al*, 1989). The behavioral effects of DSP-4 treatment are variable (Harro *et al*, 1995; Itoi *et al*, 2011; Lapiz *et al*, 2001), and in our study, we found an anxiogenic effect in SD rats with no change in WKY rats relative to their respective controls. This LC inhibition also lowered the number of maze entries SD rats made to that of WKY. Surprisingly, the DSP-4 treatment produced a robust,

dependence-like phenotype in the BNST norepinephrine regulation of SD rats. Such a response was not expected owing to the limited LC innervation of the BNST. These results may reflect feedback between the two main sources of central noradrenergic innervation through a common afferent (Van Bockstaele *et al*, 2013) and should be a point of future study. Cross-talk between noradrenergic inputs is supported by work demonstrating the importance of both medullary and coerulean norepinephrine in mediating the aversiveness (Delfs *et al*, 2000) and somatic withdrawal signs of withdrawal (Maldonado, 1997). Importantly, LC activation during opiate withdrawal is partly a result of excitatory input from the nucleus paragigantocellularis, a structure that innervates the nucleus of the solitary tract (A2). Following DSP-4 treatment, we found no change in norepinephrine regulation in WKY rats, similar to WKY rats exposed to social isolation stress. However, WKY rats were responsive to morphine withdrawal, the aversiveness of which is due to medullary norepinephrine (Delfs *et al*, 2000). WKY rats overexpress kappa opioid receptors in the LC, leaving the LC in a chronically inhibited state (Carr *et al*, 2010), a possible explanation for the low number of maze entries and lack of DSP-4 response. This persistent inhibition may attenuate any excitatory influence of CRF and partially explain the lack of noradrenergic facilitation to social isolation. Overall, these results suggest a plasticity of medullary inputs but not LC inputs in the BNST of WKY rats.

We have shown that certain stressors permit exacerbated BNST signaling that is accompanied by increased anxiety. Furthermore, we showed the signaling changes coincide with α_{2A} receptor function and are dependent on rat strain. Social isolation and persistent coerulean inhibition caused dramatic changes in the SD rat, and generated a

morphine-dependence-like phenotype. WKY rats were unresponsive to both social isolation and DSP-4 treatment. Following morphine withdrawal, they demonstrated increased anxiety and an intermediate change in norepinephrine signaling: decreased α_{2A} function without a change in norepinephrine clearance. Taken together, this differential responsivity may reflect separate noradrenergic mechanisms for adaptation that depend on the stressor or its intensity. Moreover, our data support the idea that genetic factors contribute to stress response, which may in turn generate cellular conditions that favor drug use and future substance abuse issues.

Support

We acknowledge support from the UNC Electronics Facility. This research was supported by an NIH grant to RMW. (NS 015841).

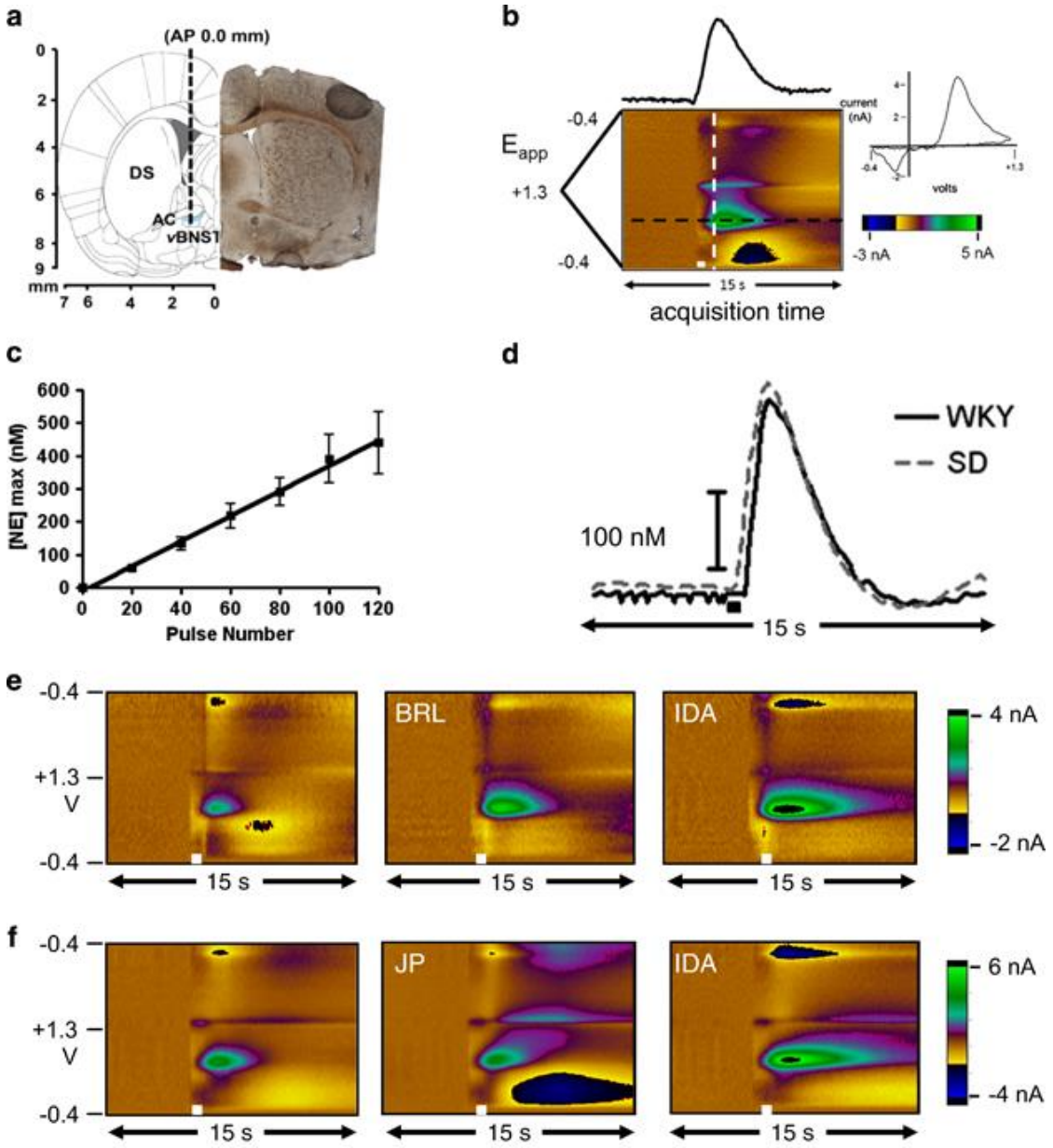

Figure 3.1: Fast-Scan Cyclic Voltammetry of norepinephrine in the vBNST. (a) Electrode tract (dashed line) and representative histology of carbon-fiber electrode placement in the vBNST (dashed circle; DS, dorsal striatum; AC, anterior commissure). (b) Norepinephrine measured in the vBNST after electrical stimulation (white bar). The cyclic voltammogram (current vs potential) is obtained from the white dashed line, and the concentration vs time trace from the black dashed line. (c) Input-output curve of [NE]max at 20, 40, 60, 80, and 120 stimulation pulses in WKY rats. (d) Representative concentration traces comparing norepinephrine release and uptake in SD and WKY rats. (e and f) Representative color plots of electrically evoked norepinephrine in the vBNST with α2A (BRL), α2C (JP), and non-selective α2 (IDA) antagonists on board in WKY rats.

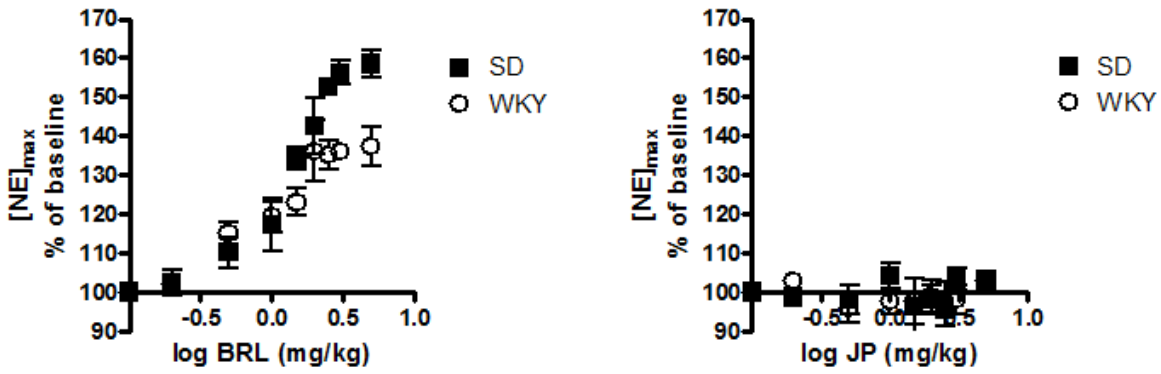

Figure 3.2: Norepinephrine release as a percent of baseline after 0.2 – 5 mg/kg (A) BRL-44408 and (B) JP-1302 in SD (black squares) and WKY (open circles) rats.

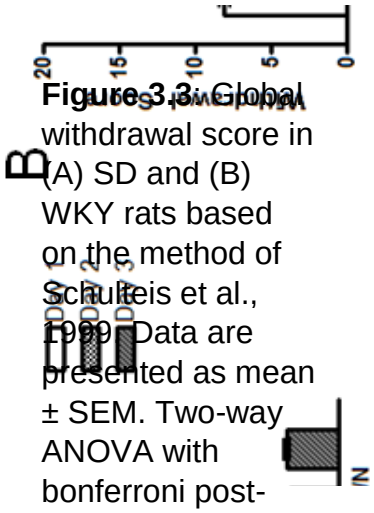

Figure 3.3: Global withdrawal score in (A) SD and (B) WKY rats based on the method of Schulteis et al., 1999. Data are presented as mean ± SEM. Two-way ANOVA with bonferroni post-hoc analysis: ***, P<0.005

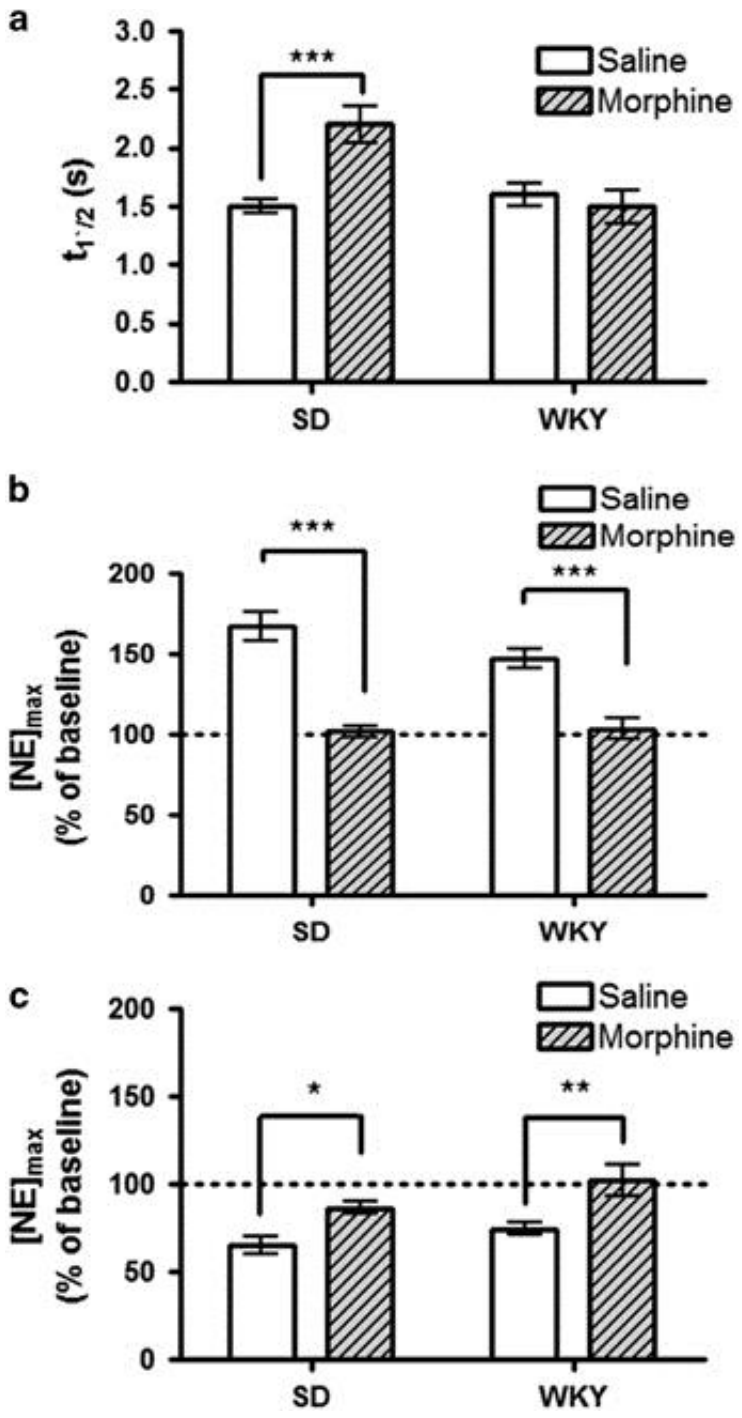

Figure 3.4: The effects of morphine dependence in Sprague-Dawley and Wistar-Kyoto rats. (a) Average norepinephrine clearance as measured by t1/2. (b and c) Average evoked norepinephrine ([NE]max) following administration of 2 mg/kg BRL-44408 (b), or guanfacine (GFC) (c) relative to pre-drug stimulated release. Data are presented as mean ± SEM. Bonferroni post hoc analysis: *P<0.05, **P<0.01, ***P<0.005.

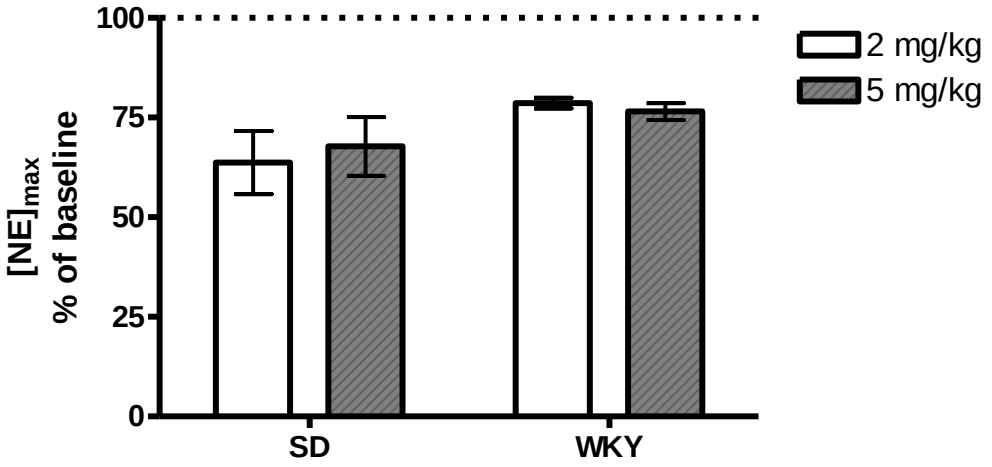

Figure 3.5: Norepinephrine response as a percent of pre-drug baseline to 2 and 5 mg/kg GFC in SD and WKY rats.

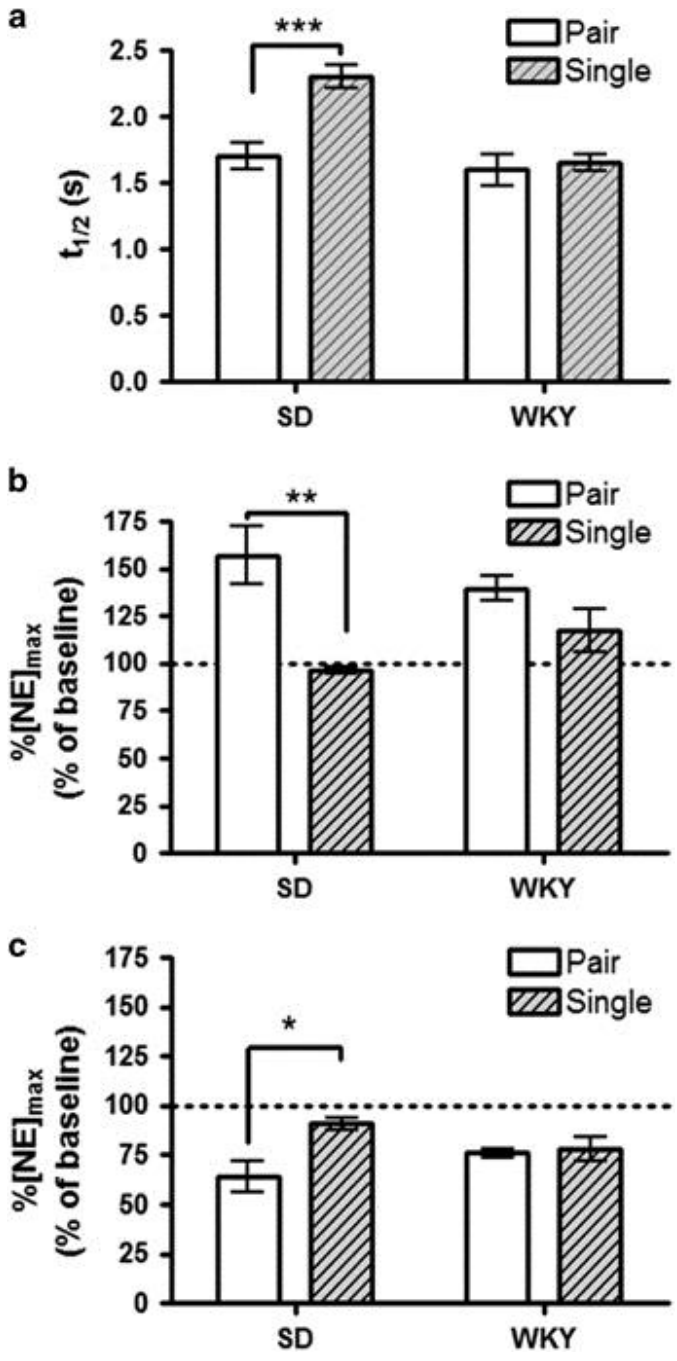

Figure 3.6: The effects of social isolation in Sprague-Dawley and Wistar-Kyoto rats. (a) Average norepinephrine clearance as measured by t1/2. (b and c) Average evoked norepinephrine ([NE]max) following administration of 2 mg/kg BRL-44408 (b), or guanfacine (GFC) (c) relative to pre-drug stimulated release. Data are presented as mean ± SEM. Bonferroni post hoc analysis: *P<0.05, **P<0.01, ***P<0.005.

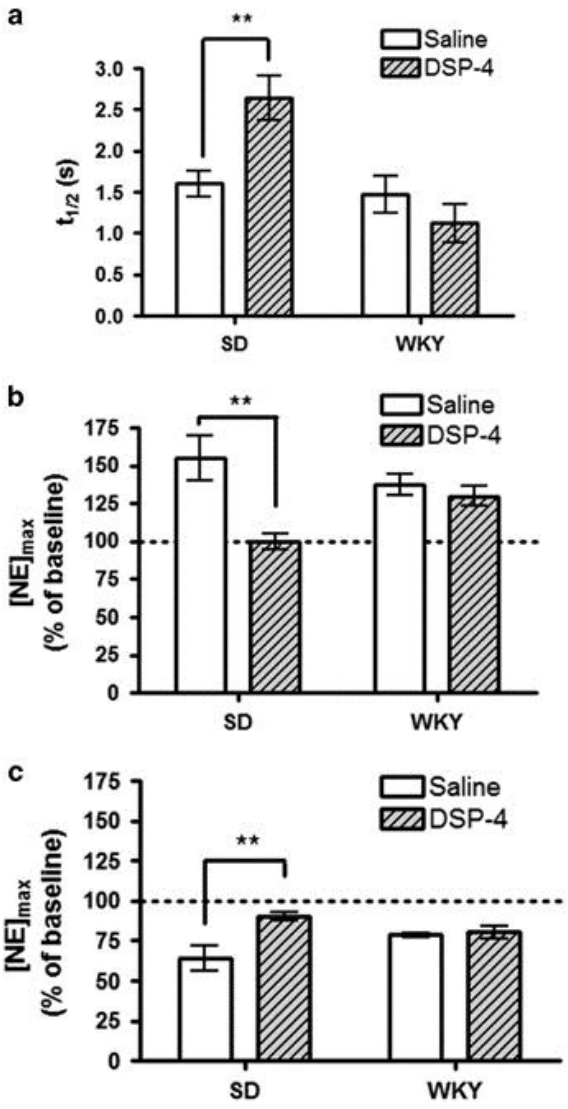

Figure 3.7: The effects of coerulean lesioning in Sprague-Dawley and Wistar-Kyoto rats. (a) Average norepinephrine clearance as measured by t1/2. (b and c) Average evoked norepinephrine ([NE]max) following administration of 2 mg/kg BRL-44408 (b) or guanfacine (GFC) (c) relative to pre-drug stimulated release. Data are presented as mean ± SEM. Bonferroni post hoc analysis: **P<0.01.

Morphine dependence	Open/Closed time	Entries	Open time	Closed time
Wistar-Kyoto				
Saline-Naloxone (*n*=8)	0.39±0.12	6±1	22±4 s	76±14 s
Morphine-Naloxone (*n*=8)	0.05±0.03*	6±1	6±3 s*	126±24 s

Table 3.1. Anxiety-like Behavior Following Morphine Withdrawal in WKY Rats. Total number of entries and time spent in the open and enclosed arms of the elevated plus maze was evaluated. An animal's preference for open arms was expressed as a ratio of open-arm time over closed-arm time. Data are presented as mean ± SEM. Treated WKY were compared with their controls using an unpaired t-test. Starred values denote significance between the treated group and the control directly above it. *P<0.05.

	Open/Closed time	Entries	Open time	Closed time
Social isolation				
Sprague-Dawley				
Pair-housed (*n*=7)	0.33±0.09	14±1	49±11 s	163±10 s
Single-housed (*n*=8)	0.12±0.05*	12±2	20±7 s*	201±12 s*
Wistar-Kyoto				
Pair-housed (*n*=8)	0.26±0.06	9±2	38±8 s	156±10 s
Single-housed (*n*=8)	0.23±0.04	9±1	32±6 s	148±9 s
Coerulean Lesioning				
Sprague-Dawley				
Saline (*n*=8)	0.26±0.01	15±2	47±6 s	165±8 s
DSP-4 lesioned (*n*=8)	0.12±0.03*	6±2*	25±6 s*	207±15 s*
Wistar-Kyoto				
Saline (*n*=8)	0.17±0.05	6±1	25±8 s	162±8 s
DSP-4 lesioned (*n*=7)	0.13±0.03	7±3	24±4 s	193±14 s

Table 3.2: Anxiety-like Behavior Following Differing Stressors.Total number of entries and time spent in the open and enclosed arms of the elevated plus maze was evaluated. An animal's preference for open arms was expressed as a ratio of open-arm time over closed-arm time. Data are presented as mean ± SEM. Treated animals were compared with their controls using a two-way ANOVA with Bonferroni *post hoc* analysis. Differences in anxiety following stress were determined for each strain by comparing treated animals with their respective controls. Starred values denote significance between the treated group and the control directly above it. *P<0.05.

CHAPTER 4: RECIPROCAL CATECHOLAMINE CHANGES DURING OPIATE EXPOSURE AND WITHDRAWAL

Introduction

Considerable evidence indicates forebrain catecholamine circuits become dysregulated during the development of addiction (Koob *et al*, 2010). The risk for addiction varies greatly following drug exposure, and repeated use causes lasting neural adaptations which converge with stress to increase the risk for relapse long after drug cessation (Hyman *et al*, 2009; Nestler, 2001; Sinha, 2008). The allostasis model describes the transition from drug use to drug-abuse as a switch from impulsive to compulsive drug taking, where positively reinforced behavior dominates early in the addiction cycle, and over time, emergence of withdrawal-induced dysphoria drives negatively reinforced drug use (Koob *et al*, 2010).

Mesolimbic dopamine modulates motivation and reward, and is implicated in the positively reinforced components of addiction. Drugs of abuse have diverse actions on dopaminergic signaling, particularly in the ventral tegmental area (VTA) and its afferents (Juarez and Han, 2016). Increased VTA dopamine transmission is thought to aid associative memory formation and drive cue-induced drug seeking (Berke and Hyman,

2000; Everitt and Robbins, 2005; Hyman *et al*, 2006). Action potentials from the VTA drive transient dopamine concentration fluctuations in the nucleus accumbens (NAc) (Sombers *et al*, 2009) that increase following drug of abuse and potentiate a drug's reinforcing properties (Covey *et al*, 2014). NAc dopamine also encodes information about negative events, as overflow is suppressed during tail-pinch delivery (Park *et al*, 2015) and aversive tastants decrease NAc dopamine transients (Roitman *et al*, 2008; Twining *et al*, 2015). Drug withdrawal is aversive, and although basal dopamine levels decrease during withdrawal (Pothos *et al*, 1991; Weiss *et al*, 1996), previous work does not address its effect on transient dopamine concentrations. Since increased and decreased dopamine signaling contribute to the addiction cycle (Koob *et al*, 2010), it is important to investigate adaptations in real-time.

Although dopamine has been the main catecholamine studied in addiction, norepinephrine also mediates drug reward (Olson *et al*, 2006) and withdrawal-aversion (Delfs *et al*, 2000). Suppression of noradrenergic signaling blocks stress-induced reinstatement (Erb *et al*, 2000; Leri *et al*, 2002; Shaham *et al*, 2000), and clonidine treatment promotes heroin-abstinence in human addicts (Kowalczyk *et al*, 2015). In the allostasis model, drug withdrawal engages the extended amygdala to produce dysphoria and advance the addiction cycle (Koob *et al*, 2010). The bed nucleus of the stria terminalis (BNST) is an important relay in the extended amygdala and a target of norepinephrine's actions in opiate intoxication/withdrawal (Aston-Jones *et al*, 1999). The ventral BNST receives dense innervation from the nucleus of the solitary tract (NTS) (Forray *et al*, 2004), the source of norepinephrine critical for morphine-reward (Olson *et al*, 2006) and withdrawal-aversion (Delfs *et al*, 2000). Chronic morphine increases basal

norepinephrine in the BNST (Fuentealba *et al*, 2000), however no work addresses phasic release. Moreover, stress-dependent adaptations in vBNST noradrenergic signaling arise following morphine-dependence (Fox *et al*, 2015; McElligott *et al*, 2013), yet the source of this plasticity is unknown.

Many studies focus on chronic drug administration (Harris and Aston-Jones, 1994; Hemby *et al*, 1995; Kaufling and Aston-Jones, 2015; Mazei-Robison and Nestler, 2012), however it is unknown how a single drug exposure paired with withdrawal influences catecholamine signaling to advance the addiction cycle. Since appetitive and aversive stimuli elicit opposing responses from catecholamines (Park *et al*, 2012; Roitman *et al*, 2008; Twining *et al*, 2015), we hypothesized dopamine and norepinephrine signal reciprocally during drug intoxication/withdrawal to prime the system for addiction. We used voltammetry to measure catecholamine release in freely moving animals exposed to morphine and naloxone-precipitated withdrawal. During drug exposure, dopamine signaling increased in the NAc but morphine did not elicit norepinephrine in the vBNST. Conversely, drug withdrawal produced vBNST norepinephrine release that coincided with specific withdrawal symptoms and suppressed NAc dopamine transients. Finally, vBNST norepinephrine, but not NAc dopamine, was attenuated after morphine/naloxone treatment. These data provide a real-time view of catecholamine signaling during exposure/withdrawal and lend insight to how catecholamine circuits become dysregulated during the development of addiction.

Materials and Methods

Animal Care

All experiments were performed in accordance with the Institutional Animal Care and Use Committee guidelines of the University of North Carolina at Chapel Hill (UNC). Sprague-Dawley rats (males, 270-350 g; Charles River, Wilmington, MA) were given food and water *ad libitum* and pair-housed in UNC animal facilities on a 12:12-hour light:dark cycle until surgery. We selected 6-7 animals per group, which is typical of voltammetric studies. Animals with misplaced electrodes were excluded from the study, as well as animals that exhibited mixed pharmacological response (See Fig 4.7). A total of 14 animals were included for dopamine measurements (7 Morphine, 7 Vehicle), and 26 for norepinephrine measurements (7 Morphine, 7 Vehicle, 6 Morphine +Idazoxan, 6 Vehicle + Idazoxan). All measurements took place during the light cycle.

Sterotaxic Surgery

Animals were anesthetized with isofluorane (4% induction, 1.5% maintenance) and affixed in a stereotaxic frame (Kopf Instruments). The scalp was removed and holes were drilled to implant guide cannulas in the right hemisphere (BASi, West Lafayette, IN) above the NAc shell (AP: +1.7 mm, ML: 0.8 mm) or vBNST (AP: 0 mm, ML: 1.2 mm), referenced from bregma and based on the atlas of Paxinos and Watson. An additional guide cannula was implanted in the left hemisphere for insertion of a Ag/AgCl reference electrode on the day of recording. A bipolar stimulating electrode (Plastics One, Roanoke, VA) was targeted to the right VTA/ventral noradrenergic bundle (VNB; AP -5.2mm, ML +1.0, DV 8.2 mm), and a dental cement skull-cap was secured with

jeweler's screws. Animals were subsequently singly housed and allowed to recover for 3-days before making measurements.

Voltammetric Catecholamine Measurements

Fast scan cyclic voltammetry (FSCV) measurements of dopamine and norepinephrine were performed in awake animals as described previously (Park *et al*, 2013). Briefly, a fresh carbon-fiber electrode (~100 µm active length) was lowered into the NAc shell or vBNST through the guide cannula with a custom-built micromanipulator. A triangular waveform (-0.4 to +1.3V, 400V/s) was applied to the electrode every 100 ms to oxidize and reduce catecholamines using HDCV for data acquisition and analysis (Bucher *et al*, 2013). After electrode placement, we recorded baseline signaling for ~10 min before giving 10 mg/kg morphine sulfate s.c. (Sigma-Aldrich, St. Louis, MO) or 1 mL/kg vehicle (saline 0.9%). 4h later, we administered 1 mg/kg naloxone HCl s.c. (Sigma-Aldrich) and scored animals for somatic indices of withdrawal (Schulteis *et al*, 1999) over 20 min. In a subset of animals, 5 mg/kg idazoxan was given with naloxone to enhance norepinephrine overflow. 1h after naloxone administration, animals were anesthetized with urethane (1.5 g/kg), and the VTA/VNB was electrically stimulated using constant current isolators (Neurologs, model NL800) to obtain voltammograms for principal component analysis (PCA)(Rodeberg *et al*, 2015). We extracted dopamine currents using PCA and converted current to concentration using an averaged in vitro calibration factor (10 nA/µM). Only dopamine transients >3 times the noise in the traces obtained by PCA were considered to be dopamine transients, and we measured increased dopamine transient frequency during the first hour of morphine administration. In awake animals, voltammetric peaks for

norepinephrine release in the vBNST were broader than expected. We suspect contribution from a noradrenergic metabolite during withdrawal because these features were mimicked in anesthetized rats with long stimulations and were eliminated following clorgyline. For this reason, we do not report norepinephrine concentrations but rather report voltammetric currents. When applicable, an averaged *in vitro* calibration factor (6 nA/μM) was used to convert norepinephrine current to concentration in anesthetized animals.

vBNST Pharmacology

At the end of awake-animal recordings, we confirmed that the signal in the vBNST was due to norepinephrine and not dopamine by measuring electrically-evoked release after 2 mg/kg s-(-)-raclopride tartrate (D2 antagonist, Sigma-Aldrich) and 5 mg/kg idaxoxan HCl (α_2 antagonist, Sigma Aldrich). Only signals that responded to idazoxan but not raclopride were classified as norepinephrine release. Signals with mixed pharmacological response were excluded as in Figure 4.7. In three separate anesthetized animals, we delivered long, lower frequency stimulations (30 Hz, 120 pulses) to the VNB to mimic the signals recorded in awake animals undergoing withdrawal. After collecting baseline release, we administered the monoamine oxidase inhibitor, clorgyline (Sigma-Aldrich, 75 mg/kg i.p.) and measured narrowed oxidative peaks at +0.6V.

Somatic Withdrawal Signs

Behavioral correlates of opiate withdrawal were measured during the first 20 min of precipitated withdrawal and assigned a global withdrawal score as described previously (McElligott *et al*, 2013; Schulteis *et al*, 1999). We manually assigned time-

stamps to each behavior and looked for presence or absence of dopamine transients or norepinephrine overflow during the withdrawal signs. Somatic withdrawal signs were either considered absent, present, or present with catecholamine signaling.

Statistics

All statistical tests were performed in Graph Pad Prism. 2-way, repeated measures analysis of variance (RM-ANOVA) with Bonferroni post-hoc were used to assess differences in dopamine transient frequency and concentration under varying drug conditions. Unpaired, Welch's corrected t-tests were used to determine significant differences between the number and magnitude of norepinephrine release events, due to significant differences in the variance between morphine- and vehicle-treated groups.

Results

Morphine-intoxication increases dopaminergic transmission in the nucleus accumbens

Drugs of abuse increase dopaminergic transmission in the NAc (Bossong *et al*, 2009; Cheer *et al*, 2007b; Di Chiara and Imperato, 1988; Phillips *et al*, 2003; Volkow *et al*, 2007), which contributes to their acutely reinforcing properties. We used a dose of morphine that, when paired with precipitated withdrawal, generates rapid dependence in rats (Schulteis *et al*, 1999). To confirm morphine's effect on dopamine in the NAc of freely moving rats (Vander Weele *et al*, 2014), we used voltammetry to record dopamine transients in locations exhibiting spontaneous activity (~2 transients min^{-1}; schematic of placement and time line in Fig 4.1A). We found that morphine increased spontaneous dopamine transient frequency in the NAc (MRP, 10 mg/kg s.c.) relative to saline (VEH, 1 mL/kg s.c.) (9.9 ± 1.5 vs. 2.1 ± 0.5 transients min^{-1}, MRP vs. VEH, n=7, respectively, t=4.976, P=.0016, Fig 1D), but the average concentration per transient

was similar under both conditions (MRP: 77.3 ± 7 vs. VEH: 72.1 ± 7 nM, *N*=7, respectively, Fig 1E).

Naloxone-precipitated withdrawal decreases dopaminergic transmission in the nucleus accumbens

We next examined the impact of drug withdrawal by administering naloxone (NAL, 1 mg/kg s.c.) 4h after initial morphine (Fox *et al*, 2015; McElligott *et al*, 2013; Schulteis *et al*, 1999). We recorded dopamine transients during the peak of somatic withdrawal signs and found decreased dopamine transient frequency in animals undergoing withdrawal relative to the initial treatment (MRP-NAL: 2.3 ± 0.5, VEH-NAL: 1.1 ± 0.1 transients min^{-1}, respectively, *N*=7, respectively, 2-way RM ANOVA; Treatment group x NAL Interaction $F(1,12)= 22.60$, $P=0.0005$; MRP treatment $F(1,12)=23.06$, $P=0.0004$, NAL treatment $F(1,12)= 40.30$, $P<0.0001$. Bonferroni post-hoc, $P<0.001$). Moreover, dopamine transient concentrations decreased during withdrawal (MRP-NAL: 57.6± 4 vs. VEH-NAL: 71.9 ± 8 nM, *N*=7, respectively. 2-way RM ANOVA; Treatment group x NAL interaction $F(1,12)= 9.667$, $P= 0.0090$, NAL $F(1,12)=10.3$, $P=0.0075$, Bonferonni post-hoc, $P<0.01$), reflecting decreased dopaminergic output. To test for adaptations after precipitated withdrawal, we anesthetized the animals and electrically stimulated the VTA. We found equivalent evoked dopamine in MRP-NAL and VEH-NAL-treated animals (1.28 ± .37 vs. 0.96 ± 0.31 µM *N*=7, respectively, $t=0.6634$, $P= 0.5196$), in agreement with previous findings of unchanged tissue content (McElligott *et al*, 2013). Similar to rewarding and aversive stimuli (Roitman *et al*, 2008), NAc dopamine signaling increased during morphine

intoxication and decreased during withdrawal; however, acute exposure/withdrawal was insufficient to elicit persistent adaptations.

Morphine-withdrawal, but not intoxication, elicits norepinephrine in the ventral bed nucleus of the stria terminalis

Norepinephrine's role in drug addiction is often overshadowed by dopamine, despite evidence that morphine reward is contingent on brainstem norepinephrine synthesis (Olson *et al*, 2006). Moreover, opiate-withdrawal aversion requires forebrain norepinephrine (Delfs *et al*, 2000), and morphine-dependence alters noradrenergic synaptic function (Fox *et al*, 2015; McElligott *et al*, 2013). We thus measured norepinephrine release in the vBNST during morphine exposure and withdrawal (schematic in Fig 4.2A). Unlike dopamine, norepinephrine concentrations in the vBNST do not fluctuate spontaneously in animals at rest, and morphine did not elicit norepinephrine overflow in the vBNST despite receiving dense projections from the NTS (Fig 4.2B). However, we observed broad norepinephrine release events during naloxone-precipitated withdrawal (Fig 4.2B). Norepinephrine release persisted for tens of seconds, in contrast to brief (~1 sec) dopamine transients recorded in the NAc. Voltammetric peaks for norepinephrine were also broader than expected, and we suspect contribution from a noradrenergic metabolite during withdrawal (Fig 4.3). Naloxone elicited norepinephrine release in some vehicle-treated animals, and release amplitudes did not differ between groups (MRP-NAL: 1.1 ± 0.1 nA, N=21 events vs VEH-NAL: 1.7 ± 0.5 nA N=3 events, t=1.669, P=0.1093, Fig 4.4E). However, the occurrence of norepinephrine release events was greater in animals undergoing morphine withdrawal relative to vehicle (MRP-NAL: 3.0 ± 0.5 vs VEH-NAL: 0.4 ± 0.2

events per animal, *N*=7, respectively; *t*=4.5, *P*=0.0028, Fig 4.4D). We next assayed norepinephrine release evoked by electrical stimulation of the VNB and found significant attenuation in animals following withdrawal (0.047 ± 0.011 vs. 0.218 ± 0.053 µM, *N*=7; *t*=3.115, *P*=0.0207, Fig 4.4F), aligning with tissue content findings (McElligott *et al*, 2013).

Catecholamine signaling differs during expression of withdrawal-related behaviors

Somatic withdrawal signs like teeth-chattering and eye-twitches are a hallmark of opiate withdrawal in rats (Schulteis *et al*, 1999). To determine if catecholamine overflow was associated with withdrawal symptoms, we recorded the timing of somatic indices and looked for concurrent dopamine or norepinephrine release. Morphine withdrawal decreased the frequency of dopamine transients, and transients 'paused' during certain behaviors (e.g. swallowing-movements, Fig 4.5A) before resuming after termination of the withdrawal sign. Dopamine release did not pause during spontaneous erection/ejaculation/penile grooming (EEP) in animals exhibiting the behavior (Fig 4.4B, 4.5C). Norepinephrine release occurred with swallowing movements (SM) and teeth-chattering (TC) in all morphine-withdrawn animals (Example in Fig 4.4C, Fig 4.5B), and in one VEH-NAL animal. Importantly, naloxone treatment produced global withdrawal scores similar to our previous reports (Fox *et al*, 2015; McElligott *et al*, 2013), and scores were significantly higher in morphine-withdrawn animals (Fig 4.5A, 2-way ANOVA, Bonferroni Post-hoc: Main effect of MRP $F(1,12) = 57.65$, $P<0.0001$. DA: MRP-NAL, 5.7± 1.0 vs. VEH-NAL, 2.0 ±0.5; NE: MRP-NAL, 7.2 ± 0.5 vs. VEH-NAL, 1.0 ± 0.4 *N*=7, respectively). To further investigate the link between norepinephrine release and somatic withdrawal signs, we administered the α_2 antagonist idazoxan with naloxone to

elicit additional norepinephrine overflow. Systemic α_2 antagonism elicited norepinephrine in VEH-NAL animals, resembling MRP-NAL, and was accompanied by withdrawal-associated behaviors in the absence of morphine (Fig 4.6).

Discussion

These findings establish that a single exposure to morphine, followed by precipitated withdrawal, elicits distinct signaling in brain regions associated with the addiction cycle. Dopaminergic signaling increased in the NAc during intoxication and decreased during withdrawal, but the single exposure did not alter evoked dopamine. Conversely, only morphine withdrawal elicited norepinephrine release in the vBNST, but acute exposure and withdrawal attenuated stimulated release. Norepinephrine release tracked two withdrawal-associated behaviors and was induced without morphine by α_2 antagonism. The combination of decreased dopamine output and recruitment of noradrenergic signaling revealed in this work suggests the negative reinforcement model of addiction begins working after a single exposure.

Drugs of abuse increase dopamine overflow in the NAc (Cheer *et al*, 2007b; Daberkow *et al*, 2013; Phillips *et al*, 2003), which helps drive their acutely reinforcing properties, and a recent study showed intravenous morphine administration produces similar efflux (Vander Weele *et al*, 2014). We gave morphine s.c. since i.v. catheters require rats to be singly housed and social-isolation produces a stress profile similar to morphine-addicted rats (Fox *et al*, 2015). We found dopamine transients increased in frequency for a much longer duration (>60 min) than in (Vander Weele *et al*, 2014). This could be due to differences in baseline stress, or might arise from the slower time-course of drugs delivered s.c. compared with i.v. Regardless, both methods of morphine

administration increased dopamine overflow in the NAc, confirming its actions on the mesolimbic dopamine system. When animals underwent naloxone-precipitated withdrawal, dopamine transients appeared to 'pause' during somatic withdrawal signs, and decreased in both frequency and magnitude in the MRP/NAL treated group. This effect was not solely due to naloxone, because transient concentrations only decreased in animals exposed to morphine. Withdrawal symptoms were most apparent during pauses in dopamine transients. Consistent with this, activation of D2 receptors in the NAc attenuates withdrawal symptoms (Harris *et al*, 1994). Additionally, the decrease in dopamine transients during naloxone aligns with studies on reduced basal dopamine concentrations during withdrawal (Pothos *et al*, 1991; Weiss *et al*, 1996). Decreased dopaminergic output supports the allostasis model (Koob *et al*, 2010) and likely contributes to the withdrawal-induced negative affect.

The role of norepinephrine in drug addiction is often overshadowed by that of dopamine (Weinshenker and Schroeder, 2006), despite evidence that brainstem norepinephrine synthesis is crucial for establishing morphine self-administration (Davis *et al*, 1975) and conditioned place preference (Olson *et al*, 2006). The vBNST receives dense noradrenergic projections from the nucleus of the solitary tract (NTS) (Forray *et al*, 2004), and thus is a likely downstream target for norepinephrine's actions in morphine reward. Surprisingly, we did not detect norepinephrine release in the vBNST during morphine, although it is possible elevated norepinephrine in the BNST develops after chronic drug exposure (Fuentealba *et al*, 2000). Alternatively, the NTS projects to a number of brain regions, including the VTA and NAcsh, where it may regulate dopaminergic activity (Moore and Bloom, 1979) to drive reinforcement and reward.

BNST norepinephrine is traditionally implicated in the aversive aspects of opiate-withdrawal (Aston-Jones *et al*, 1999), and its regulation of the hypothalamic-pituitary-adrenal axis (Forray *et al*, 2004) positions it to integrate the stressful and negative aspects of drug addiction. Indeed, direct infusion of adrenergic antagonists into the BNST suppresses stress-induced reinstatement of drug seeking and conditioned place preference (Leri *et al*, 2002; Wang *et al*, 2001), and three days of morphine paired with withdrawal produces noradrenergic plasticity in the vBNST (McElligott *et al*, 2013). When we induced withdrawal with naloxone, we found robust norepinephrine release in the vBNST that coincided with somatic withdrawal behaviors. In particular, norepinephrine was linked with swallowing movements and the neurons responsible for this reflex are located in the NTS (Kessler and Jean, 1985). In some vehicle-treated animals, norepinephrine was released after administration of naloxone. We believe this to be a result of removing endogenous opiate tone, as some withdrawal signs were also noted in VEH-NAL animals. Norepinephrine release in the VEH-NAL group could also arise due to injection stress, and the split population in control animal response could reflect differences in baseline stress-reactivity. Regardless, the occurrence of release events was much greater in animals undergoing withdrawal relative to control. Additionally, when the α_2 antagonist idazoxan was given with naloxone, both norepinephrine overflow and withdrawal behaviors were elicited in the absence of morphine, highlighting its role in withdrawal-aversion. Interestingly, releasable norepinephrine concentrations were depleted after withdrawal, reflecting signaling adaptations after the first withdrawal episode. This effect is consistent with previous work showing reduced norepinephrine tissue content in the vBNST after repeated

morphine-withdrawal (McElligott *et al*, 2013). Overall, these data support links between norepinephrine overflow and withdrawal symptoms, and provide mechanistic insight for adrenergic receptor therapy in treating human addicts (Kowalczyk *et al*, 2015). Moreover, the norepinephrine release during withdrawal uncovered here is the likely source of adrenergic receptor plasticity in the vBNST (McElligott *et al*, 2013).

Dopamine and norepinephrine exhibit opposing responses to rewarding and aversive stimuli. Oral infusion of an appetitive tastant produces enhanced dopamine (Park *et al*, 2012; Roitman *et al*, 2008), whereas aversive tastants attenuate dopamine release and increase norepinephrine signaling. This effect is also seen in animals undergoing reward learning and its extinction (Park *et al*, 2013), and during presentation of a painful stimulus (Park *et al*, 2015). Reciprocal catecholamine signaling has interesting implications in the context of the aversive stimulus of drug withdrawal, due to norepinephrine's potential influence on dopaminergic signaling. Glutamatergic inputs from the vBNST exert strong excitatory influence over VTA dopamine neurons (Georges *et al*, 2002), and norepinephrine's actions through α_{2A} receptors decrease excitatory transmission in the vBNST (Egli *et al*, 2004). Thus, norepinephrine release during withdrawal may act through α_2 receptors in the vBNST to suppress VTA activity and decrease dopaminergic output as a consequence. Indeed, activation of α_2 receptors with clonidine suppresses dopamine concentrations in the NAc (Murai *et al*, 1998). In addition, norepinephrine causes $GABA_A$ inhibition of VTA-projecting BNST neurons (Dumont *et al*, 2004), which may serve as an additional source of reduced dopaminergic output via VTA inhibition. This is further supported by the decreased dopamine concentrations we found during withdrawal, but not after morphine treatment. When

animals underwent withdrawal, elevated norepinephrine concentrations in the vBNST may have suppressed VTA activity thereby reducing dopamine transient concentrations. This effect was relieved at the end of the treatment, and direct electrical stimulation of the VTA resulted in equivalent dopamine release regardless of an animal's exposure to withdrawal, in agreement with tissue-content findings (McElligott *et al*, 2013). The reciprocal actions of dopamine and norepinephrine seen here during intoxication and withdrawal reflect important feedback between catecholamine circuits during rewarding and aversive stimuli.

Overall, the increased dopaminergic signaling we observed during intoxication supports a rich literature on dopamine's role in the rewarding properties of drugs. Additionally, the enhanced noradrenergic overflow concurrent with withdrawal signs underscores norepinephrine's importance in mediating opiate-withdrawal aversion. The combination of decreased dopaminergic output and enhanced noradrenergic overflow revealed in this work supports the allostasis model, and suggest negative reinforcement may emerge after the first exposure. Taken together, this real-time view of reciprocal catecholamine signaling provides insight as to how catecholamine circuits in the ventral forebrain become dysregulated after drug exposure and withdrawal. These adaptations may converge with stress or other risk factors to drive the development of addiction in susceptible individuals, and how they progress longitudinally should be a topic of future investigations.

Support:

Nathan Rodeberg contributed to this chapter. This work was supported by NIH grant DA10900 to RMW.

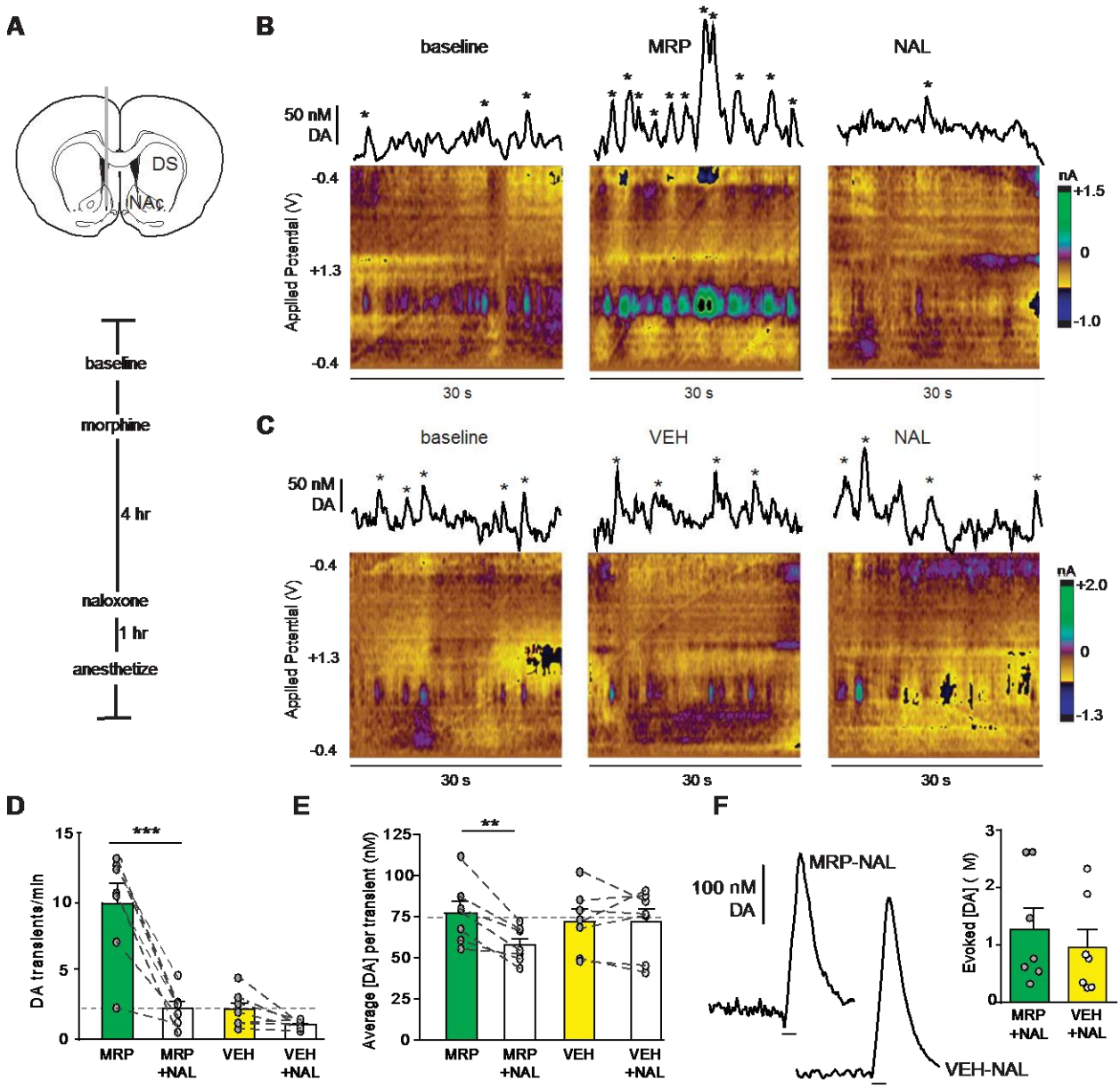

Figure 4.1. Dopamine efflux in the nucleus accumbens (NAc) varies with morphine intoxication and withdrawal. (A) Schematic of electrode placement and experimental timeline. (B) Representative dopamine (DA) transients at baseline, after morphine (MRP), and after naloxone (NAL). Principal component analysis identified concentrations marked with asterisks as DA transients. (C) Representative DA transients at baseline, after saline (VEH), and after NAL. (D) Transient frequency and (E) average DA transient concentration under MRP or VEH and subsequent NAL. Average frequency and concentration of dopamine transients at baseline are indicated by the gray dashed lines (F) Representative evoked [DA] in MRP or VEH-treated animals. Inset shows data from all subjects. Bar graphs show average ±SEM with individual subjects overlaid. **, P<0.01, ***, P<0.001, 2-way RM ANOVA, Bonferroni post-hoc.

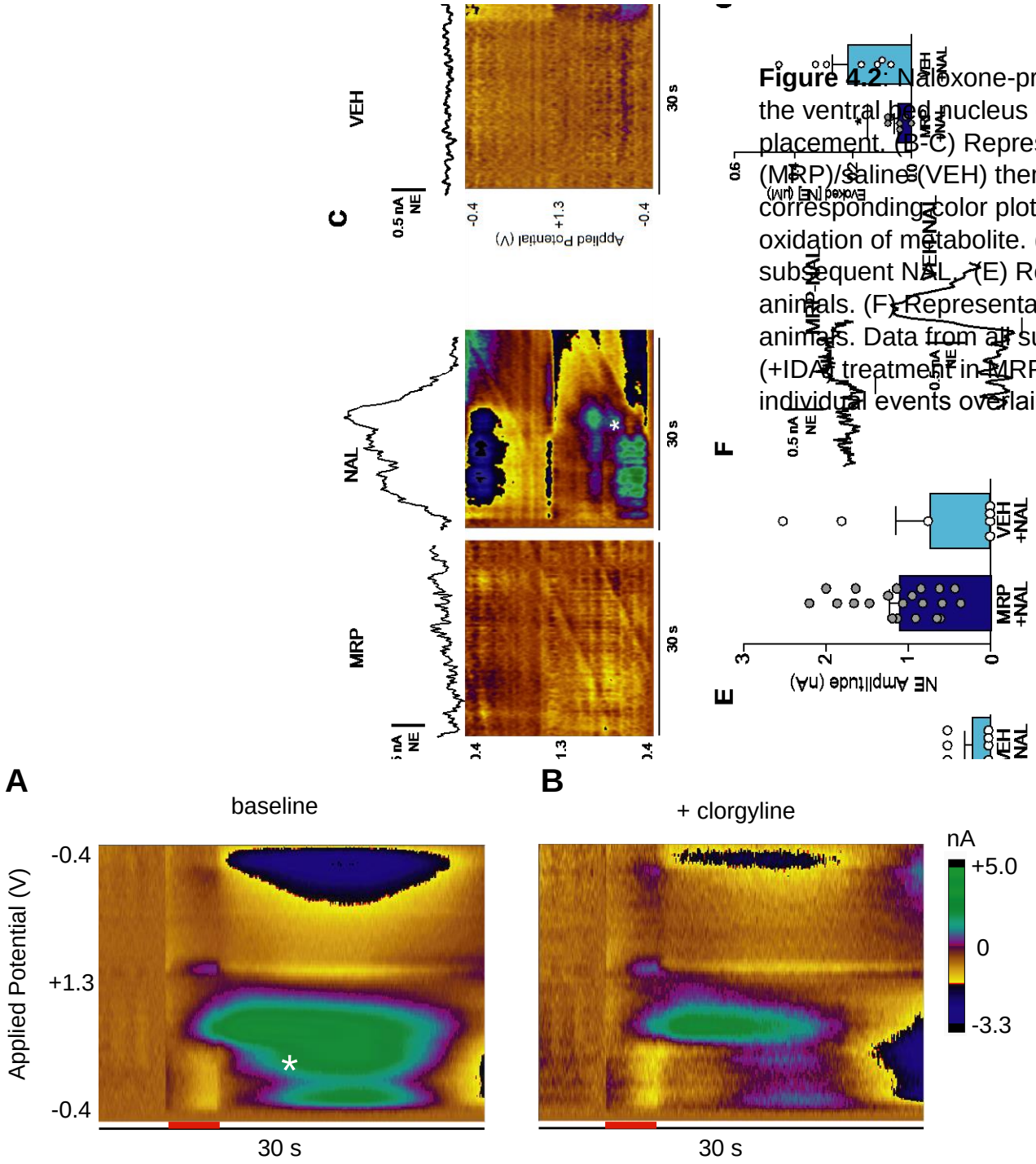

Figure 4.2: Naloxone-precipitated w
the ventral tegmental nucleus of the stria t
placement. (B-C) Representative no
(MRP)/saline (VEH) then naloxone (
corresponding color plots using prin
oxidation of metabolite. (D) Total NE
subsequent NAL. (E) Release ampl
animals. (F) Representative evoked
animals. Data from all subjects inset
(+IDA) treatment in MRP/VEH-NAL
individual events overlaid. *, P<0.05

Figure 4.3: MAO-inhibitor clorgyline suppresses oxidative current accompanying norepinephrine release. (a) A 30 Hz, 120 pulse electrical stimulation (red bar) elicits norepinephrine release accompanied by positive current at ~+0.4V (asterisk). (b) Inhibition of monoamine oxidase with clorgyline (75 mg/kg i.p.) attenuates the current at ~+0.4V, suggesting oxidative current at this potential is due to a catecholamine metabolite.

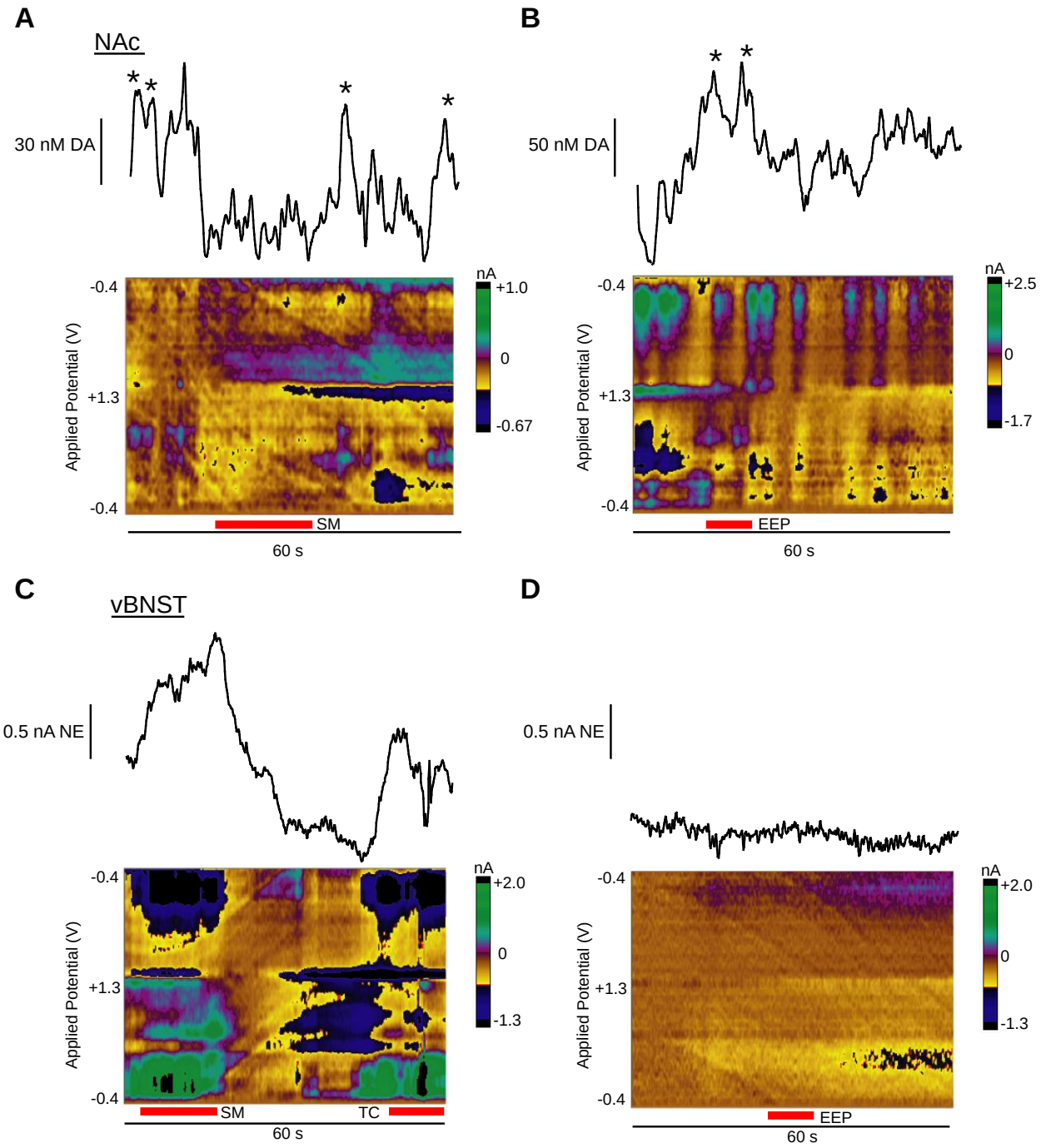

Figure 4.4: Somatic withdrawal signs produce variable catecholamine release in the nucleus accumbens and ventral bed nucleus of the stria terminalis. (A-B) Dopamine transients pause during swallowing movements (SM) and occur during spontaneous erection/ejaculation/penile grooming (EEP). Asterisks denote dopamine transients extracted with PCA from the corresponding color plot. (C-D) Norepinephrine release occurs during SM and teeth chattering (TC) and is absent during EEP as extracted from the corresponding color plot. Red bars beneath color plots denote duration of withdrawal behaviors.

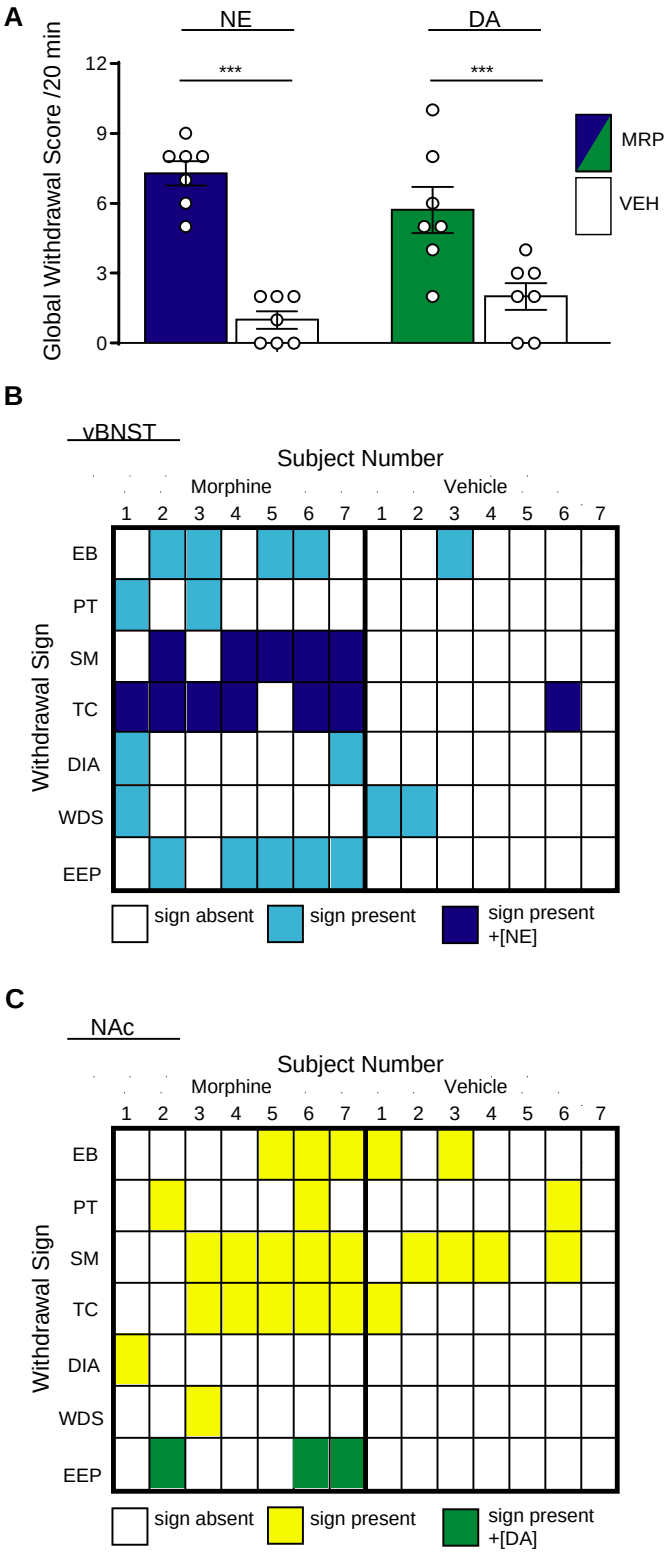
A
NE
DA
***
***
Global Withdrawal Score /20 min
12
9
6
3
0
MRP
VEH
B
vBNST
Subject Number
Morphine
Vehicle
1 2 3 4 5 6 7 1 2 3 4 5 6 7
EB
PT
SM
TC
DIA
WDS
EEP
Withdrawal Sign
sign absent
sign present
sign present +[NE]
C
NAc
Subject Number
Morphine
Vehicle
1 2 3 4 5 6 7 1 2 3 4 5 6 7
EB
PT
SM
TC
DIA
WDS
EEP
Withdrawal Sign
sign absent
sign present
sign present +[DA]

Figure 4.5: Catecholamine signaling coincides with specific withdrawal behaviors. (A) Global withdrawal score in morphine-naloxone (MRP, blue/green) or vehicle-naloxone (VEH, white) treated animals. Average ±SEM with individual subjects overlaid. ***, P<0.0001. (B) Heat map illustrating withdrawal signs coinciding with norepinephrine signaling in individual subjects. Light blue, sign present; dark blue, sign occurs with norepinephrine overflow; white, sign absent. (C) Heat map illustrating withdrawal signs coinciding with dopamine signaling. Yellow, sign present; green, sign occurs with dopamine transients; white, sign absent. Abbreviations: EB, excessive eye blinks; PT, ptosis; SM, swallowing movements; TC, teeth-chattering; DIA, diarrhea; WDS, wet dog shakes; EEP, spontaneous erection/ejaculation/penile grooming.

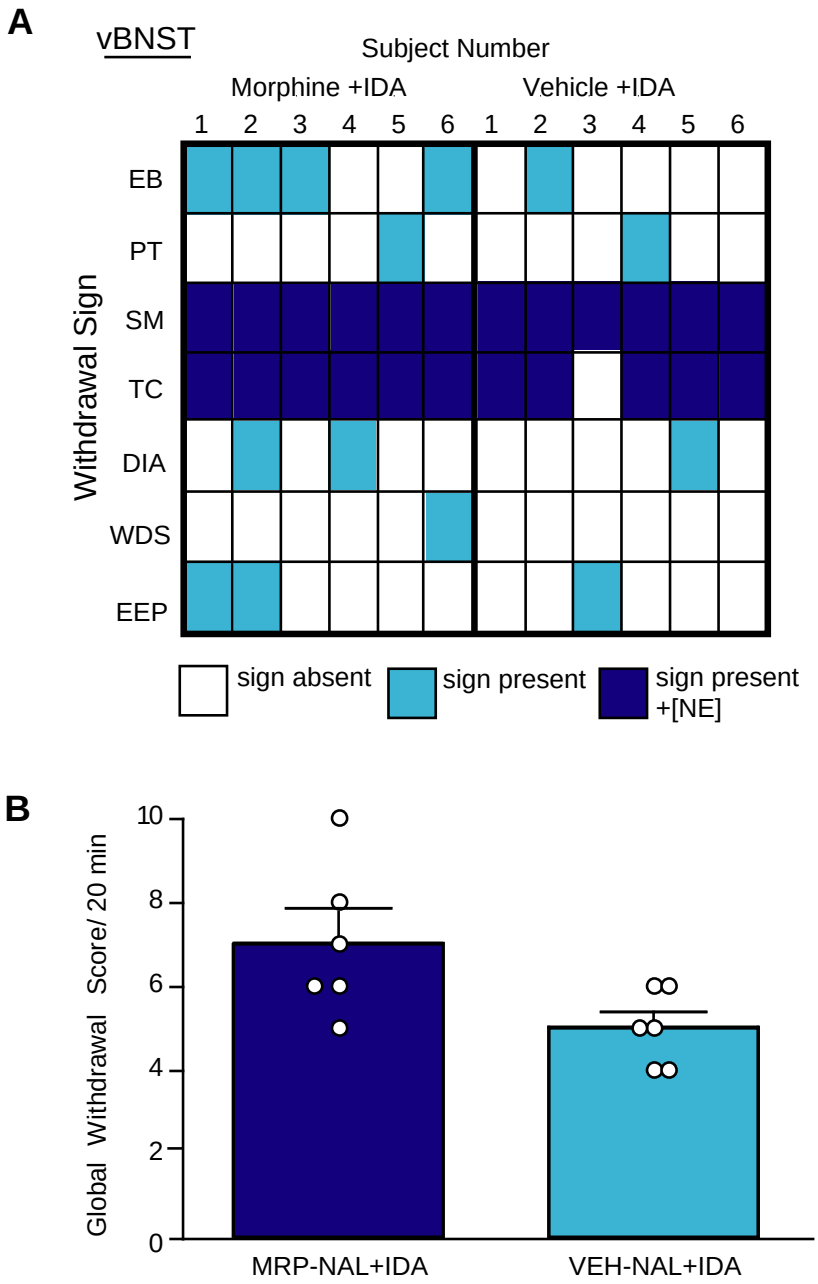

Figure 4.6: Idazoxan enhances naloxone-precipitated withdrawal signs. (A) Heat map illustrating withdrawal signs in individual subjects that coincide with norepinephrine signaling. Light blue indicates presence of sign, dark blue indicates presence occurring simultaneously with norepinephrine overflow, white indicates absence of sign. Abbreviations: EB, excessive eye blinks; PT, ptosis; SM, swallowing movements; TC, teeth-chattering; DIA, diarrhea; WDS, wet dog shakes; EEP, spontaneous erection/ejaculation and penile grooming. (B) Global withdrawal score in morphine or vehicle-treated animals given 5 mg/kg idazoxan in conjunction with naloxone.

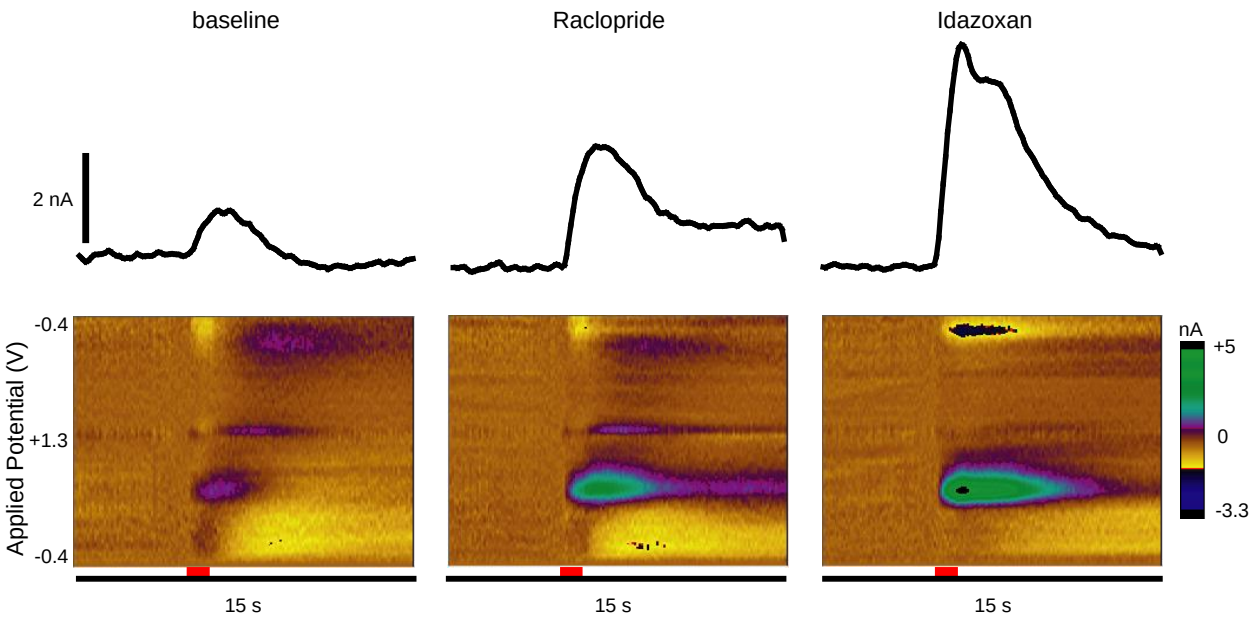

Figure 4.7: Mixed catecholamine recording locations respond to dopamine and norepinephrine drugs. Representative location of electrically evoked catecholamine release under baseline, 2 mg/kg raclopride, and 5 mg/kg idazoxan. Signals that responded in this way were excluded from analysis.

CHAPTER 5: CROSS HEMISPHERIC DOPAMINE PROJECTIONS HAVE FUNCTIONAL SIGNIFICANCE[3]

Introduction

Dopamine neurotransmission modulates arousal and motivation, and is important in expressing reward-seeking behavior. Dopamine is released on a subsecond timescale during unexpected reward (Sugam *et al*, 2012; Wassum *et al*, 2012), and becomes time-locked to cues that predict reward (Day *et al*, 2007; Owesson-White *et al*, 2008; Phillips *et al*, 2003; Roitman *et al*, 2004; Saddoris *et al*, 2015a). Dopamine transients in the nucleus accumbens (NAc) occur as a result of cell-firing in the ventral tegmental area (VTA) (Cacciapaglia *et al*, 2011; Sombers *et al*, 2009), and reach concentrations of 50-200 nM in rats before returning to baseline (Robinson *et al*, 2002; Wightman *et al*, 2007). Striatal dopamine transients also occur spontaneously during periods of rest (Robinson *et al*, 2002; Wightman *et al*, 2007), reflecting endogenous dopamine modulation. The magnitude and frequency of dopamine transients increases following drugs of abuse (Cheer *et al*, 2007b; Stuber *et al*, 2005), which is thought to contribute to their reinforcing properties (Covey *et al*, 2014). Although numerous studies

[3] This chapter originally appeared as an article in Proceedings of the National Academy of Sciences of the United States of America. The original citation is as follows: Fox, ME; Mikhailova, MA; Bass, CE; Takmakov, P; Gainetdinov, RR; Budygin, EA; Wightman, RM. (2016). "Cross-hemispheric dopamine projections have functional significance." Proc Natl Acad Sci U S A: *In press*

have summarized the function of dopamine circuits in reward-based behaviors (Berridge and Robinson, 1998; Schultz, 2015) and motor control (Baik *et al*, 1995; Costa *et al*, 2006; Crocker, 1997), anatomical descriptions of dopamine projections are conflicting (Andén NE, 1966; Geisler and Zahm, 2005; Jaeger *et al*, 1983; Nauta *et al*, 1978). Recent evidence suggests some dopamine neurons project contralateral to their origin (Geisler *et al*, 2005; Jaeger *et al*, 1983), contradictory to the uncrossed dopamine system described previously (Andén NE, 1966; Nauta *et al*, 1978). To date, the significance of contralaterally projecting dopamine neurons has not been established, nor how they may contribute to cross-hemispheric signaling.

A potential role for contralateral dopamine projections emerged in a recent study on brain stimulation reward (Steinberg *et al*, 2014). When rats were trained to self-stimulate the VTA, infusion of dopamine receptor antagonists in the NAc suppressed stimulation. This effect was seen whether the infusion was contralateral or ipsilateral to the stimulation site, reflecting cross-hemispheric modulation of the behavior. Furthermore, following unilateral stimulation, c-Fos was elevated in both hemispheres. Since this study did not examine dopamine release from VTA stimulations, the functional influence of contralateral projections could not be confirmed. Contralateral projections may also play a role in the neural adaptations in Parkinson's disease, which is characterized by a loss of midbrain dopamine. A hemiparkinsonian state can be modeled with unilateral 6-hydroxydopamine (6-OHDA) lesions, and recent studies describe alteration of synaptic signaling following dopamine depletion (Capper-Loup and Kaelin-Lang, 2013; Day *et al*, 2006; Fieblinger *et al*, 2014; Gerfen, 2000; Thiele *et al*, 2014). If contralateral dopamine projections have functional significance, dopamine

arising from these intact projections may influence signaling in the lesioned hemisphere (Nieoullon *et al*, 1977). Understanding the influence of contralateral projections may afford new ways to implement therapies such as deep brain stimulation for Parkinson's disease.

In this study, we demonstrate that contralaterally projecting dopamine neurons are functional and influence cross-hemispheric striatal signaling. We measured spontaneous and stimulated dopamine release in rats with fast-scan cyclic voltammetry (FSCV). In freely moving rats, we found spontaneous synchronous dopamine release in both hemispheres that further synchronized following amphetamine. We show that electrical or optogenetic stimulation of dopamine neurons elicits physiologically relevant dopamine release in the contralateral NAc and dorsomedial striatum (DMS). Using pharmacology, we discovered dopamine projections are differentially regulated by D2 receptors. We also extend these findings into 6-OHDA lesioned animals and characterize functional adaptations following unilateral depletion.

Materials and Methods

Animal Care

Experiments were performed in accordance with the Institutional Animal Care and Use Committee guidelines of the University of North Carolina at Chapel Hill (UNC) and Wake Forest School of Medicine. Sprague-Dawley rats (males, 270-400 g; Charles River, Wilmington, MA) were given food and water *ad libitum* and pair-housed in UNC or Wake Forest animal facilities on a 12:12-hour light:dark cycle. All experiments took place during the light cycle. To reduce number of animals and suffering, we limited awake measurements to 3 per treatment group, sufficient to demonstrate the effect in

every animal. For anesthetized experiments, we selected 5-10 animals, typical of voltammetric studies. In total, 3 animals were used for bilateral transient measurements, 20 for 6-OHDA studies, 53 for mapping/pharmacology, and 10 for optogenetic experiments.

Spontaneous dopamine measurements

Rats were anesthetized with isofluorane (4% induction, 1.5% maintenance) and affixed in a stereotaxic frame. The scalp was removed and holes were drilled to implant guide cannulas (BASi, West Lafayette, IN) bilaterally in the NAc (AP +1.3 mm, ML ±2.1 mm, ±10º to the perpendicular). A bipolar stimulating electrode (Plastics One, Roanoke, VA) was implanted in the right ventral tegmental area (AP -5.2mm, ML +1.0 mm, DV -8.5 mm). A third cannula was implanted in the left hemisphere for inserting a Ag/AgCl reference electrode on the day of recording. Cannulas were secured with dental cement and jewelers screws. Rats were subsequently singly housed and allowed to recover. After 3 days of recovery, carbon-fiber microelectrodes were lowered bilaterally into the NAc of awake animals through microdrives. Voltammetric measurements of spontaneous dopamine transients were as described previously (Bass *et al*, 2013; Saddoris *et al*, 2015a) using HDCV. A triangular scan (-0.4 to +1.3V, 400 V/s) was applied to the working electrode every 100 ms to detect changes in dopamine concentration. Spontaneous dopamine efflux was measured for 30 min after saline (VEH, 1 mL/kg, i.p.), and 30 min after d-amphetamine (AMPH, 2.5mg/kg, i.p., Sigma-Aldrich, St Louis, MO). Animals were then anesthetized (urethane,1.5 g/kg) and VTA stimulations were delivered to construct voltammograms for principle component analysis using an *in vitro* calibration factor (10 nA/µM) (Rodeberg *et al*, 2015). Only

transients >3 times the standard deviation of the noise in dopamine traces obtained by principle component regression were considered spontaneous dopamine.

Spontaneous dopamine measurements-hemispheric synchrony

Dopamine concentrations were extracted from color plots using principle component analysis as described above. We used a headstage that allows for simultaneous measurements at two electrodes, and thus aligned dopamine transient concentrations with respect to recording time at both electrodes. Dopamine transients were considered synchronous if their peaks occurred at the same time (e.g., t=127 s) and asynchronous if they did not occur at the same time (e.g., t=97 s, t=100 s).

Lidocaine infusions

Treatment-naïve rats were anesthetized with urethane (1.5g/kg), affixed in a stereotaxic frame, and holes were drilled in the NAc, DMS, VTA, and SN as above. A carbon-fiber electrode was lowered into the right DMS or NAc. A cannulated stimulating electrode (Plastics-One) was lowered into either the right SN (-7.8mm DV) or right VTA (-8.4 mm) and secured with dental cement. A second stimulating electrode was lowered into the left SN or VTA. Electrical stimulations were delivered every 2 min with Neurologs, alternating between contralateral and ipsilateral SN/VTA to establish baseline release. Lidocaine was subsequently delivered to the ipsilateral SN/VTA (350 nmol/0.5µL) and evoked dopamine was compared with baseline release over 40 min.

Stereotaxic virus infusion

Briefly, male Sprague-Dawley rats were anesthetized with ketamine HCl (100 mg/kg, i.p. and xylazine HCl, 20 mg/kg, i.p.) and affixed in a stereotaxic frame. The scalp was removed and a small hole was drilled above the right SN (from bregma, AP -

5.8 mm, ML, 2.0 mm) or right VTA (AP -5.8 mm, ML 0.7 mm) and an optic-fluid cannula (Doric Lenses, Canada) was implanted (DV -7.3 mm). 1.3 µL of pseudotyped AAV2/10 virus was slowly injected over 3 min via a Hamilton syringe connected to the optic-fluid cannula. We used a previously characterized combinatorial targeting system, in which a Cre dependent ChR2 (EF1α-DIO-ChR2-EYFP) is co-infused with a tyrosine hydroxylase (TH) promoter-Cre-AAV, resulting in ChR2 expression only in TH+ neurons. A dental-cement skull cap was secured over the exposed skull using jeweler's screws.

Optogenetic stimulations

Optical stimulations (60Hz, 60 p, 4ms width) were delivered to transduced cells from a 473 nm laser (Beijing Viasho Technology Co., Ltd, Beijing, China), controlled using TTL pulses generated by a programmable function generator (Hewlett-Packard model 8116A). Average laser power output delivered by the optical fiber was 2.3 mW, measured using a commercial power meter (Newport Model 1815C).

Immunohistochemistry

Animals were deeply anesthetized with isoflurane and then transcardially perfused with 50 ml saline followed by 500 ml of 10% formalin. The brains were removed, postfixed for 2 h in 10% formalin, and then cryoprotected in 20% sucrose in PBS containing azide overnight. The brains were sectioned on a sliding microtome at 40 µm. Tissue sections were incubated with a 1% H_2O_2 phosphate buffered saline-Tween20 (PBST) solution for 30 min, rinsed three times with PBS, and incubated with a rabbit anti-GFP antibody (1:20,000, Invitrogen, catalog no. A6455) overnight at room temperature. Sections were rinsed three times with PBS and incubated with biotin-SP-conjugated AffiniPure Donkey anti-Rabbit IgG (H+L) (1:1000, Jackson

ImmunoResearch Labs, cat. no. 711-065-152) for 1 hr. After three more rinses the sections were incubated with ABC reagent (Vectorlabs cat. no. PK-6100) and stained with diaminobenzidine (DAB, Sigma). Sections were then mounted and coverslipped with Permount. Images were collected on an Apiero slide scanner.

Mapping contralateral dopamine release

Treatment-naive rats were anesthetized with urethane (1.5 g/kg), affixed in a stereotaxic frame, and the scalp removed. Holes were drilled for working (NAc: AP + 1.3 mm, ML +1.3 mm; DMS: AP +1.2 mm, ML +2.0 mm) and stimulating (VTA: AP -5.2, ML±1.0 mm; SN: AP -5.8 mm, ML ±2.0 mm; PPTg: AP-7.8mm, ML ± 2.0mm) electrodes. A bipolar stimulating electrode (Plastics One) was placed at a constant depth contralateral to the working electrode (VTA: -8.4 mm DV, SN: -7.8 mm DV) while a carbon-fiber microelectrode was lowered ventrally through the striatum in 200 µm increments to map release.

300 µA electrical stimulations (60Hz, 1s) were applied with Neurologs (NL800). Once maximal dopamine release was attained at the working electrode, the stimulating electrode was adjusted ventrally by 200 µm intervals to map the effect of stimulation location on release. The stimulating electrode was removed from the contralateral and lowered ventrally through the ipsilateral hemisphere. In a subset of animals (5 DMS, 5 NAc), 10 Hz stimulations were delivered to the contralateral SN/VTA. We also examined dopamine release in the dorsolateral striatum (AP +0.5 mm, ML +3.5 mm, N=5), and as evoked by PPTg stimulations (AP -7.8, ML ± 2.0mm, N=5).

6-hydroxydopamine lesions

Rats were anesthetized with isofluorane and affixed in a stereotaxic frame. The scalp was removed and a hole for a bipolar, cannulated stimulating electrode (Plastics-One) was lowered into the right SN (AP -5.8 mm, ML +2.0 mm, DV -7.8 mm) and secured with dental cement. 3 µL of 10 mM 6-hydroxydopamine hydrobromide/ 0.01% w/v ascorbic acid (Sigma-Aldrich) in sterile saline (0.9%), or saline (sham-lesioned) was administered through the cannula at a rate of 1 µL/min. The infusion needle (33 ga, 10 mm long) was left in place for 10 min to minimize spread up the tract Rats recovered from 6-OHDA lesions for 2-weeks before being placed in a clear plastic bowl (30 cm diameter, 20 cm high) and videotaped for spontaneous rotational behavior after 2.5 mg/kg AMPH. 3-days after scoring rotations, rats were anesthetized (urethane, 1.5 g/kg) and a second stimulating electrode was placed in the left SN (AP -5.8, ML -2.0, DV -7.8 mm). A carbon-fiber electrode was lowered into the right DMS (AP +1.2, ML +2.0, DV -4.0 to -6.2 mm) in 200 µm intervals. A Ag/AgCl reference electrode was placed contralateral to the working electrode. Dopamine release was evoked using 1s, 300 µA stimulation pulses applied at 60 Hz using constant current isolators (Neurolog, NL800) and compared between hemispheres. In a subset of animals, a carbon-fiber electrode was lowered in the DMS of freely moving animals (DV -6.0 mm). Spontaneous dopamine transients were recorded after vehicle (1mL/kg saline) and AMPH (2.5 mg/kg). Animals were then anesthetized (urethane, 1.5 mg/kg) and electrical stimulations were delivered to treated and contralateral SN to confirm lesion efficacy.

Spontaneous Rotational Behavior

Rats were habituated to the chamber for 10 min before given 1 mL/kg saline i.p. A rotation was defined as four consecutive 90º turns in the same direction and summed over a 60 min trial. Subsequently, 2.5 mg/kg d-amphetamine (Sigma-Aldrich) was administered i.p. and rotations were measured for an additional 60 min. The number of rotations contralateral to the lesion (i.e., counter-clockwise) was subtracted from the number of rotations ipsilateral to the lesion (i.e., clock-wise) and plotted as net-rotations over the 1 hr recording period. Videos were scored after the trials by an experimenter blind to the treatment.

Pharmacology

Baseline release was recorded for 20 min by repeating 1 s electrical stimulations every 2 min. Release was monitored for 30 min after D2 receptor antagonisism (s-(-)-raclopride HCl, 2 mg/kg i.p., Sigma-Aldrich), and 30 min after subsequent dopamine transporter inhibition (GBR-12909, 15 mg/kg i.p.,Sigma-Aldrich).

Histology

At the end of FSCV experiments, a constant current (20 μA,10 s) was applied to the carbon fiber to mark the electrode recording location. In most 6-OHDA animals, 3 μL of 2% Chicago sky blue was infused through the cannulated stimulating electrode to mark the lesion boundaries. Brains were removed and fixed in 10% formalin for >24 hr. 50 μm sections were taken on a cryostat (Leica, Germany) and viewed under a light microscope to identify electrode placements. In two 6-OHDA lesioned animals, we stained for tyrosine hydroxylase in 40μm sections using Rabbit anti TH (1:500, Fisher) and Goat anti rabbit IgG-Alexa 514 (1:500, Invitrogen). Sections were incubated with anti-TH for 18hr at 4º after 2 hr incubation in 10% normal goat serum/ 0.3% triton x-100

blocking solution. Sections were washed in PBS, and then incubated in anti-rabbit IgG-Alexa 514 for 2 hr in 2% bovine serum albumin at room temperature. Sections were rinsed with PBS before being mounted, dried, and coverslipped, then imaged with an Olympus FV1000 microscope.

Statistics

Statistical analysis was performed using Graph Pad Prism and no data were removed. Mainly one-way ANOVAs with Bonferroni post-hoc determined significant differences between groups. A two-way repeated-measures ANOVA determined significant increases in dopamine transients and ipsilateral rotations after amphetamine. A two-tailed, unpaired T-test determined differences in raclopride response between 6-OHDA and sham lesioned animals.

Results

Spontaneous dopamine transients synchronize in the NAc.

FSCV has been used to measure dopamine fluctuations in a number of studies; however, all awake-animal measurements have been restricted to a single hemisphere (Cacciapaglia *et al*, 2011; Cheer *et al*, 2007b; Daberkow *et al*, 2013; Day *et al*, 2007; Hamid *et al*, 2016; Howe *et al*, 2013; Owesson-White *et al*, 2008; Phillips *et al*, 2003; Robinson *et al*, 2002; Roitman *et al*, 2004; Saddoris *et al*, 2015a; Sombers *et al*, 2009; Stuber *et al*, 2005; Sugam *et al*, 2012; Syed *et al*, 2016; Wassum *et al*, 2012; Wheeler *et al*, 2015; Wightman *et al*, 2007). To investigate connectivity between hemispheres, we measured dopamine transients bilaterally in the NAc of freely moving rats. We recorded from dual carbon-fiber electrodes, as previously employed in anesthetized animals (Park *et al*, 2011). We targeted guide cannulas over the NAc (Fig 5.1a) and

optimized recording locations for spontaneous dopamine release (Fig 5.1c-d). We found dopamine transients of similar magnitudes (L: 92.1 ± 5.23 nM, R: 96.4 ± 5.92 nM, Fig 5.1e) and frequency (L: 8.5 ± 1.6, R: 7.7 ± 0.6, transients min^{-1}, Fig 5.1f) in both hemispheres. Interestingly, 74 ± 5.3 % of dopamine transients occurred simultaneously between hemispheres in animals at rest (Fig 5.1g). We next administered d-amphetamine (AMPH, 2.5 mg/kg, i.p.) and transient magnitude increased in both hemispheres (L: 157.2 ± 30.6 nM, R 184.3 ± 39.2 nM, 2-way RM ANOVA, effect of AMPH, $F_{(1,4)}$=11.3, P<0.05, Fig 5.1e). Following AMPH, all dopamine transients synchronized and increased in frequency (15.9 ± 2.0 transients min^{-1}, 2-way RM ANOVA, effect of AMPH, $F_{(1,4)}$=13.7, P<0.05, Fig 5.1f-g). When animals were anesthetized and the VTA stimulated unilaterally, we measured dopamine at both electrodes (Fig 5.1b).

Stimulation of dopamine neurons elicits release in the contralateral hemisphere.

Given that electrical stimulation of the VTA resulted in dopamine in both hemispheres, we characterized contralaterally evoked release to ascertain if it was restricted to the NAc and if it contributed to coupled dopamine transients. We implanted a carbon-fiber electrode into either the NAc or DMS (schematics in Fig 5.2a,d) of anesthetized rats and lowered it ventrally through the striatum with the stimulating electrode in the contralateral VTA (8.8 mm DV) or substantia nigra (SN, 7.6 mm DV). We found multiple locations that supported release (examples in Fig 5.2b,e). In the NAc, contralateral dopamine release peaked $(DA]_{con}/[DA_{con\text{-}max}$) in the core (6.4 mm DV) and in the shell (7.4 mm DV, Fig 5.2c). In the DMS, maximal dopamine release elicited by

contralateral SN stimulations was restricted to a smaller range (6.2-6.4 mm, DV, Fig 5.2f).

We examined interhemispheric differences using within-animal comparisons of dopamine evoked contralateral vs. ipsilateral to the stimulation site (schematic in Fig 5.3a,c). With the recording electrode at a constant depth, (NAc: 7.4 mm DV, DMS: 6.2 mm DV) maximal release was achieved by stimulating similar VTA or SN depths in both hemispheres. Notably, in the NAc, ipsilateral stimulation elicited ~20x more dopamine release than contralateral (8.8 mm DV, Fig 5.3a). In contrast, ipsilateral and contralateral SN stimulations evoked dopamine release of equal magnitude in the DMS (7.6 mm DV, Fig 5.3c). We obtained similar release in the DMS by stimulating contralateral and ipsilateral peduncolopontine tegmental nucleus (PPTg), an excitatory input to the SN (Fig 5.4). Recording in the dorsolateral striatum revealed equal release was unique to the DMS (Fig 5.5).Additionally, contralateral release was not due to electrical spread to the ipsilateral hemisphere, as lidocaine infusions in the ipsilateral SN/VTA did not affect release evoked by contralateral stimulation (Fig 5.6).

We confirmed the origin of contralateral release using optogenetics to activate only dopaminergic neurons. We drove unilateral channelrhodopsin-2 (ChR2) expression in dopamine neurons using a tyrosine hydroxylase promoter (Bass *et al*, 2013; Gompf *et al*, 2015). Light stimulations of the VTA elicited dopamine release in the contralateral NAc roughly equivalent to electrical stimulations (Examples in Fig 5.3b). We found similar release in the DMS following stimulations of the contralateral SN (Examples in Fig 3d). ChR2 expression was confirmed in the contralateral striatum and was not due to viral spread between hemispheres (Fig 5.7, 5.8).

Contralateral dopamine release is differentially regulated

To investigate the differences in dopamine released from contralateral and ipsilateral projections, we administered D2 antagonist raclopride (RAC; 2 mg/kg, i.p.) and dopamine transporter inhibitor GBR-12909 (GBR; 15 mg/kg, i.p.) and measured their effects on evoked dopamine.There were no differences in D2-like regulation between contralateral and ipsilateral projections to the DMS (Fig 5.9a). In contrast, D2 autoreceptors in the NAc exerted more control over dopamine release from contralateral compared to ipsilateral projections, evidenced by a much larger RAC response on the contralateral side (525 ± 135.3% vs 204 ± 26.5%, n=7, respectively, $F_{(3,22)}$ =4.9, P<0.05, Fig 5.9b). Thus, enhanced regulation by D2 may account for the discrepancy in dopamine concentrations evoked in ipsilateral and contralateral NAc. We also found an increased response to GBR in the DMS following contralateral SN stimulation relative to ipsilateral (1260 ± 301% vs 694 ± 199%, n=7, respectively, $F_{(3,26)=}$5.7, P<0.05), but not NAc (Fig 5.9a-b). To exclude the effects of supraphysiological stimulation frequency on dopamine release, we delivered 10 Hz stimulations to the contralateral VTA and SN, resulting in small, physiologically relevant concentrations (Fig 5.10).

Contralateral release is not solely compensatory

Parkinson's disease is often modeled with unilateral 6-OHDA lesions. Although small dopamine concentrations remain in lesioned animals (Zigmond *et al*, 1992), the extent to which contralateral projections compensate for depletion is unknown. Since the DMS exhibited hemispherically equivalent release, we chose it as a site to monitor changes in contralateral dopamine release after depletion. We used unilateral 6-OHDA lesions of the SN and recorded dopamine in the lesioned hemisphere. Two-weeks after

treatment, we validated the lesion by measuring ipsilaterally biased rotations after AMPH (2.5 mg/kg, Fig 5b. RM 2-way ANOVA, effect of 6-OHDA treatment $F_{(1,12)}$=38.32; effect of AMPH $F_{(1,12)}$=49.55, P<0.001). After 3-days, animals were anesthetized and we recorded dopamine in the DMS ipsilateral to the lesion. Stimulations were delivered to ipsilateral (lesioned) and contralateral SN (Fig 5.11a, examples in Fig 5.11c). Ipsilateral dopamine efflux was ablated following lesioned SN stimulation relative to controls (0.03 ± 0.007 µM vs 0.15± 0.024 µM, n=7, respectively, $F_{(3,24)}$=8.3, P<0.001, Fig 5.11d). Stimulation of the contralateral/untreated SN resulted in dopamine release in the same recording location (Fig 5.11d). Surprisingly, lesioned and control animals showed no differences in dopamine release following contralateral SN stimulation, suggesting that contralateral projections in 6-OHDA treated rats do not compensate via increased release (Fig 5d, 0.10 ± 0.01 µM vs. 0.12 ± 0.02 µM, n=7, respectively P>0.05, Fig 5.11d).

Dopamine denervation drives homeostatic changes in striatal signaling (Zigmond *et al*, 1990), such as increased D2 expression in indirect pathway neurons (Gerfen, 2000). To test for D2-like adaptations in intact contralateral projections after unilateral dopamine depletion, we measured the effect of D2 antagonist RAC (2mg/kg i.p.) on release in the lesioned DMS. RAC produced a larger increase in contralaterally evoked dopamine in lesioned relative to control animals (674 ±98.3% vs 401±79.9%, n=7, respectively, $t_{(13)}$=2.2, P<0.05), confirming adaptations after dopamine depletion.

Finally, we measured spontaneous dopamine efflux in awake animals two-weeks after unilateral 6-OHDA. We found spontaneous dopamine transients in the DMS of sham-lesioned animals that increased following AMPH (Fig 5.11e) in agreement with

previous studies (Daberkow *et al*, 2013). In 6-OHDA lesioned animals, spontaneous dopamine transients in the DMS ipsilateral to the SN lesion were not present under vehicle, but elicited by AMPH (Fig 5.11f). Thus, AMPH-induced dopamine release appears to arise from intact contralateral projections in unilaterally lesioned animals.

Discussion

These studies reveal previously undescribed interhemispheric communication in the mesencephalic dopamine system of rats. First, we found that optogenetic and electrical stimulation of dopamine cells elicited physiologically relevant release in the contralateral striatum. Contralateral projections from the VTA released less dopamine in the NAc and were more tightly controlled by D2 autoreceptors compared to ipsilateral projections. In contrast, dopamine release in the DMS was equivalent following contralateral or ipsilateral SN stimulation and accompanied similar D2 control in both hemispheres. Next, we found that ~75% of spontaneous NAc dopamine transients synchronized between hemispheres in freely moving rats, which increased to 100% following amphetamine. Finally, we showed that contralateral projections from SN neurons are functional in the hemiparkinsonian state, but do not compensate with increased dopamine release. Instead, D2 control on contralateral projections is increased after unilateral 6-OHDA. Contralateral SN projections can be stimulated with AMPH to evoke dopamine transients in the lesioned striatum of awake animals. These results establish for the first time that transient dopamine concentrations are synchronous between hemispheres, and that the dopamine system has functional contralateral projections with implications for interhemispheric adaptations in

Parkinson's disease. Furthermore, the data indicate that psychostimulants such as AMPH play a role in coupling dopamine transients between hemispheres.

Anatomical studies describe ~5% of midbrain dopamine neurons as projecting contralaterally to their origin (Geisler *et al*, 2005; Jaeger *et al*, 1983). In agreement with this, we measured smaller dopamine concentrations in the NAc following contralateral VTA stimulation compared to ipsilateral (Fig 5.3a). Interestingly, dopamine release from contralateral VTA neurons was more regulated by D2 autoreceptors. Dopamine released from ipsilateral projections may occupy D2 receptors on terminals from the contralateral hemisphere, attenuating release from contralateral VTA. Under intense stimulation, or when regulation mechanisms are disrupted, dopamine can be released from these fibers. Consistent with this, dopamine receptor antagonism in the contralateral NAc suppressed intra-VTA self-stimulation in the ipsilateral hemisphere (Steinberg *et al*, 2014), corroborating cross-hemispheric functionality and providing behavioral significance.

Surprisingly, when we placed our recording electrode in the DMS and stimulated contralateral or ipsilateral SN, we found similar release amplitudes regardless of stimulated hemisphere (Fig 5.3c). This property was unique to the DMS, as the evoked dopamine ratio in the dorsolateral striatum was more similar to the NAc (Fig 5.5). Similar D2 regulation in both hemispheres accompanied hemispherically equivalent release in the contralateral DMS, in contrast to D2 regulation of contralateral/ipsilateral VTA projections. Since our findings were confirmed using optogenetics, contralateral dopamine release is driven by dopamine neurons. However, optical activation does not

preclude the effects of glutamate co-release (Zhang *et al*, 2015), which may facilitate hemispherically equivalent release.

Dopamine transients increase following administration of drugs of abuse (Cheer *et al*, 2007b), and this appears to mediate their reinforcing properties (Covey *et al*, 2014). Dopamine transients have been studied extensively, (Cacciapaglia *et al*, 2011; Cheer *et al*, 2007b; Daberkow *et al*, 2013; Day *et al*, 2007; Hamid *et al*, 2016; Howe *et al*, 2013; Owesson-White *et al*, 2008; Phillips *et al*, 2003; Robinson *et al*, 2002; Roitman *et al*, 2004; Saddoris *et al*, 2015a; Sombers *et al*, 2009; Stuber *et al*, 2005; Sugam *et al*, 2012; Syed *et al*, 2016; Wassum *et al*, 2012; Wheeler *et al*, 2015; Wightman *et al*, 2007); however, previous measurements were restricted to a single hemisphere, including those using a MRI-compatible dopamine reporter (Lee *et al*, 2014), and few microdialysis experiments measure bilaterally (Buck and Ferger, 2008). In this work, we measured spontaneous dopamine efflux with millisecond time resolution in both hemispheres simultaneously and found synchronicity in release. In agreement with previous reports (Wightman *et al*, 2007), synchronized dopamine concentrations exhibited variability on a sub-minute timescale (Fig 5.1d), but on average, transient concentrations over 30 min were comparable between hemispheres (Fig 5.1e). The apparent bilateral synchrony in NAc dopamine release shows that although transients are heterogeneous within subregions (Wightman *et al*, 2007), their occurrence is coupled between hemispheres.

Interestingly, after AMPH, all dopamine efflux became synchronized between hemispheres. Since NAc dopamine transients originate from VTA cell firing (Cacciapaglia *et al*, 2011; Sombers *et al*, 2009), and AMPH-induced dopamine release

occurs in an action-potential dependent manner (Covey *et al*, 2016), coupled dopamine transients reflect synchronicity within the VTA that could arise from several mechanisms. During psychostimulant-induced excitation, VTA cells display slow rhythmic oscillations (Shi *et al*, 2004). Oscillations enable neurons to become more sensitive to precise timing of synaptic inputs and aid in synchronizing patterns of neuronal activity (Volgushev *et al*, 1998). Thus, AMPH may synchronize firing in the VTA between hemispheres, or synchronize contralaterally and ipsilaterally projecting neurons within a hemisphere. Synchronicity in dopamine transients may result from neurotensin release in the VTA. Intra-VTA neurotensin activates dopamine neurons and contributes to behavioral sensitization after psychostimulants (Panayi *et al*, 2005). The parabrachial nucleus is one source of neurotensinergic projections to the VTA (Geisler and Zahm, 2006) and projects bilaterally to midbrain dopamine neurons (Watabe-Uchida *et al*, 2012).

Regardless of mechanism, the synchronicity in dopamine release between hemispheres uncovered here establishes that chemical signaling, like physiological activity (Shen *et al*, 2015), is tightly coupled across the brain. Since amphetamine-induced dopamine transients remain in unilaterally lesioned animals, it is apparent that interhemispherical connectivity contributes to psychostimulant induced dopamine fluctuations. Dopamine transients, demonstrated to be important in drug abuse (Covey *et al*, 2014), clearly arise from bilateral interactions. Furthermore, AMPH is used to treat attention deficit hyperactivity disorder (ADHD), and ADHD patients have abnormal frontostriatal asymmetry (Silk *et al*, 2015). The observed synchronicity in dopamine signaling after AMPH may contribute to its therapeutic effects in individuals with ADHD.

While further research is needed to establish the mechanisms that coordinate dopamine transient coupling, the present work establishes that dopamine fluctuations display synchrony between hemispheres.

Contralateral projections may balance dopamine concentrations between hemispheres after dopamine depletion. However, when the SN was 6-OHDA lesioned, we found dopamine release from the contralateral, unlesioned SN was equivalent in lesioned and control animals. This was surprising, because these projections are thought to compensate for depletion via increased release (Nieoullon *et al*, 1977). Instead, we found enhanced D2 control over release in the lesioned hemisphere, supporting prior findings of increased D2 expression after dopamine depletion (Gerfen, 2000).

When we extended our measurements into awake animals, we found spontaneous transients in the DMS of sham-lesioned animals that were not present in the 6-OHDA group. However, dopamine transients were elicited in the lesioned hemisphere with amphetamine. Since D2 receptors exerted more control over contralateral dopamine release in lesioned animals, and AMPH attenuates D2 function (Calipari *et al*, 2014b), we believe this release arises from intact contralateral projections. With the perturbation introduced by amphetamine, contralateral projections may release dopamine into the depleted hemisphere. Indeed, dopamine cell firing between hemispheres normalizes after activation of dopamine receptors in 6-OHDA lesioned animals (Chen *et al*, 2001). Previous work in primates (Salvatore *et al*, 2009) and rats (Yang *et al*, 2007) has alluded to interhemispheric adaptations following

nigrostriatal damage. The data presented here establish a functional role for interhemispheric dopamine projections after unilateral 6-OHDA treatment.

In summary, this work demonstrates the functional significance of interhemispheric communication in dopaminergic signaling. Activation of midbrain dopamine neurons evokes physiologically relevant dopamine release in the contralateral striatum of rats that synchronizes between hemispheres. D2 autoreceptors from contralateral VTA projections exert more control over NAc dopamine release relative to the ipsilateral projections, in contrast to DMS release via SN stimulation. Selective activation confirmed that dopaminergic neurons drive contralateral release. Furthermore, we found contralateral release was not solely compensatory because similar amounts of dopamine were evoked after contralateral SN stimulations in 6-OHDA treated and control rats. These data are the first to demonstrate the functional nature of cross-hemispheric dopamine projections and provide new context for plasticity of striatal synapses after unilateral manipulation. Crossing projections likely facilitate the observed coupling of dopamine transients. Moreover, our findings provide additional insight for recently reported receptor alterations (Capper-Loup *et al*, 2013; Day *et al*, 2006; Fieblinger *et al*, 2014; Gerfen, 2000; Thiele *et al*, 2014) as the lesioned hemisphere is not completely dopamine-deprived. Small concentrations released from contralateral projections, such as those reported here after amphetamine, likely influence receptor sensitivity in the lesioned hemisphere, and should be accounted for in future studies. The previously unappreciated cross-hemispheric functionality revealed here may also be useful in devising new therapies for treating dysregulated dopamine signaling.

Support

This work was funded by NIH (DA10900 to RMW, AA022449 to EAB) and by the Russian Science Foundation (4-50-00069 to RRG). The authors thank Michael Bruno for immunohistochemistry assistance and Dr. Elyse Dankoski for manuscript comments.

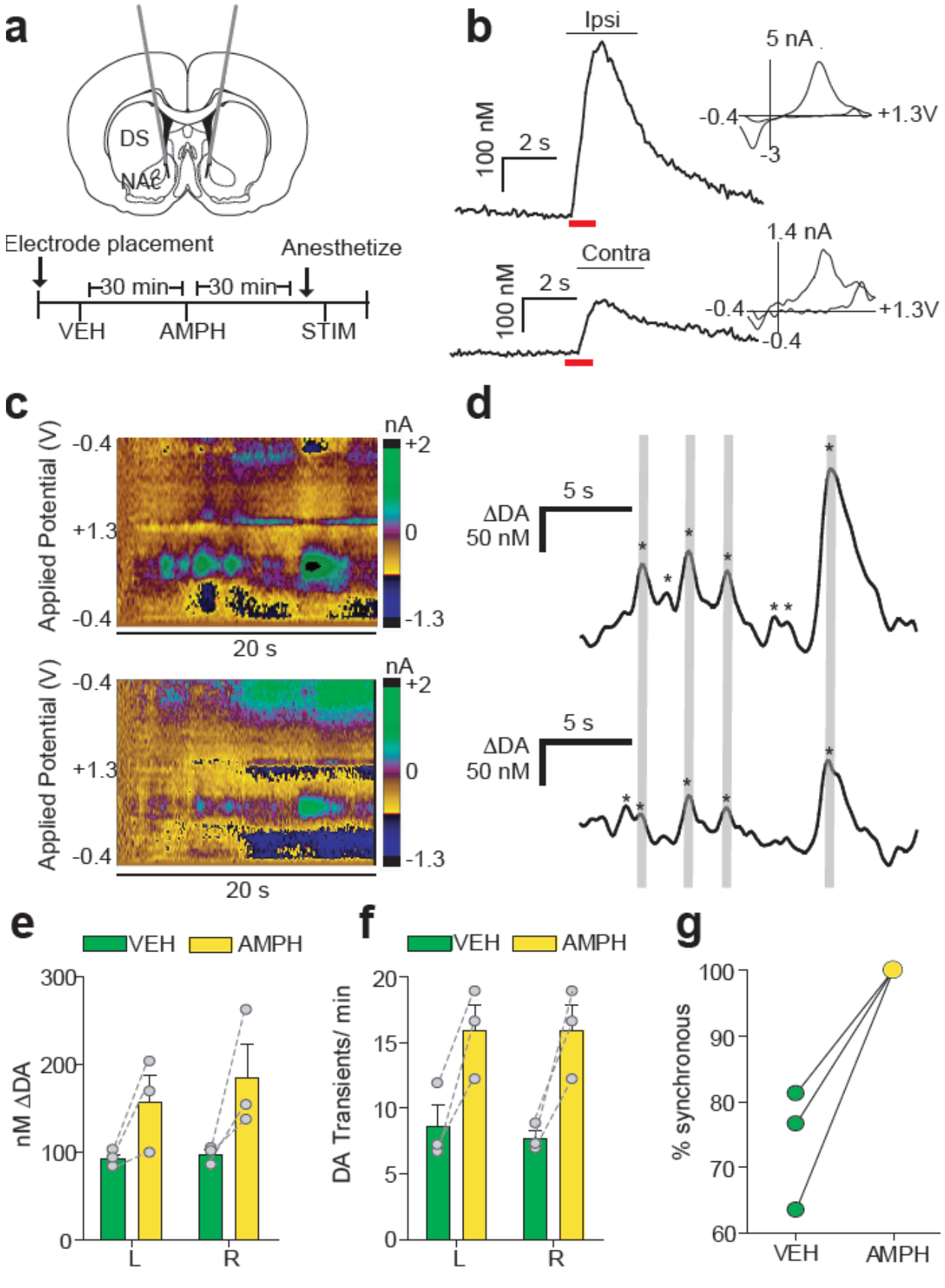
a
DS
NAc
Electrode placement
Anesthetize
30 min
30 min
VEH
AMPH
STIM
b
Ipsi
5 nA
100 nM
2 s
-0.4
+1.3V
-3
Contra
1.4 nA
100 nM
2 s
-0.4
+1.3V
-0.4
c
Applied Potential (V)
-0.4
+1.3
-0.4
nA
+2
0
-1.3
20 s
Applied Potential (V)
-0.4
+1.3
-0.4
nA
+2
0
-1.3
20 s
d
5 s
ΔDA
50 nM
5 s
ΔDA
50 nM
e
VEH
AMPH
nM ΔDA
300
200
100
0
L
R
f
VEH
AMPH
DA Transients/ min
20
15
10
5
0
L
R
g
% synchronous
100
90
80
70
60
VEH
AMPH

Figure 5.1: Spontaneous dopamine transients synchronize bilaterally in the nucleus accumbens. (a) Schematic of electrode implantation for simultaneous dopamine transient measurements. (b) Representative dopamine release in the right and left NAc following stimulation (red bar) of the right VTA with voltammograms inset. (c) Representative color plots demonstrating synchronous dopamine transients in both hemispheres with applied potential on the ordinate, recording time on the abscissa, and current encoded in false color. (d) Changes in dopamine concentration (asterisks) in both hemispheres extracted from (c) using principle component analysis. Gray lines indicate synchronized transients; asterisks alone indicate asynchronous dopamine release. (e) Average ± SEM dopamine transient concentration in left (L) and right (R) NAc after saline (VEH, green) and 2.5 mg/kg amphetamine (AMPH, yellow) (f) Average ± SEM number of dopamine transients per min in L and R NAc after VEH and AMPH. (g) Within-animal comparison of % transient synchrony after VEH and AMPH. N=3 animals.

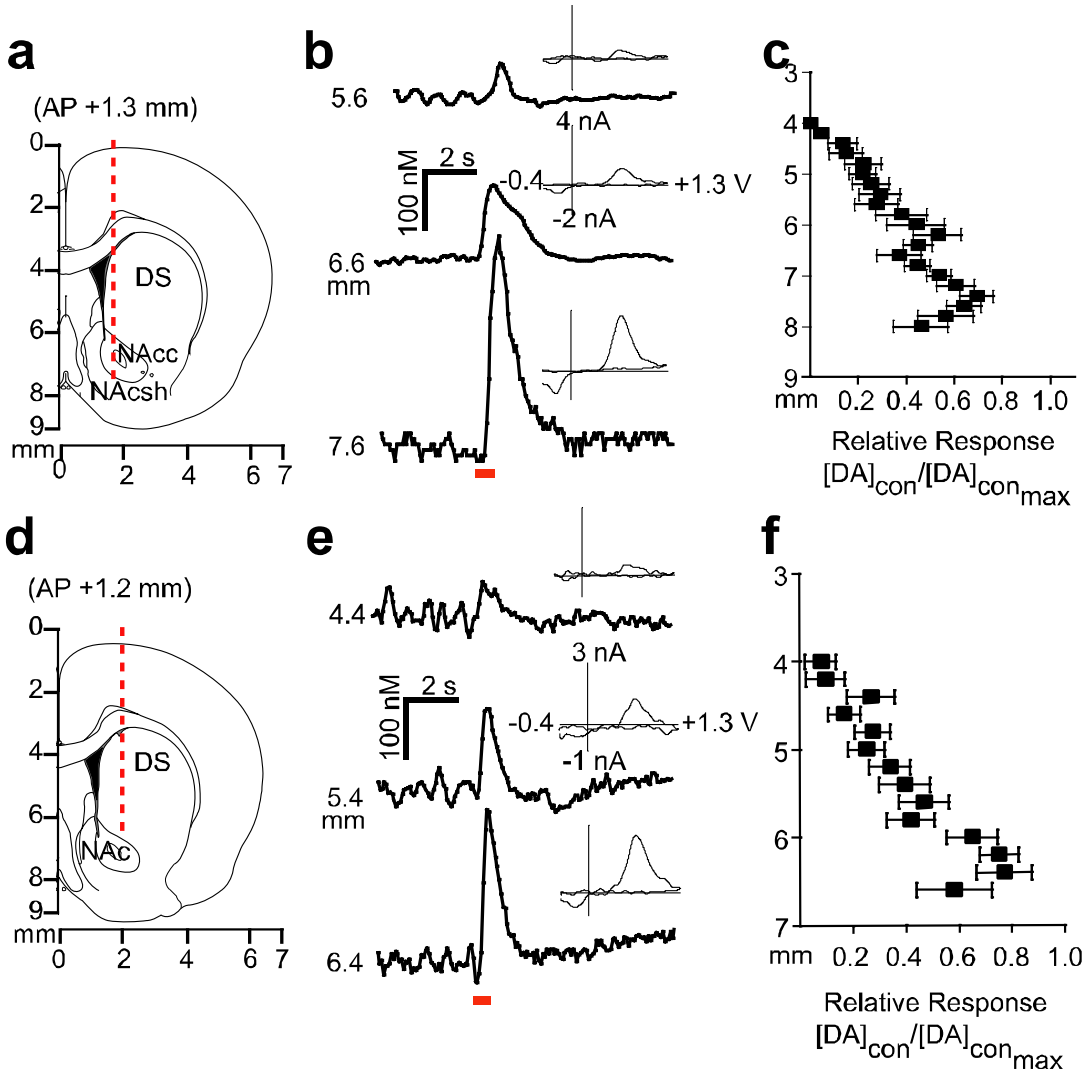

Figure 5.2: Stimulation of dopamine neurons produces localized release in the contralateral striatum. Electrode trajectories are shown superimposed on coronal sections in (a) and (d). Dopamine release at the terminals was dependent on recording electrode depth with example traces shown in (b) and (e). Insets are the cyclic voltammograms recorded at maximum release. Dopamine response (DA_{con}) following electrical stimulations of the contralateral VTA (c) or SN (f), normalized to maximum dopamine release ($DA_{con\text{-}max}$) and plotted as a function of working electrode depth. N= 10 animals per group, average ± SEM.

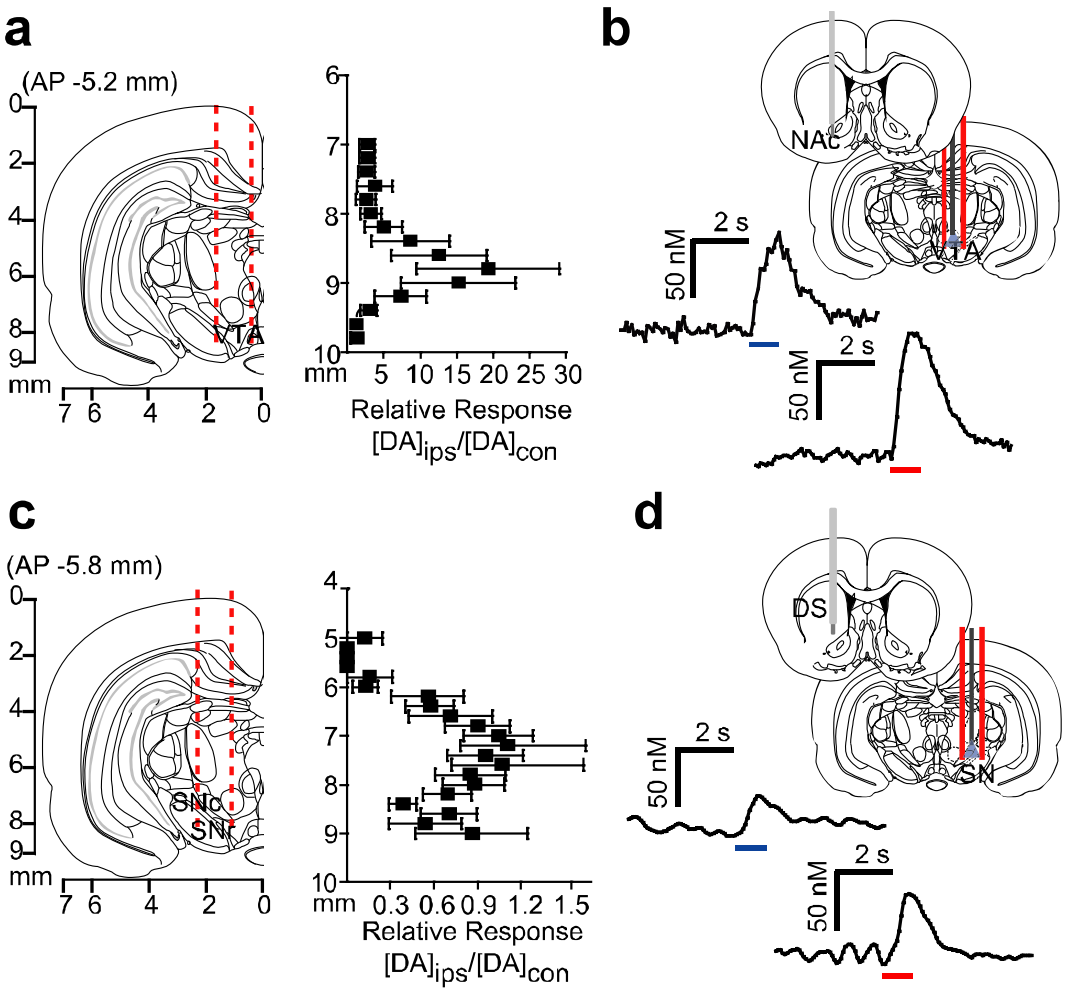

Figure 5.3: Stimulation of contralateral dopamine neurons produces variable dopamine release in the striatum. Coronal section showing stimulating electrode tracts in the VTA (a) and SN (c), and within-animal comparison of NAc and DMS effluxes, respectively, resulting from ipsilateral stimulation (DA_{ips}) compared with contralateral stimulation (DA_{con}) at identical depths. N= 10 animals per group, average ± SEM. Representative dopamine response in the contralateral NAc (b) and DMS (d) to optogenetic (blue) and electrical (red) stimulation of VTA or SN.

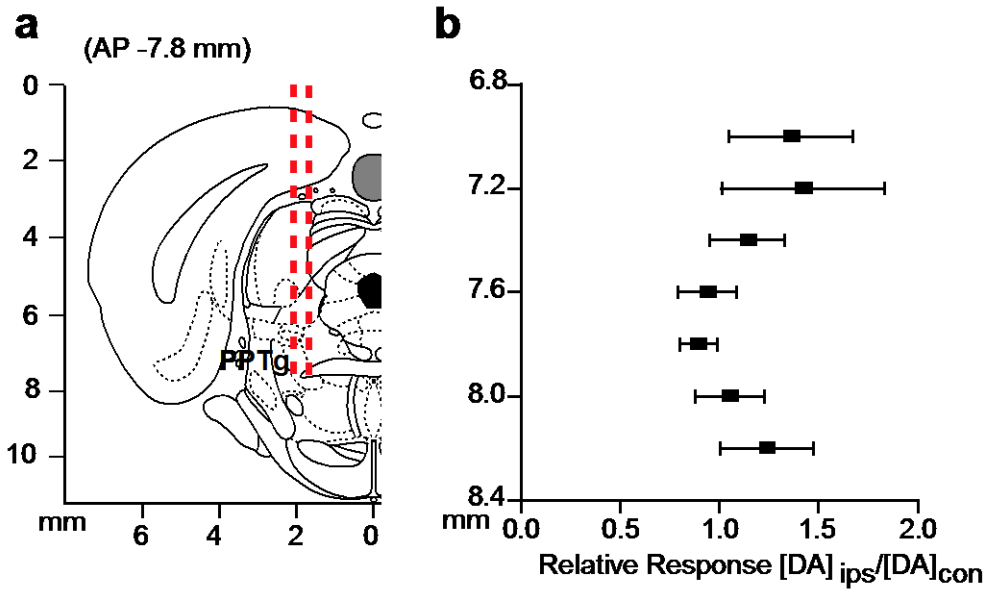

Figure 5.4: Stimulation of the peduncolopontine tegmental nucleus elicits release in the contralateral DMS. (a) Coronal section showing stimulating electrode tracts in the PPTg, and (b) within-animal comparison of DMS effluxes resulting from ipsilateral (DA_{ips}) compared to contralateral stimulation (DA_{con}) at identical depths. N=5 animals, average ± SEM.

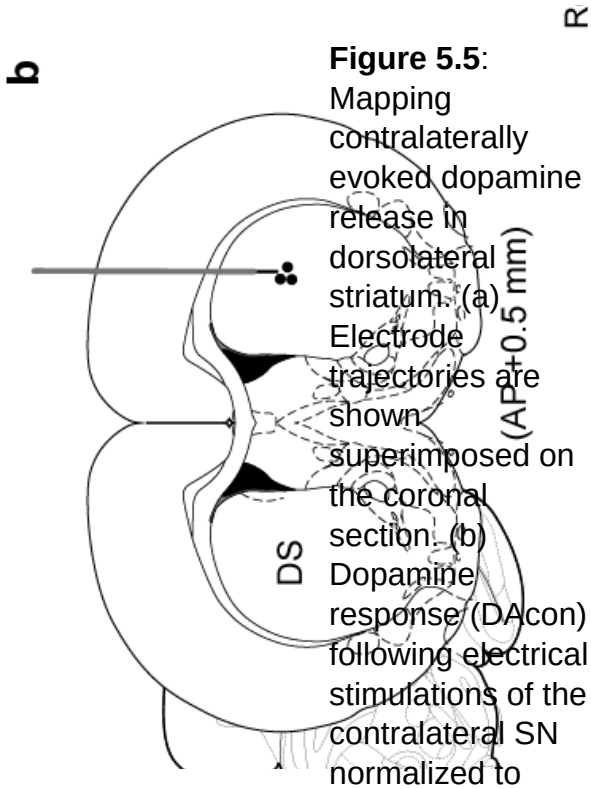

Figure 5.5: Mapping contralaterally evoked dopamine release in dorsolateral striatum. (a) Electrode trajectories are shown superimposed on the coronal section. (b) Dopamine response (DAcon) following electrical stimulations of the contralateral SN normalized to maximum dopamine release (DAcon-max) and plotted as a function of working electrode depth. N= 5 animals, average ± SEM.

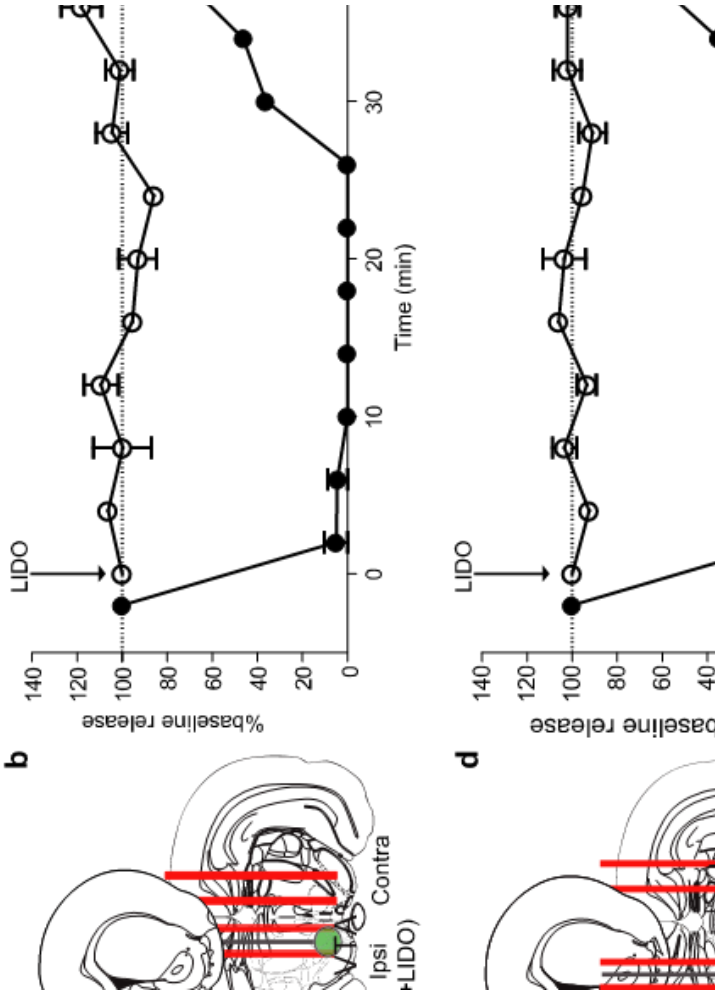

Figure 5.6: Contralateral dopamine release is not a result of electrical spread between hemispheres. Schematics of carbon-fiber electrode in the (a) NAc, or (c) DMS, with cannulated stimulating electrode in the ipsilateral VTA/SN for delivery of lidocaine, and stimulating electrode in the contralateral VTA/SN. Dopamine release as a percent of baseline in (b) the NAc, or (d) DMS, resulting from contralateral and ipsilateral stimulations of VTA/SN. Lidocaine (350 nmol/0.5µL) delivery is

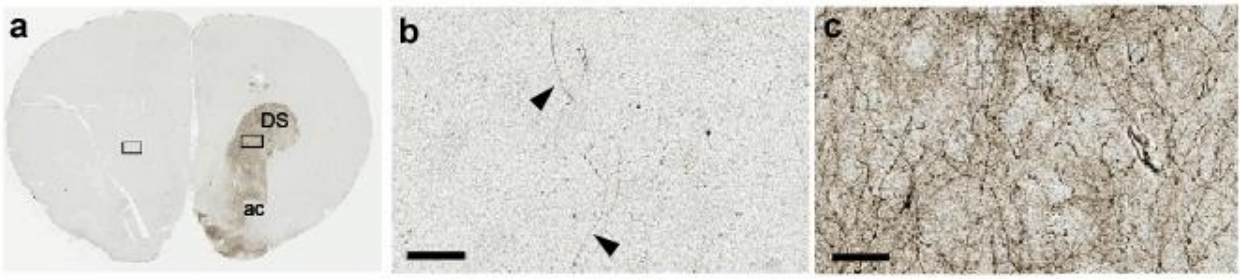

Figure 5.7: Channelrhodopsin-2 expression in the contralateral striatum. (a) Low magnification images of ChR2-eYFP expression in the striatum after immunohistochemistry with GFP antibody. High magnification images ChR2-eYFP expression in (b) contralateral and (c) ipsilateral striatum as highlighted in (a). Scale bar =80 m.

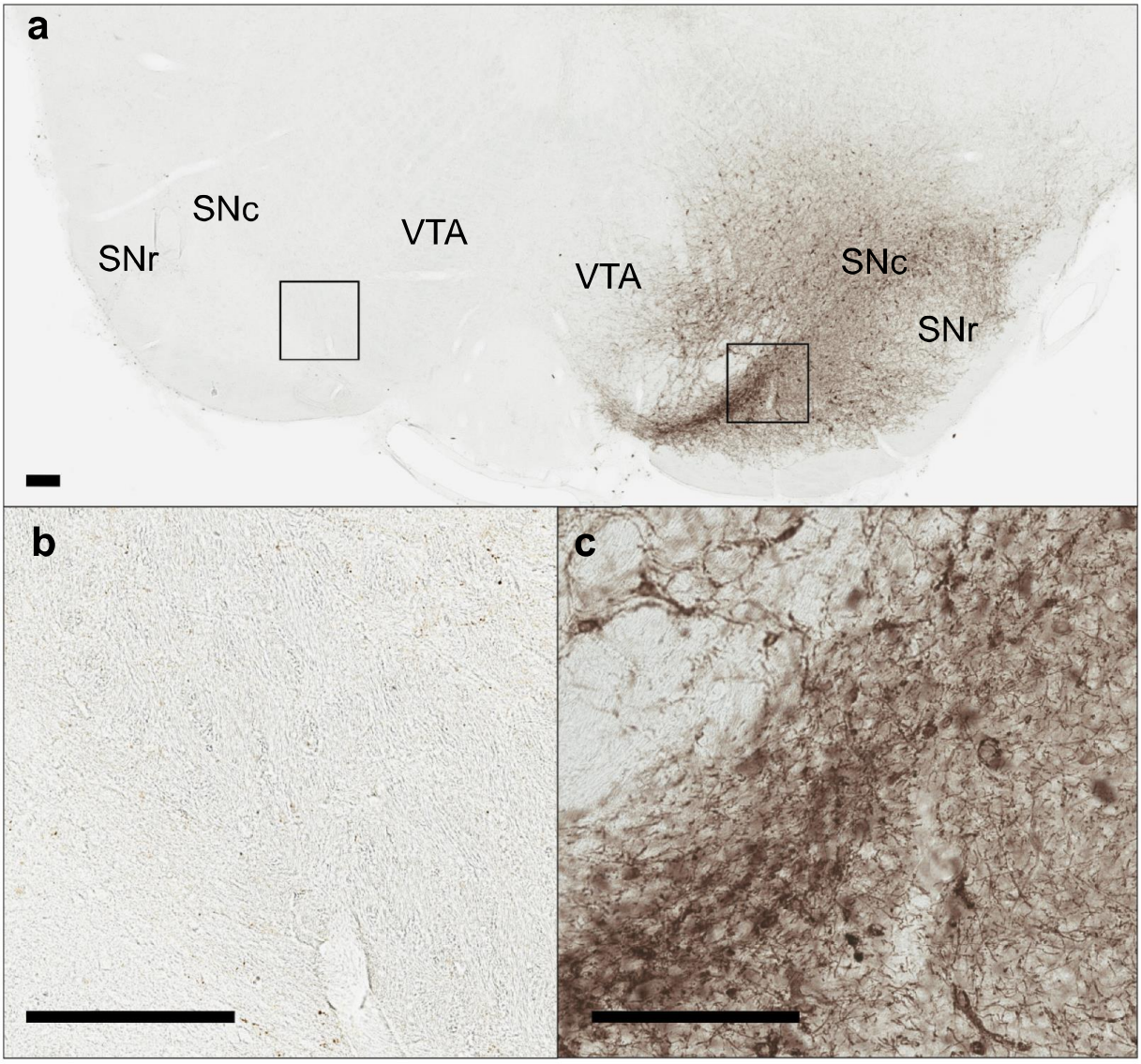

Figure 5.8: Channelrhodopsin-2 expression is restricted to one hemisphere in the midbrain. (a) Low magnification images of ChR2-eYFP expression at the level of the SN/VTA after immunohistochemistry with GFP antibody. Higher magnification images ChR2-eYFP expression in (b) contralateral and (c) ipsilateral midbrain as highlighted in (a). Scale bar = 200µm.

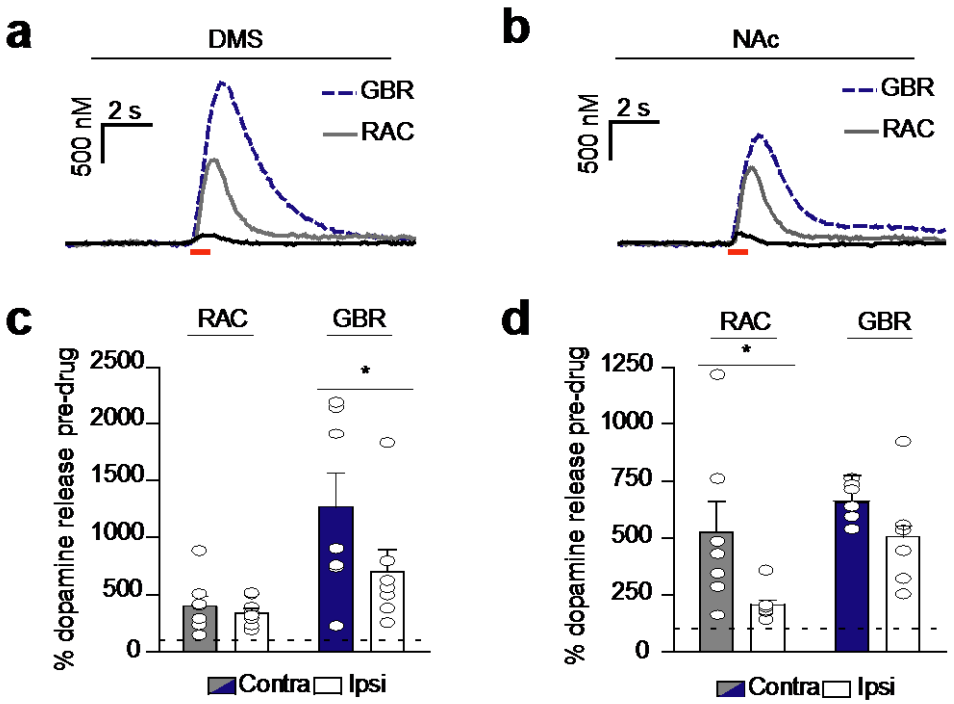

Figure 5.9: Contralateral dopamine release is differentially regulated in the dorsomedial striatum and nucleus accumbens. (a-b) Representative contralateral dopamine efflux in the DMS (a) and NAc (b) after administration of D2 antagonist raclopride (RAC, 2 mg/kg, i.p., gray line) and subsequent transporter blockade (GBR-12909, 15 mg/kg, i.p., blue line) compared to baseline (black). (c-d) Average increase in contralaterally (gray/blue bars) or ipsilaterally (white bars) evoked dopamine after raclopride and GBR-12909 administration as a percent of baseline. N=6-8 animals per group. Data are average ± SEM with individual experiments overlaid. ANOVA with Bonferonni post-hoc, *, P<0.05.

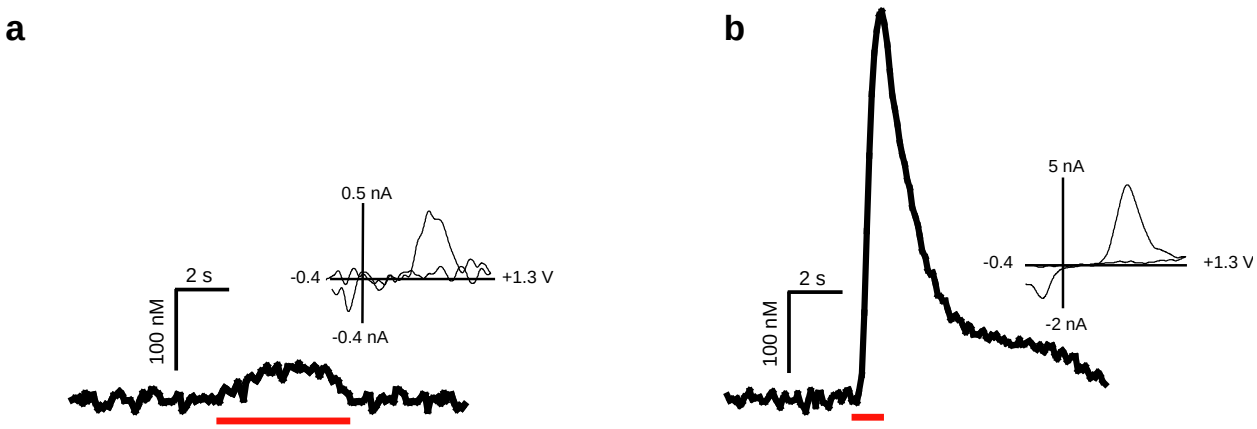

Figure 5.10: Effect of stimulation frequency on contralateral dopamine release. Representative traces with inset cyclic voltammograms in the NAc of a single animal following 5-second, 10 Hz stimulation (a) and 1-second, 60 Hz stimulation (b) of the contralateral VTA. Red bars denote stimulation duration.

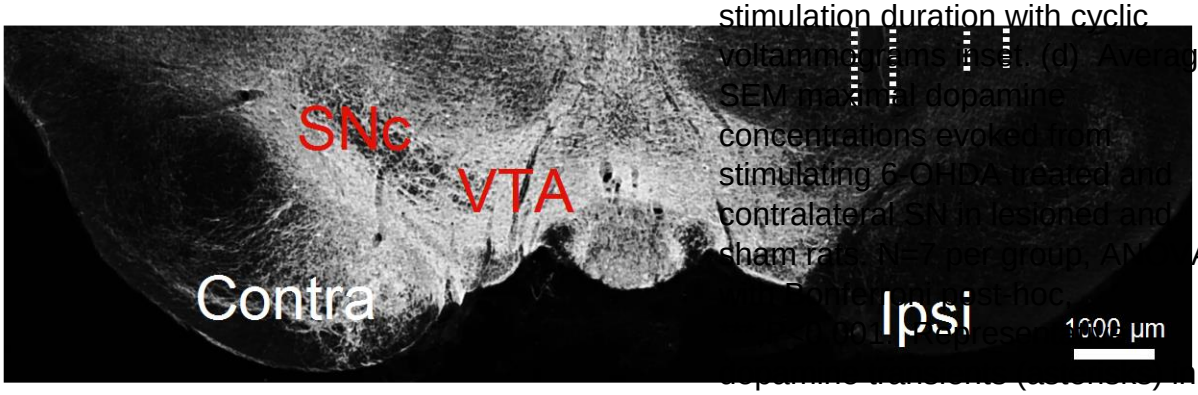

Figure 5.12: Tyrosine hydroxylase immunoreactivity is reduced in the SN after unilateral infusion with 6-OHDA. Hashed lines show tract of cannulated stimulating electrode for 6-OHDA infusion

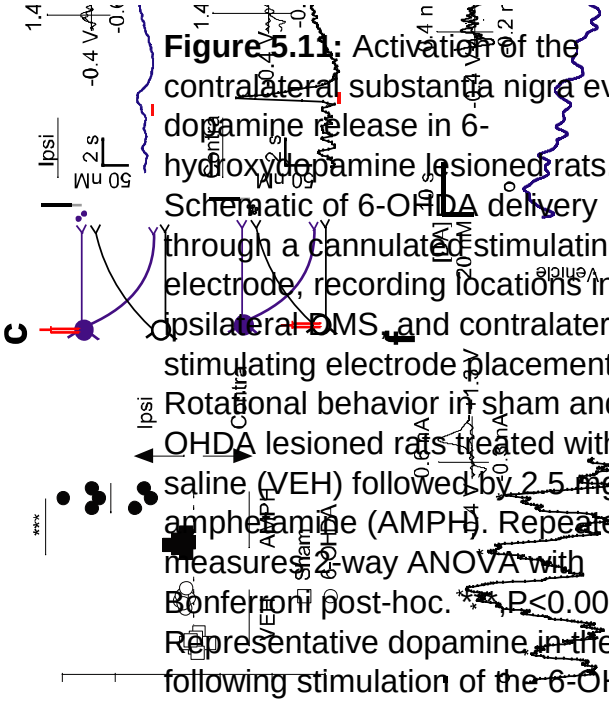

Figure 5.11: Activation of the contralateral substantia nigra evokes dopamine release in 6-hydroxydopamine lesioned rats. (a) Schematic of 6-OHDA delivery through a cannulated stimulating electrode, recording locations in the ipsilateral DMS, and contralateral stimulating electrode placement. (b) Rotational behavior in sham and 6-OHDA lesioned rats treated with saline (VEH) followed by 2.5 mg/kg d-amphetamine (AMPH). Repeated-measures 2-way ANOVA with Bonferroni post-hoc. ***, P<0.001 (c) Representative dopamine in the DMS following stimulation of the 6-OHDA treated SN (purple) and contralateral (black) SN. Red bar denotes stimulation duration with cyclic voltammograms inset. (d) Average ± SEM maximal dopamine concentrations evoked from stimulating 6-OHDA treated and contralateral SN in lesioned and sham rats. N=7 per group, ANOVA with Bonferroni post-hoc [illegible] (e) Representative dopamine transients (detected) in the DMS in awake sham-lesioned (e, black line), or 6-OHDA treated (f, purple line) rats following vehicle and amphetamine. Inset cyclic voltammograms correspond to the dopamine transient marked with a circle.

CHAPTER 6: CROSS-HEMISPHERIC NOREPINEPHRINE RELEASE IN THE VBNST ARISES FROM THE NUCLEUS OF THE SOLITARY TRACT

Introduction

Norepinephrine signaling is important in mediating a variety of processes including learning and memory, drug reward and withdrawal, and the behavioral and physiological responses to stress (Berridge and Waterhouse, 2003; Cecchi *et al*, 2002; Delfs *et al*, 2000; Forray *et al*, 2004; Olson *et al*, 2006). Dysregulation of noradrenergic signaling is implicated in disorders ranging from drug addiction (Koob, 2009) to Alzheimer's disease (Weinshenker, 2008), and the ventral bed nucleus of the stria terminalis (vBNST) is a site of some of the densest noradrenergic innervation in the brain (Kilts *et al*, 1986). Limbic, forebrain, and brainstem inputs converge in the BNST to relay information about stressors and generate an appropriate physiological response through regulation of the hypothalamic-pituitary adrenal axis (Forray *et al*, 2004). The BNST receives noradrenergic input primarily from medullary neurons (A1/A2) coursing through the ventral noradrenergic bundle (VNB) and, to a lesser extent, from the neurons of the locus coeruleus (LC) through the dorsal noradrenergic bundle (DNB) (Forray *et al*, 2004; Robertson *et al*, 2013). Norepinephrine is released in the vBNST during presentation of an aversive tastant, omission of an expected reward, and delivery of a noxious stimulus (Park *et al*, 2015; Park *et al*, 2013; Park *et al*, 2012). Furthermore, the vBNST is an important structure in the mediation of the aversive components of drug-

withdrawal (Aston-Jones et al., 1999; Delfs et al., 2000) and norepinephrine signaling in the vBNST undergoes robust plasticity following stress or drug-withdrawal in a strain-dependent manner (Fox *et al*, 2015; McElligott *et al*, 2013). Regulation of norepinephrine in the vBNST is an important topic of investigation, since it integrates information about aversive and stressful stimuli to generate an appropriate physiological response.

Like all monoamine neurons, norepinephrine neurons are thought to project solely to one hemisphere (Andén NE, 1966). However, we recently uncovered an unexpected population of dopamine neurons that cross the midline to release dopamine in the contralateral striatum (Fox *et al*, 2016a). Although norepinephrine and dopamine traditionally signal in opposition of each other (Park *et al*, 2013; Park *et al*, 2012), we hypothesized that some norepinephrine neurons might also project bilaterally and contribute to norepinephrine release. We used fast-scan cyclic voltammetry combined with retrograde tracing to identify functional cross-hemispheric norepinephrine projections. In this work we found that noradrenergic axon pathways can release norepinephrine in the vBNST contralateral to their origin. While characterizing the origin of contralateral release, we serendipitously discovered that LC and DNB stimulations produce norepinephrine overflow indirectly. Instead, the direct bilateral projections to the vBNST originate in the nucleus of the solitary tract.

Materials and Methods

Volammetric Norepinephrine Measurements

Norepinephrine release was measured in anesthetized animals as described previously (Fox *et al*, 2015). For bilateral norepinephrine measurements, rats were anesthetized with urethane (1.5 g/kg) and placed in a stereotaxic frame. Holes were drilled for the BNST (AP 0mm, ML +1.2mm), the D/VNB (AP -5.2mm, ML +1.2mm), and the LC(AP -9.8mm, ML +1.3mm) referenced from bregma and based on the atlas of Paxinos and Watson. A Ag/AgCl reference electrode was placed in the left hemisphere and secured with a jeweler's screw. A carbon-fiber microelectrode (~100 µm active length) was lowered into the BNST (7-7.5mm DV) and the stimulating electrode was lowered ipsilaterally to the carbon-fiber electrode to the dorsal (-6.5mm DV) or ventral (-8.0mm DV) noradrenergic bundle or LC (-7mm DV) until maximal NE release was attained. Both stimulating and carbon-fiber electrodes were subsequently secured with dental cement. A second carbon-fiber microelectrode was lowered into the ipsilateral BNST (7-7.5mm DV) until maximal norepinephrine was achieved. A total of 10 animals were used for these studies.

For mapping experiments and stimulation duration studies, first a carbon-fiber electrode was lowered into the vBNST until maximal release with ipsilateral VNB stimulations was attained. Next, the stimulating electrode was raised to the DNB to determine maximum ipsilatateral release. Then, the stimulating electrode was lowered through the contralateral hemisphere in 200 µm increments to map the effect of contralateral stimulating electrode placement in the vBNST. 60 Hz stimulations of varying duration (20-120 pulses) were delivered at depths corresponding to maximal

release from contralateral DNB and VNB stimulations and plotted vs. stimulation duration. We compared maximal norepinephrine evoked by ipsilateral and contralateral DNB and VNB stimulations at the same recording electrode location. A total of 6 animals were used for these experiments.

DSP-4 treatment

Adolescent rats (150 – 200 g) were administered DSP-4 (N-(2-chloroethyl)-N-ethyl-2-bromobenzylamine) in two doses (0.5 mL, 50 mg/kg, i.p.) provided 3 days apart (Fox *et al*, 2015). Voltammetric (n=5 DSP-4, n=5 control) and tissue content (n=6 DSP-4, n=5 control) experiments were conducted 10 to 15 days after the last dose.

Tissue Content Analysis

A separate group of rats were anesthetized with urethane (1.5 mg/kg) and decapitated, and their brains were rapidly removed and placed on ice. Coronal sections (300 µm thick) containing the BNST or AV were collected with a VF-200 Compresstome (Precisionary Instruments Greenville, NC) in ice cold artificial cerebral spinal fluid (aCSF). The aCSF contained (in mM) 126 NaCl, 25 $NaHCO_3$, 2.45 KCl, 12 NaH_2PO_4, 1.2 $MgCl_2$, 2.4 $CaCl_2$, 20 HEPES, and 11 glucose, and was adjusted to pH 7.4 and saturated with 95% O_2 /5% CO_2. Tissue containing the vBNST or AV was excised bilaterally with a 1 mm punch, and collected into pre-weighed tubes. The samples were mixed with 200 µL of 0.1 N $HClO_4$ containing 1 µM hydroquinone, the internal standard, and subsequently homogenized using a sonic dismembrator (Fisher Scientific, Model 60, Pittsburgh, PA). The homogenate was spun down at 6000 rpm for 10 minutes, and the supernatant was removed and filtered using a 0.2 µm syringe filter. High performance liquid chromatography was performed using the methods of Mefford and

Lähdesmäki *et al* (Lahdesmaki *et al*, 2002; Mefford, 1981). Briefly, 20 µL injections were made onto a revered-phase column (5 µm, 4.6 x 5 mm, Waters Atlantis, Milford, MA, USA). The mobile phase consisted of 0.1 M citric acid, 1 mM sodium hexylsulfate, 0.1 mM EDTA (pH = 3), and 10% methanol organic modifier at a flow rate of 1.0 mL/min. Norepinephrine and dopamine were detected with a thin layer radial electrochemical cell (BASi, West Lafayette, IN, USA) at a potential of +800 mV vs Ag/AgCl. Data were collected at 60 Hz using a LabVIEW stripchart recorder program (Jorgenson Lab, UNC) and custom-made electronics. Concentration was determined by a ratio of analyte peak area to internal standard peak area, and normalized to wet tissue weight.

6-hydroxydopamine lesions

Rats underwent stereotaxic surgery under isofluorane anesthesia, and an incision was made in the scalp to drill bilateral holes targeting the LC (AP -9.8mm, ML±1.4). An infusion cannula (Plastics One) was lowered to a depth of 7.0mm from brain surface, and 1µL of 10 mM 6-hydroxydopamine hydrobromide (6-OHDA)/ 0.01% w/v ascorbic acid (Sigma-Aldrich) in sterile saline (0.9%), or saline (sham-lesioned) was infused into each hemisphere with an infusion needle (33 ga, 10 mm, Plastics One) over 5 min. The scalp was closed with Vet Bond (3M) and rats were allowed to recover for 2 weeks before being anesthetized with urethane for voltammetric norepinephrine measurements.

Knife-cut experiments

Rat were anesthetized with urethane (1.5 g/kg) and affixed in a stereotaxic frame. Holes were drilled for the vBNST, VNB, and LC as described above. Once

maximal release was attained with VNB stimulations, the stimulating electrode was moved to the LC and adjusted for maximal release. The stimulating electrode was subsequently removed, and a surgical blade was lowered 0.2mm past the depth of maximal LC release. The stimulating electrode was repositioned in the LC, and norepinephrine release was measured after subsequent LC stimulations. A total of 5 animals were used for these experiments.

FluoroGold Tracing

Rats underwent stereotaxic surgery under isoflurane anesthesia (4% induction, 1.5% maintenance). A small incision was made in the scalp and a hole was drilled in the skull to target the BNST (AP 0.0mm, ML 1.2mm) and a 2 µL Hamilton syringe was lowered to a depth of 7.2 mm from brain surface. 200 nL of FluoroGold (4% w/v in 0.9% saline, Fluorochrome, Denver, CO) in was infused slowly over 5min using a microinjection unit (Model 500, Kopf, Tujunga, CA). The syringe was left in place for an additional 5 min to minimize spread up the tract. The scalp was closed with vet bond (3M, St Paul, MN) and rats were allowed to recover for 2 weeks. Rats were then anesthetized with urethane (1.5 g/kg) and transcardially perfused with 0.1M phosphate buffered saline (PBS, pH 7.4), followed by 4% paraformaldehyde dissolved in PBS. Brains were subsequently removed and post-fixed for >24 hr in 4% paraformaldehyde. The fixed tissue was cryoprotected for >24 hr in 30% sucrose before 30 µm sections were collected in PBS using a freezing microtome (Leica, Germany).

Free-floating sections were incubated in 1%$NaBH_4$/0.1M PBS for 15 min to quench endogenous fluorescence, and then rinsed in PBS 3x 15 min. Sections were blocked in 10% Normal Goat Serum (NGS)/ 0.3% Triton x-100 for 2 hr at RT. After

blocking, sections were incubated in 1:1000 Rabbit-anti-FluoroGold (Fluorochrome) in 3% NGS 0.1%Triton x-100 overnight at 4ºC. Sections were washed in PBS before being incubated for 2 hr in 1:500 Goat anti Rabbit-FITC in 2% bovine serum albumin/0.1M PBS at RT. Sections were rinsed 3x in PBS, then mounted, dried, and coverslipped with fluoromount (Sigma Aldrich) for imaging on an Olympus FV1000 confocal microscope.

Ibotenic Acid Infusion

Electrical stimulation of the DNB was repeated every 3 min over a 1 h period to establish a baseline for norepinephrine release. Thereafter the stimulating electrode was removed and the tip of a 2 µL Hamilton syringe containing sterile saline was positioned 500 µm dorsal to the original stimulation depth. The saline was infused manually with a microinjection unit (Model 500, Kopf, Tujunga, CA, USA) over a 20 min period and the syringe was removed for reinsertion of the stimulating electrode. Stimulations commenced for another 1 h period before the infusion procedure was repeated with 2 µL ibotenic acid (130 mM in 2% Chicago Sky Blue prepared in sterile saline, Abcam, Cambridge, MA, USA). The last 15 min of data collected for baseline, post-saline and post-IBA were used in analysis

Results

Stimulation of noradrenergic axons elicits release in the contralateral vBNST

To determine if norepinephrine in the vBNST could be elicited by contralateral stimulations, we lowered carbon-fiber electrodes bilaterally into the vBNST and a stimulating electrode into the VNB (Schematic in Fig 6.1A). Unilateral VNB stimulation produced norepinephrine release at both electrodes (Examples in Fig 6.1B). We next mapped contralateral release by holding a carbon-fiber at a fixed depth in the vBNST (-

7.2mm DV), and lowered the stimulating electrode ventrally in 200 µm increments through the contralateral hemisphere. Contralateral norepinephrine release was seen over a large dorsal-ventral range, but it peaked at locations corresponding to the DNB (6.4 mm DV) and VNB (8.0 mm DV Fig 6.1C). Norepinephrine release evoked by DNB and VNB stimulation was linear with increasing stimulation duration (DNB slope= 0.146 ± 0.007 r^2=0.97; VNB slope=0.170 ± 0.005, r^2=0.98; Fig 6.1D). On average, maximal norepinephrine release in the vBNST was of similar magnitude following stimulations of the contralateral DNB or VNB (DNB: 0.214 ± 0.066 µM; VNB: 0.192 ± 0.038 µM, *n*=10, respectively), and ipsilateral DNB and VNB (DNB: 0.228 ± 0.063µM; VNB: 0.191 ± 0.029 µM, *n*=10, respectively). In a subset of animals, we performed within-animal comparisons of ipsilateral vs contralateral release by lowering the stimulating electrode ventrally through the ipsilateral, then contralateral hemisphere. The ratio of ipsilateral to contralateral release was equal between hemispheres, regardless of DNB/VNB stimulation (Ipsi/Contra, VNB: 1.3± 0.20; DNB:1.0 ±0.08, n=6 animals, *P*>0.05, Fig 6.1E).

DSP-4 treatment does not attenuate vBNST norepinephrine release

The DNB mainly contains axons originating from the LC, and the vBNST receives very little coerulean innervation. Since both DNB and VNB stimulations produced surprisingly similar release amplitudes, we next placed our stimulating electrode in the LC to ascertain its influence over contralateral release. Stimulations of the contralateral and ipsilateral LC produced norepinephrine release to an equal extent (Ipsi: 0.163 ± 0.082 µM; Contra 0.250 ± 0.115µM, *n*=5, *P*>0.05). To examine the possibility that release was due to off-target effects we employed the selective neurotoxin DSP-4 to

lesion norepinephrine from the LC. Tissue content analysis revealed the treatment effectively eliminated some LC innervation, as concentrations were reduced in the anteroventral thalamus (AV), a brain region receiving exclusively coerulean input (Table 6.1). Control values for the vBNST and the AV are similar to those previously reported from our lab (McElligott *et al*, 2013; Park *et al*, 2009) and others (Kilts *et al*, 1986; Oke *et al*, 1983). DSP-4 treatment significantly reduced norepinephrine and dopamine in the AV (unpaired student's t-test, NE: $t(9)=3.579$, $P=0.006$; DA: $t(9)=2.586$, $P=0.029$), but did not exhibit an effect on the catecholamine content of the vBNST (NE: $t(9)=0.959$, $P=0.363$; DA: $t(9)=0.371$, $P=0.719$).

DSP-4 treatment did not affect release with VNB stimulations, in agreement with our previous work (Fox *et al*, 2015) and tissue content analysis (Control vs. DSP-4, 0.281± 0.046 vs 0.408 ±0 .104 µM, n=5 animals, respectively, Fig 6.2A). Surprisingly, DSP-4 treatment did not reduce norepinephrine evoked by DNB or LC stimulations (Control vs. DSP-4, DNB: 0.288 ± 0.046 vs 0.386±-0.154; LC 0.163 ± 0.032, 0.237± 0.073 µM, n=5 animals, respectively, P>0.05 Fig 6.2A).

Physical, but not 6-OHDA LC lesions attenuate vBNST norepinephrine release

Since DSP-4 does not lesion the LC with 100% efficacy (Bortel, 2014), and its actions on the LC noradrenergic system have been called into question (Szot *et al*, 2010) we next used bilateral 6-hydroxydopamine (6-OHDA) lesions targeted to the LC to corroborate the DSP-4 findings. 2-weeks after 6-OHDA treatment, we anesthetized animals and recorded norepinephrine evoked from electrical stimulations. Similar to DSP-4 treatment, 6-OHDA lesions of the LC had no measurable effect on vBNST norepinephrine release (Sham vs 6-OHDA; DNB: 0.364 ± 0.092 vs 0.342 ± 0.054 µM;

VNB: 0.339 ± 0.065 vs 0.457± 0.072 µM; LC 0.213 ± 0.082 vs 0.278± 0.060 µM, n=5 animals, respectively, *P*>0.05 Fig 6.2B). Given that chemical ablations did not reduce norepinephrine release, we turned to a physical disconnection approach by performing a knife-cut at the level of the LC. Cutting the LC reduced LC-evoked norepinephrine release in the vBNST to ~10% of its original value (9.0 ±6.1%, n=5 animals).

A2, but not LC neurons project bilaterally to the vBNST

Since a physical, but not chemical lesion of the LC reduced norepinephrine overflow, we asked if the LC was sending projections to the vBNST that might be spared by the chemical treatments. We unilaterally injected fluorogold into the vBNST, and looked for retrograde labeling in the LC and the nucleus of the solitary tract (A2) (schematic in Fig 6.3A, representative injection site Fig 6.3B). Even after signal amplification with an antibody against fluorogold, we did not find any retrogradely labeled cells in the LC (Fig 6.3C,D). Instead, we found bilateral fluorogold labeling in the A2 (Fig 6.3E-G). The number of labeled cells ipsilateral to the tracer infusion was greater than those in the contralateral hemisphere (27± 1.7 vs 5.3±1.2 cells, n=3 animals).

DNB stimulations produce vBNST norepinephrine indirectly

The LC sends most of its forebrain projections through the DNB (Nakazato, 1987; Ungerstedt, 1971). Since the LC was not labeled with fluorogold, we hypothesized that DNB stimulations produced norepinephrine release through an indirect mechanism. To test the possibility that another midbrain structure was mediating norepinephrine release, we delivered ibotenic acid (IBA) through a cannulated stimulating electrode targeted to the DNB (Schematic in Fig 6.4A). IBA is an

excitotoxic agent that causes cell loss within an area closely confined to the locus of its injection, but does not target afferent terminals or fibers of passage (Jarrard, 1989). IBA infusions reduced vBNST norepinephrine release elicited by DNB stimulations compared with saline infusions (Saline: 77.9 ± 3.3% vs. IBA: 20.3 ±3.8 %, n=5 respectively, 2-way RM ANOVA: Drug x region interaction $F(2,16)=16.52$, Effect of region $F(2,16) =21.47$, Effect of drug $F(2,16) =46.67$, Fig 6.4 B,C). IBA treatment did not reduce evoked norepinephrine in the AV, consistent with the lack of effect this toxin has on axons of passage (Saline: 68.0± 4.3% vs IBA: 70.8± 10.4%, n=5 animals, Fig 6.4 B,C). Post hoc analysis revealed significant attenuation of vBNST, but not AV release compared with saline (Bonferroni, Saline vs IBA $p<0.001$). Thus, DNB evoked NE in the vBNST, but not AV, arose from an indirect mechanism

Discussion

In this study, we found norepinephrine release was elicited in the vBNST contralateral to the electrical stimulation location. Stimulations of the DNB, VNB, and LC evoked norepinephrine of equal magnitude in both hemispheres. Norepinephrine evoked from LC stimulations occurred via nonspecific activation, as only physical, but not selective chemical lesions of the LC attenuated release. DNB stimulations also elicited norepinephrine in a non-specific way, since inactivation of cells proximal to the DNB reduced evoked vBNST norepinephrine. Furthermore, fluorogold tracing revealed the A2, but not LC, sends bilateral projections to the vBNST. Taken together, these data show that although norepinephrine is released in both hemispheres with unilateral activation, only the projections from the A2 are directly responsible for cross-hemispheric release in the vBNST.

Anatomical studies describe noradrenergic neurons as projecting primarily unilaterally (Andén NE, 1966; Ungerstedt, 1971). Recent reports have uncovered that a small percentage of dopamine neurons project contralateral to their origin (Geisler *et al*, 2005; Jaeger *et al*, 1983) and support dopamine release in the striatum (Fox *et al*, 2016a), however no studies have described cross-hemispheric noradrenergic projections originating in the A2. In this work we found norepinephrine was released in both hemispheres after VNB stimulations, supported by bilateral retrograde labeling in the A2. Surprisingly, release elicited by VNB stimulations was equivalent between hemispheres, despite the smaller number of projections originating in the contralateral A2. This equivalent release could arise from a number of mechanisms. First, norepinephrine concentrations are tightly regulated and require much longer stimulation trains compared with dopamine (Miles *et al*, 2002; Park *et al*, 2011). Since norepinephrine concentrations released from contralateral projections were linear with respect to stimulation duration, similar to ipsilaterally evoked concentrations (McElligott *et al*, 2013), this might indicate that norepinephrine release is “capped” from ipsilateral projections. Although there are more ipsilateral than contralateral projections, regulation mechanisms may attenuate the amount of norepinephrine released from ipsilateral projections to create hemispherically equivalent release. Alternatively, norepinephrine neurons may co-release glutamate, which was recently demonstrated to occur from some dopamine terminals (Zhang *et al*, 2015). Co-release of other neurotransmitters may depolarize norepinephrine terminals in the vBNST and partially explain the apparent hemispheric equivalence. Regardless, these data reveal that norepinephrine in the vBNST is similar to dopamine release in the dorsomedial striatum

(Fox *et al*, 2016a) in that it is of equivalent magnitude with ipsilateral or contralateral stimulations.

The vBNST is thought to receive a small input from the LC (Forray *et al*, 2004; Robertson *et al*, 2013), and in a previous study, we characterized norepinephrine overflow with LC stimulations (Park *et al*, 2009). In this work, we found that stimulation of the LC and its projections through the DNB produced equivalent norepinephrine release in both hemispheres. However, this release arises from a non-coeruelan mechanism since selective chemical lesions of the LC did not attenuate norepinephrine release, and fluorogold was not retrogradely transported from the vBNST to the LC. In our initial characterization of LC-evoked norepinephrine, release was suppressed after delivery of lidocaine to the stimulation site (Park *et al*, 2009). Similar to lidocaine, we found a knife-cut of the LC drastically attenuated norepinephrine overflow in the BNST. This finding brings up two important points. First, selective chemical inactivation with DSP-4 and 6-OHDA strongly suggest that noradrenergic neurons of the LC are not responsible for release in the vBNST. However, both lidocaine and knife-cut would prevent the propogation of action potentials traveling down axons near the LC. It is therefore possible that projections from medullary noradrenergic neurons close to the LC are responsible for this release. Indeed, an anterograde tracing study revealed A2 neurons innervate regions proximal to the LC (Geerling and Loewy, 2006). Second, the A2 projects to the nucleus paragigantocellularis (PGi) (Reyes and Van Bockstaele, 2006), which in turn, sends projections to the LC (Ennis and Aston-Jones, 1988). Therefore, stimulating the LC may antidromically activate the PGi and subsequently the A2 to produce norepinephrine release. Cross-talk between noradrenergic cell groups is

supported by work demonstrating both coerulean and medullary norepinephrine contribute to opiate withdrawal syndrome (Delfs *et al*, 2000; Maldonado, 1997), and coerulean lesions produce adaptations in norepinephrine signaling originating from the A2 (Fox *et al*, 2015). Regardless of mechanism, the selective chemical lesions reveal that although the LC can produce release in both ipsilateral and contralateral vBNST, it does so indirectly.

Stimulations of the DNB also produced release in the ipsilateral and contralateral vBNST, and when we infused IBA into the DNB we found blunted release in the vBNST. IBA is a glutamate analog that, through excitotoxicity, selectively inactivates cell bodies while leaving fibers of passage intact (Jarrard, 1989). Therefore its neurotoxicity is not expected to impact the axons of the DNB. In agreement with this, norepinephrine was not significantly altered in the AV, supporting that norepinephrine release in this region is mediated by direct activation of the DNB. However release was markedly attenuated in the vBNST after IBA treatment, suggesting other midbrain nuclei are mediating release. At the coordinates used in this study, the DNB courses by several structures including the periaqueductal gray (PAG). Fluorogold infusions into the ventrolateral portion of the PAG bilaterally labels neurons in the A2 region (Chang *et al*, 2012b). Thus, one possible explanation for contralateral norepinephrine release produced by DNB stimulations may be through a PAG mechanism. PAG stimulation may antidromically activate the A2 group to elicit vBNST release in both hemispheres and future efforts should address this possibility. Regardless, the results of the chemical lesions of both DNB and LC suggest that DNB-evoked norepinephrine release arises via an indirect mechanism.

Unilateral manipulation of catecholaminergic neurons is often used to model neurodegenerative conditions such as Parkinson's disease (Zigmond *et al*, 1990). Additionally, unilateral knife-cut of the DNB was used in a recent report to rule out contributions of LC norepinephrine to measured catecholamine release in the medial prefrontal cortex (Shnitko *et al*, 2014b). The cross-hemispheric projections found from the A2 call into question the nature of LC projections. Indeed, LC neurons project bilaterally to some regions (Simpson *et al*, 1997) and may release physiologically relevant concentrations in the contralateral hemisphere. It is clear from these findings that care must be taken when performing unilateral disconnection studies, since the unilateral monoamine projections originally described by Ungerstedt (Andén NE, 1966; Ungerstedt, 1971) are now being called into question.

In summary, this work demonstrates that stimulation of noradrenergic pathways elicits release in the contralateral vBNST. These projections arise from the A2, and stimulations of the VNB produce hemispherically equivalent release. While projections from the LC also elicit norepinephrine release in the vBNST, they do so indirectly. This previously undescribed property or norepinephrine neurons should be taken into account when performing unilateral manipulations.

Support.

Elizabeth Bucher contributed to this work. This work was funded by NIH grant DA10900 to RMW.

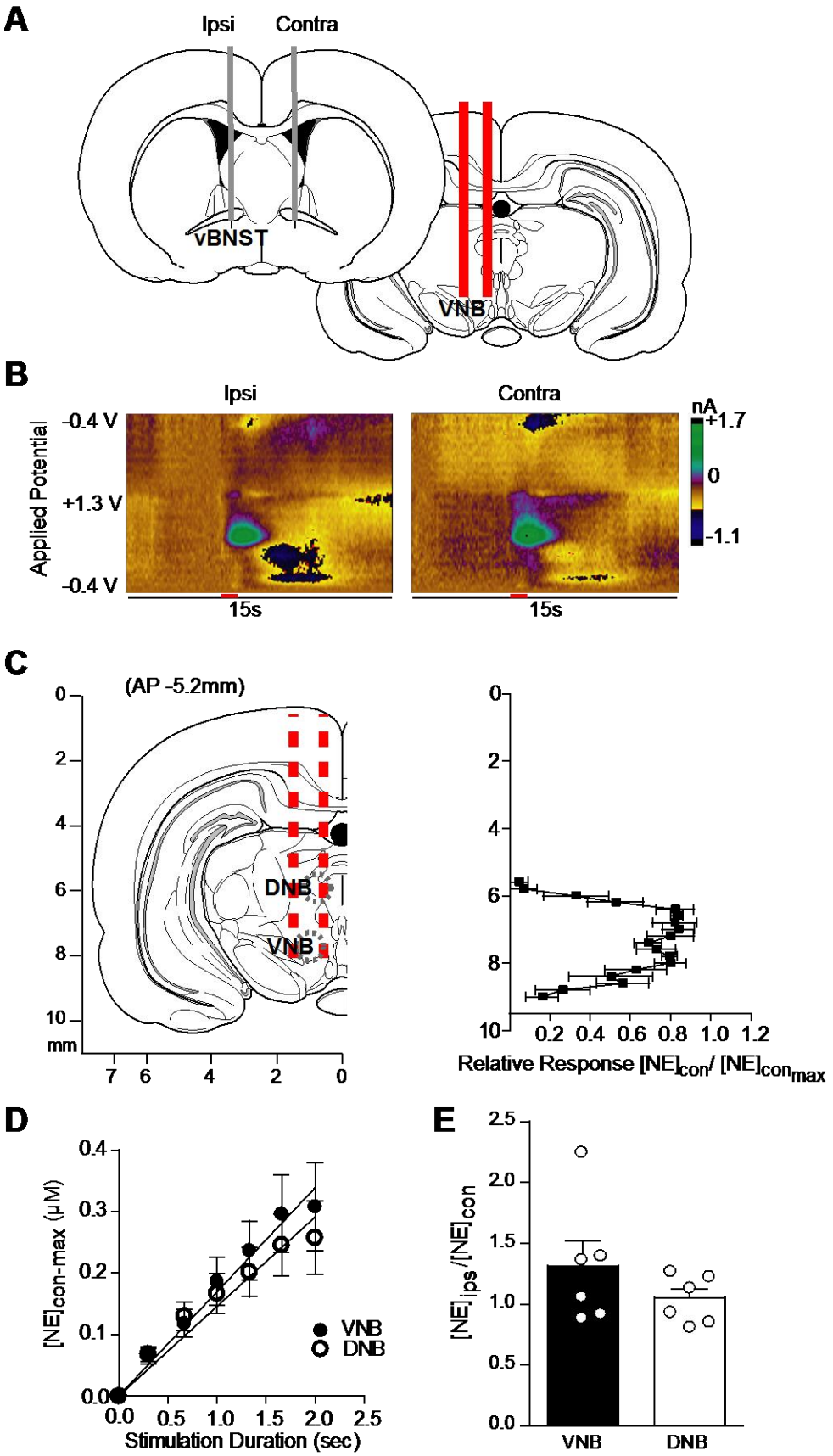
A
Ipsi
Contra
vBNST
VNB
B
Ipsi
Contra
nA
+1.7
0
-1.1
Applied Potential
-0.4 V
+1.3 V
-0.4 V
15s
15s
C
(AP -5.2mm)
DNB
VNB
mm
Relative Response [NE]con/ [NE]conmax
D
[NE]con-max (μM)
VNB
DNB
Stimulation Duration (sec)
E
[NE]ips /[NE]con
VNB
DNB

Figure 6.1. Stimulation of noradrenergic axon bundles produces hemispherically equivalent norepinephrine release in the vBNST. (A) Schematic of dual carbon-fiber electrodes in the vBNST with unilateral stimulating electrode in the VNB. (B) Representative color plots demonstrating norepinephrine release to a 1 s electrical stimulation (red bar) of the VNB, recording ipsilateral (Ipsi) and contralateral (Contra) to the stimulation. Applied potential is plotted on the absiscca, recording time on the ordinate, and current is encoded in false color. (C) Effect of stimulation electrode placement on contralateral norepinephrine release. Data are plotted as norepinephrine release [NE]con over maximal norepinephrine release [NE]con-max as elicited by contralateral stimulations and are presented as average±SEM. (D) Effect of stimulation duration on norepinephrine release evoked by contralateral DNB and VNB. Average±SEM (E) Within-animal comparison of norepinephrine release in the vBNST as elicited by ipsilateral and contralateral DNB and VNB stimulations. Average±SEM with individual experiments overlaid.

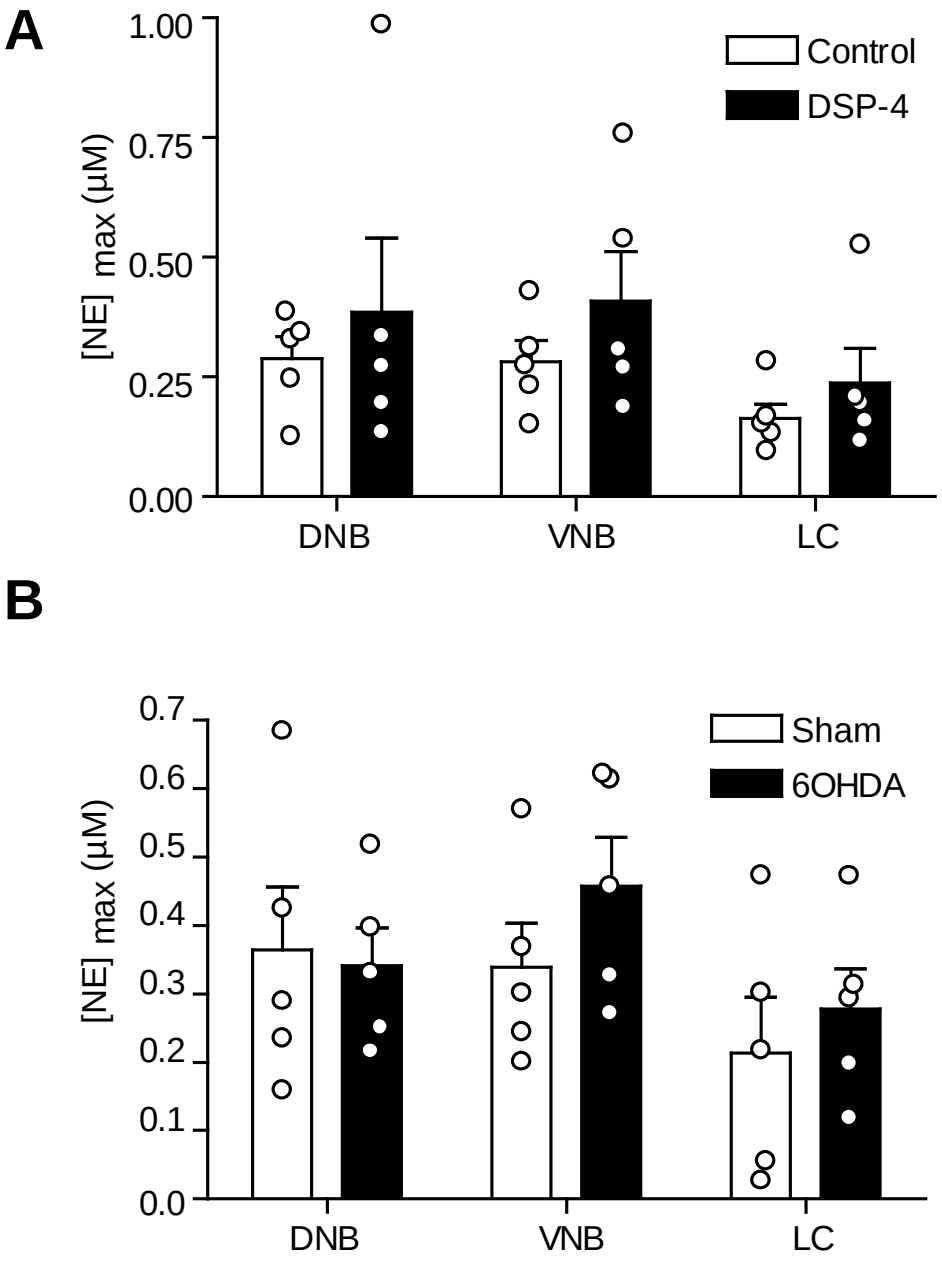

Figure 6.2: Chemical lesions of the LC do not impact vBNST norepinephrine release. (A) Maximal norepinephrine concentrations elicited by DNB, VNB, and LC stimulations in control (white, 5 animals) and DSP-4 treated rats (black, 5 animals). (B) Maximal norepinephrine concentrations elicited by DNB, VNB, and LC stimulations in sham (white, 5 animals), and 6-OHDA lesioned rats (black, 5 animals). Average±SEM with individual experiments overlaid.

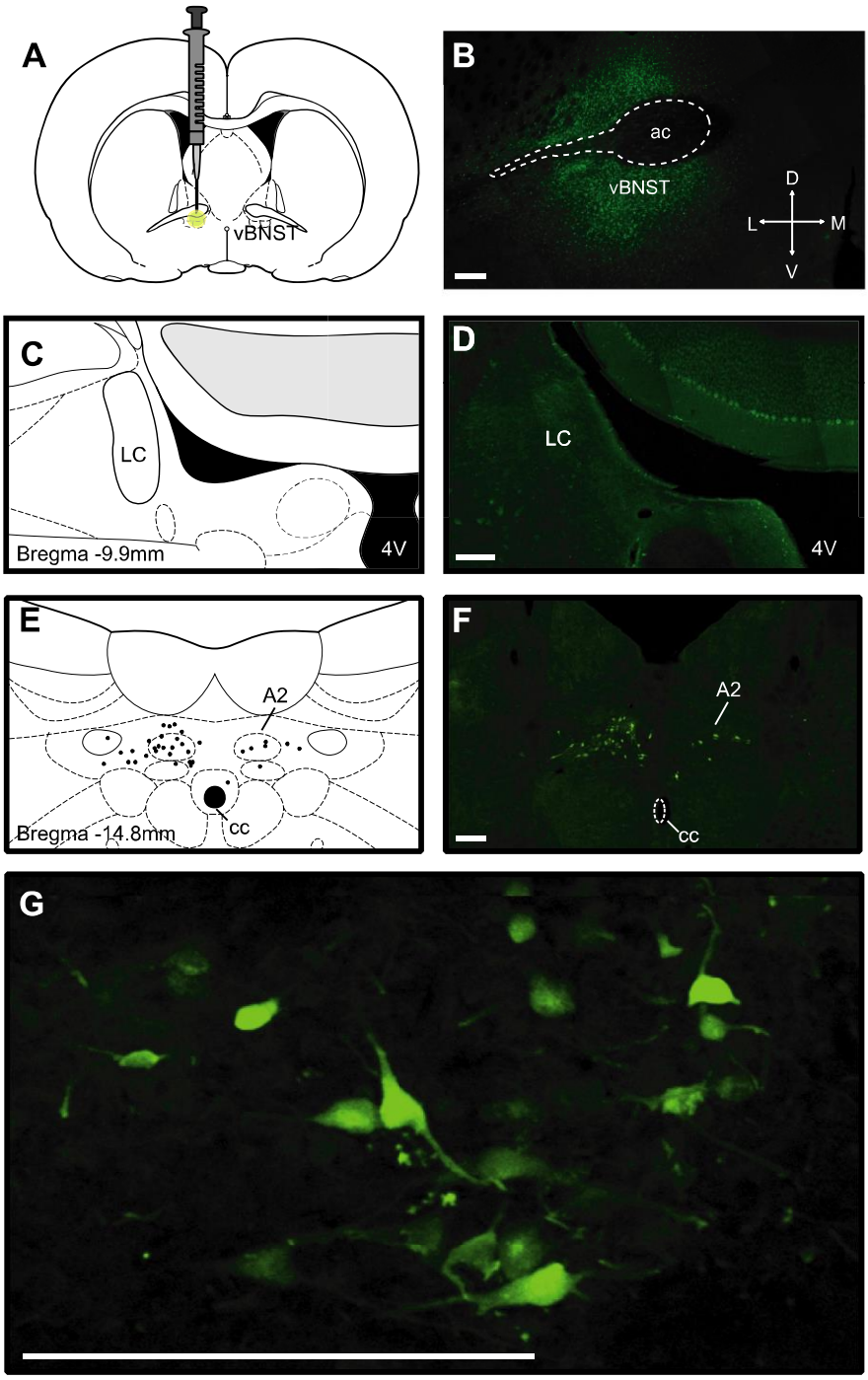

Figure 6.3: Unilateral fluorogold tracing in the vBNST. (A-B) Schematic and representative infusion site of FG into the vBNST. (C-D) Apparent lack of FG-positive cells in the LC and atlas section corresponding to the photomicrograph. (E-F) FG-positive cells in the A2 and atlas section corresponding to the photomicrograph. (G) Higher magnification image of FG-positive cells in the A2. Scale bars are 200µm. Abbreviations: vBNST, ventral bed nucleus of the stria terminalis; LC, locus coeruleus, cc, central canal; 4V, fourth ventricle.

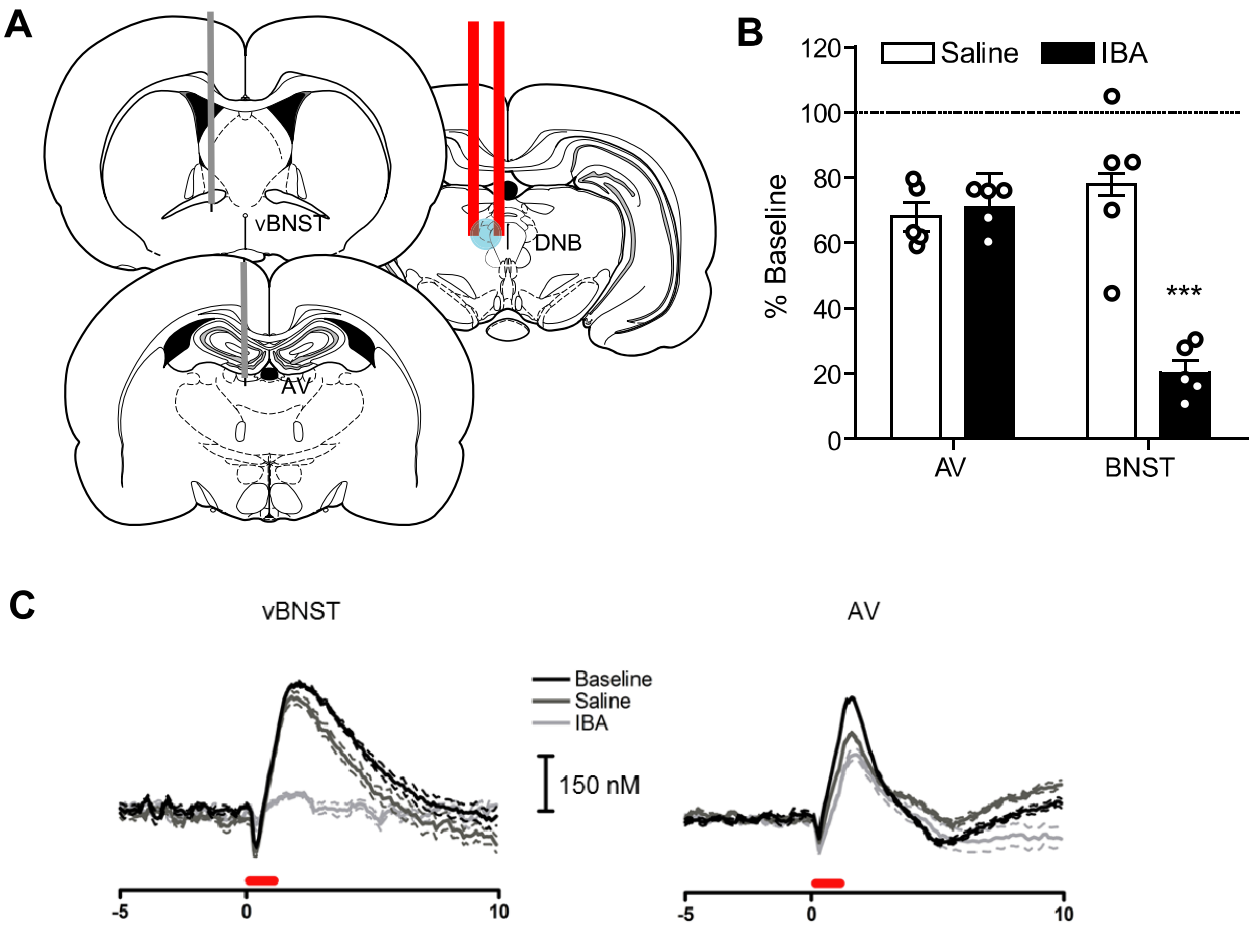

Figure 6.4. Ibotenic acid infusions in the DNB attenuate norepinephrine release in the vBNST, but not AV. (A) Schematic of recording locations and infusion of IBA in the DNB. (B) Effect of saline (white) and IBA (black) infusions on norepinephrine release in the vBNST and AV as a percent of baseline release (hashed line).***, P<0.01, 2-way RM ANOVA with Bonferroni post-hoc (C) Representative evoked norepinephrine in the vBNST and AV after saline and IBA infusions. Red bar denotes electrical stimulation.

	NE (µg/g Tissue)		DA (µg/g Tissue)	
	Untreated	DSP-4	Untreated	DSP-4
vBNST	2.98 ± 0.80	2.14 ± 0.58	0.82 ± 0.25	0.84 ± 0.17
AV	1.82 ± 0.50	0.18 ± 0.10**	1.62 ± 0.52	0.34 ± 0.20*

Table 6.1. Catecholamine tissue content in target regions for untreated and DSP-4-treated animals. Values are shown as mean ± SEM. *P < 0.05, **P < 0.01, compared to untreated values. Abbreviations: NE, norepinephrine; DA, dopamine.

CHAPTER 7: CONCLUSION

Adaptations in in vivo norepinephrine regulation

The goal of this work was to measure functional adaptations to norepinephrine signaling *in vivo*. Prior studies established that FSCV could be used to measure norepinephrine overflow and regulation in intact animals (Herr *et al*, 2012; Park *et al*, 2009). With the careful pharmacological and histological verification described in Chapter 1, we were able to selectively monitor norepinephrine in the vBNST. Since noradrenergic signaling plays a key role in stress and aversion, and vBNST norepinephrine can activate the HPA axis (Forray *et al*, 2004), we first used animal models with divergent HPA axis function to examine how noradrenergic signaling may differ with varying stress-susceptibility. The results of these experiments are described in Chapters 2 and 3 (Fox *et al*, 2015; McElligott *et al*, 2013). In this work, we found a correlation between anxiety-like behavior and norepinephrine signaling in the vBNST. In the inbred Lewis rat, a model of PTSD, we found increased norepinephrine tissue content, a slow rate of norepinephrine clearance, and blunted α_2 receptor control over norepinephrine release. In the inbred Wistar-Kyoto (WKY) rat, a model of depression, we found norepinephrine regulation mechanisms similar to those of the outbred Sprague-Dawley (SD) rat, with correspondingly low levels of anxiety-like behavior. When we subjected each rat strain to a host of stressors, adaptations in noradrenergic signaling varied dependent on HPA axis function. For example, morphine-dependent SD rats exhibited reduced α_2 function, slowed norepinephrine clearance, and increased

anxiety-like behavior. In contrast, morphine-dependent Lewis rats did not become more anxious, nor were vBNST norepinephrine control mechanisms altered as compared with baseline. WKY rats exhibited an intermediate phenotype with decreased α_2 function and increased anxiety without an accompanying change in norepinephrine clearance rate. Following the stress of social-isolation, noradrenergic synaptic function in SD rats was similar to that of morphine-dependent SD, whereas WKY rats were unaffected by social isolation. Additionally, depletion of LC norepinephrine produced an anxious/morphine-dependent profile in SD rats without changing the behavior or noradrenergic regulation mechanisms in WKY rats. The findings detailed in Chapters 2 and 3 demonstrate that noradrenergic signaling can undergo robust plasticity in response to different manipulations. The response of the noradrenergic system to stress and drug-exposure is dependent on genetic factors and correlated with anxiety-like behavior. Furthermore, they suggest that genetic factors may interact with stress to predispose individuals to drug-addiction, since after stress, noradrenergic synaptic function resembles a drug-dependent phenotype.

Real-time catecholamine overflow during drug-intoxication and withdrawal

Since vBNST norepinephrine regulation underwent robust plasticity after morphine-dependence, we measured neurochemical signaling in awake animals during a single-drug exposure and withdrawal episode to elucidate the mechanism. We compared norepinephrine in the vBNST with dopamine in the NAc after morphine exposure and naloxone-precipitated withdrawal. The results of these experiments are described in Chapter 4. In the NAc, we found increased dopamine transients during drug exposure, in contrast to a lack of norepinephrine overflow in the vBNST. When the

animals underwent naloxone precipitated withdrawal, dopamine transients decreased in frequency and magnitude in the NAc, and we measured broad norepinephrine release events in the vBNST that occurred with somatic withdrawal behaviors. Norepinephrine and withdrawal behaviors were elicited in the absence of morphine by administering an α_2 antagonist with naloxone. Remarkably, at the end of the treatment, norepinephrine concentrations were depleted in the vBNST, in agreement with the reduced norepinephrine tissue content in Chapter 2. This was in stark contrast to unchanged NAc dopamine after the treatment. These findings provide a real-time picture of how noradrenergic synaptic function becomes dysregulated in morphine dependent animals. During withdrawal, norepinephrine is released in the vBNST where it can bind α_2 receptors. The continued occupation of α_2 receptors by norepinephrine can result in α_2 desensitization, which we describe in Chapters 2 and 3. This disruption in control over norepinephrine release by α_2 autoreceptors likely facilitates the development of anxiety and the negative affect via exacerbated norepinephrine signaling. Additionally, dopamine concentrations decreased in the NAc during withdrawal. In the allostasis model, the transition to drug abuse is characterized by both deficits in dopaminergic signaling and enhanced noradrenergic signaling (Koob *et al*, 2010). How the opposing responses of these catecholamines develop longitudinally should be a topic of future investigation.

Unexpected cross-hemispheric catecholamine projections

In characterizing aspects of catecholamine release and regulation, we serendipitously discovered an unexpected property of catecholamine neurons which is described in Chapters 5 and 6. Traditionally, catecholamine neurons were thought to

project solely unilateral to their origin (Andén NE, 1966). We found that stimulations of the VTA and SN elicited dopamine in the contralateral dorsal and ventral striatum. Transient dopamine concentrations were synchronized between hemispheres in the NAc, and D2 regulation of dopamine release was different between contralateral and VTA projections. Furthermore, in a hemiparkinsonian model, intact contralateral projections from the SN could be stimulated with amphetamine to restore dopamine transients in an otherwise depleted dorsomedial striatum. Similar to our findings with dopamine, stimulations of noradrenergic cell groups and their afferent projections also elicited release in the contralateral vBNST. Subsequent characterization revealed only those arising from the A2 group produced release directly. These findings highlight the importance of combining functional measurements with anatomical tracing. Our measurements provide new insight regarding the function of catecholamine neurons. In the case of dopamine neurons, both nigrostriatal and mesolimbic groups directly produced contralateral release; in contrast, only norepinephrine neurons from the A2 were directly responsible for cross-hemispheric norepinephrine in the vBNST.

Future Directions

Over the last four decades, voltammetry has been used to characterize release and uptake of catecholamines. The technology has sufficiently advanced to allow for measurements in awake and behaving animals, and numerous works have focused on dopamine fluctuations during a variety of tasks. Yet it is only within the last ten years that FSCV has been used for norepinephrine measurements in awake animals. Although dopamine and norepinephrine appear to signal in opposition of each other, it is too soon to make sweeping generalizations about the function of dopamine vs.

norepinephrine in shaping action selection and behavior. For convenience we tend to think about patterns of signaling that arise after an animal is well trained. Dopamine is released during presentation of reward-predicting cues; norepinephrine is released during omission of a reward. Dopamine increases during a positive stimulus; norepinephrine increases during a negative stimulus. However, it is important to note that even within a rewarding-seeking paradigm there are aspects that might be aversive to rodents. Although an audiovisual cue may eventually predict reward and elicit dopamine, presentation of a noise and a light may initially be aversive to an animal. How does catecholamine signaling change during learning about rewards? How does it change while learning about avoiding negative stimuli? Are these patterns maintained in other catecholamine containing regions such as the prefrontal cortex? How do they change in individuals with Parkinson's or Alzheimer's disease? Furthermore, the last several decades of work has focused on signaling in outbred rats, despite evidence that signaling exhibits incredible variability in diverse genetic models. Dopamine transients are heterogeneous in outbred SD rats (Wightman *et al*, 2007), however this may not hold true in other strains. Additionally, most measurements have been restricted to male animals, even though sex plays a role in the development of drug addiction (Becker and Koob, 2016). Great strides have been made in understanding the dynamic processes controlling release and uptake of catecholamines, but there are many unresolved questions with respect to their function in shaping behavior.

REFERENCES

Addy NA, Daberkow DP, Ford JN, Garris PA, Wightman RM (2010). Sensitization of rapid dopamine signaling in the nucleus accumbens core and shell after repeated cocaine in rats. *J Neurophysiol* **104**(2): 922-931.

Allen JA, Yadav PN, Setola V, Farrell M, Roth BL (2011). Schizophrenia risk gene CAV1 is both pro-psychotic and required for atypical antipsychotic drug actions in vivo. *Transl Psychiatry* **1**: e33.

Amitai N, Liu J, Schulteis G (2006). Discrete cues paired with naloxone-precipitated withdrawal from acute morphine dependence elicit conditioned withdrawal responses. *Behav Pharmacol* **17**(3): 213-222.

Andén NE DA, Fuxe K, Larsson K, Olson L, Ungerstedt U. (1966). Ascending Monoamine Neurons to the Telencephalon and Diencephalon. *Acta Physiol Scand*(67): 313-326.

Anstrom KK, Miczek KA, Budygin EA (2009). Increased phasic dopamine signaling in the mesolimbic pathway during social defeat in rats. *Neuroscience* **161**(1): 3-12.

APA (2013). Diagnostic and statistical manual of mental disorders : DSM-5.

Armstrong JM, Lefevre-Borg F, Scatton B, Cavero I (1982). Urethane inhibits cardiovascular responses mediated by the stimulation of alpha-2 adrenoceptors in the rat. *J Pharmacol Exp Ther* **223**(2): 524-535.

Aston-Jones G, Delfs JM, Druhan J, Zhu YAN (1999). The Bed Nucleus of the Stria Terminalis: A Target Site for Noradrenergic Actions in Opiate Withdrawal. *Ann N Y Acad Sci* **877**(1): 486-498.

Badrinarayan A, Wescott SA, Vander Weele CM, Saunders BT, Couturier BE, Maren S*, et al* (2012). Aversive stimuli differentially modulate real-time dopamine transmission dynamics within the nucleus accumbens core and shell. *J Neurosci* **32**(45): 15779-15790.

Baik JH, Picetti R, Saiardi A, Thiriet G, Dierich A, Depaulis A*, et al* (1995). Parkinsonian-like locomotor impairment in mice lacking dopamine D2 receptors. *Nature* **377**(6548): 424-428.

Bass CE, Grinevich VP, Gioia D, Day-Brown JD, Bonin KD, Stuber GD*, et al* (2013). Optogenetic stimulation of VTA dopamine neurons reveals that tonic but not phasic patterns of dopamine transmission reduce ethanol self-administration. *Front Behav Neurosci* **7**: 173.

Beaulieu JM, Gainetdinov RR (2011). The physiology, signaling, and pharmacology of dopamine receptors. *Pharmacol Rev* **63**(1): 182-217.

Becker JB, Koob GF (2016). Sex Differences in Animal Models: Focus on Addiction. *Pharmacol Rev* **68**(2): 242-263.

Belle AM, Owesson-White C, Herr NR, Carelli RM, Wightman RM (2013). Controlled iontophoresis coupled with fast-scan cyclic voltammetry/electrophysiology in awake, freely moving animals. *ACS Chem Neurosci* **4**(5): 761-771.

Bergquist F, Ludwig M (2008). Dendritic transmitter release: a comparison of two model systems. *J Neuroendocrinol* **20**(6): 677-686.

Berke JD, Hyman SE (2000). Addiction, Dopamine, and the Molecular Mechanisms of Memory. *Neuron* **25**(3): 515-532.

Berridge CW, Waterhouse BD (2003). The locus coeruleus-noradrenergic system: modulation of behavioral state and state-dependent cognitive processes. *Brain research Brain research reviews* **42**(1): 33-84.

Berridge KC, Robinson TE (1998). What is the role of dopamine in reward: hedonic impact, reward learning, or incentive salience? *Brain Res Brain Res Rev* **28**(3): 309-369.

Berrios J, Stamatakis AM, Kantak PA, McElligott ZA, Judson MC, Aita M*, et al* (2016). Loss of UBE3A from TH-expressing neurons suppresses GABA co-release and enhances VTA-NAc optical self-stimulation. *Nat Commun* **7**: 10702.

Blanchard BA, Steindorf S, Wang S, Glick SD (1993). Sex differences in ethanol-induced dopamine release in nucleus accumbens and in ethanol consumption in rats. *Alcohol Clin Exp Res* **17**(5): 968-973.

Bortel A (2014). Nature of DSP-4-Induced Neurotoxicity. In: Kostrzewa MR (ed). *Handbook of Neurotoxicity*. Springer New York: New York, NY, pp 219-236.

Bossong MG, van Berckel BN, Boellaard R, Zuurman L, Schuit RC, Windhorst AD*, et al* (2009). Delta 9-tetrahydrocannabinol induces dopamine release in the human striatum. *Neuropsychopharm* **34**(3): 759-766.

Brady S, Siegel, G., Albers, R. W., Price, D. (2005). *Basic Neurochemistry: Molecular, Cellular and Medical Aspects*, Seventh edn. Elsevier.

Brodie MS, Pesold C, Appel SB (1999). Ethanol Directly Excites Dopaminergic Ventral Tegmental Area Reward Neurons. *Alcohol Clin Exp Res* **23**(11): 1848-1852.

Bucher ES, Brooks K, Verber MD, Keithley RB, Owesson-White C, Carroll S*, et al* (2013). Flexible software platform for fast-scan cyclic voltammetry data acquisition and analysis. *Anal Chem* **85**(21): 10344-10353.

Bucher ES, Fox ME, Kim L, Kirkpatrick DC, Rodeberg NT, Belle AM*, et al* (2014). Medullary norepinephrine neurons modulate local oxygen concentrations in the bed nucleus of the stria terminalis. *J Cereb Blood Flow Metab* **34**(7): 1128-1137.

Buck K, Ferger B (2008). Intrastriatal inhibition of aromatic amino acid decarboxylase prevents l-DOPA-induced dyskinesia: a bilateral reverse in vivo microdialysis study in 6-hydroxydopamine lesioned rats. *Neurobiol Dis* **29**(2): 210-220.

Budygin EA, Kilpatrick MR, Gainetdinov RR, Wightman RM (2000). Correlation between behavior and extracellular dopamine levels in rat striatum: comparison of microdialysis and fast-scan cyclic voltammetry. *Neurosci Lett* **281**(1): 9-12.

Budygin EA, Phillips PE, Robinson DL, Kennedy AP, Gainetdinov RR, Wightman RM (2001). Effect of acute ethanol on striatal dopamine neurotransmission in ambulatory rats. *J Pharmacol Exp Ther* **297**(1): 27-34.

Butler TR, Ariwodola OJ, Weiner JL (2014). The impact of social isolation on HPA axis function, anxiety-like behaviors, and ethanol drinking. *Front Integr Neurosci* **7**: 102.

Cacciapaglia F, Saddoris MP, Wightman RM, Carelli RM (2012). Differential dopamine release dynamics in the nucleus accumbens core and shell track distinct aspects of goal-directed behavior for sucrose. *Neuropharmacology* **62**(5-6): 2050-2056.

Cacciapaglia F, Wightman RM, Carelli RM (2011). Rapid dopamine signaling differentially modulates distinct microcircuits within the nucleus accumbens during sucrose-directed behavior. *J Neurosci* **31**(39): 13860-13869.

Cachope R, Mateo Y, Mathur BN, Irving J, Wang HL, Morales M*, et al* (2012). Selective activation of cholinergic interneurons enhances accumbal phasic dopamine release: setting the tone for reward processing. *Cell Rep* **2**(1): 33-41.

Calipari ES, Ferris MJ, Jones SR (2014a). Extended access of cocaine self-administration results in tolerance to the dopamine-elevating and locomotor-stimulating effects of cocaine. *J Neurochem* **128**(2): 224-232.

Calipari ES, Sun H, Eldeeb K, Luessen DJ, Feng X, Howlett AC*, et al* (2014b). Amphetamine self-administration attenuates dopamine D2 autoreceptor function. *Neuropsychopharm* **39**(8): 1833-1842.

Capper-Loup C, Kaelin-Lang A (2013). Locomotor velocity and striatal adaptive gene expression changes of the direct and indirect pathways in Parkinsonian rats. *J Parkinsons Dis* **3**(3): 341-349.

Carr GV, Lucki I (2010). Comparison of the kappa-opioid receptor antagonist DIPPA in tests of anxiety-like behavior between Wistar Kyoto and Sprague Dawley rats. *Psychopharmacology (Berl)* **210**(2): 295-302.

Cecchi M, Khoshbouei H, Javors M, Morilak DA (2002). Modulatory effects of norepinephrine in the lateral bed nucleus of the stria terminalis on behavioral and neuroendocrine responses to acute stress. *Neuroscience* **112**(1): 13-21.

Chaijale NN, Curtis AL, Wood SK, Zhang XY, Bhatnagar S, Reyes BA*, et al* (2013). Social stress engages opioid regulation of locus coeruleus norepinephrine neurons and induces a state of cellular and physical opiate dependence. *Neuropsychopharm* **38**(10): 1833-1843.

Chang S-Y, Kim I, Marsh MP, Jang DP, Hwang S-C, Van Gompel JJ*, et al* (2012a). Wireless Fast-Scan Cyclic Voltammetry to Monitor Adenosine in Patients With Essential Tremor During Deep Brain Stimulation. *Mayo Clin Proc* **87**(8): 760-765.

Chang Z, Okamoto K, Bereiter DA (2012b). Differential ascending projections of temporomandibular joint-responsive brainstem neurons to periaqueductal gray and posterior thalamus of male and female rats. *Neuroscience* **203**: 230-243.

Chaudhury D, Liu H, Han MH (2015). Neuronal correlates of depression. *Cell Mol Life Sci* **72**(24): 4825-4848.

Chavkin C (2013). Dynorphin--still an extraordinarily potent opioid peptide. *Mol Pharmacol* **83**(4): 729-736.

Cheer JF, Aragona BJ, Heien ML, Seipel AT, Carelli RM, Wightman RM (2007a). Coordinated accumbal dopamine release and neural activity drive goal-directed behavior. *Neuron* **54**(2): 237-244.

Cheer JF, Wassum KM, Heien ML, Phillips PE, Wightman RM (2004). Cannabinoids enhance subsecond dopamine release in the nucleus accumbens of awake rats. *J Neurosci* **24**(18): 4393-4400.

Cheer JF, Wassum KM, Sombers LA, Heien ML, Ariansen JL, Aragona BJ*, et al* (2007b). Phasic dopamine release evoked by abused substances requires cannabinoid receptor activation. *J Neurosci* **27**(4): 791-795.

Chen MT, Morales M, Woodward DJ, Hoffer BJ, Janak PH (2001). In vivo extracellular recording of striatal neurons in the awake rat following unilateral 6-hydroxydopamine lesions. *Exp Neurol* **171**(1): 72-83.

Chen P, Fan Y, Li Y, Sun Z, Bissette G, Zhu MY (2012). Chronic social defeat up-regulates expression of norepinephrine transporter in rat brains. *Neurochem Int* **60**(1): 9-20.

Chiti Z, Teschemacher AG (2007). Exocytosis of norepinephrine at axon varicosities and neuronal cell bodies in the rat brain. *FASEB J* **21**(10): 2540-2550.

Choi DC, Furay AR, Evanson NK, Ostrander MM, Ulrich-Lai YM, Herman JP (2007). Bed Nucleus of the Stria Terminalis Subregions Differentially Regulate Hypothalamic–Pituitary–Adrenal Axis Activity: Implications for the Integration of Limbic Inputs. *J Neurosci* **27**(8): 2025-2034.

Cohen H, Zohar J, Gidron Y, Matar MA, Belkind D, Loewenthal U*, et al* (2006). Blunted HPA Axis Response to Stress Influences Susceptibility to Posttraumatic Stress Response in Rats. *Biol Psychiatry* **59**(12): 1208-1218.

Cone JJ, Chartoff EH, Potter DN, Ebner SR, Roitman MF (2013). Prolonged high fat diet reduces dopamine reuptake without altering DAT gene expression. *PLoS One* **8**(3): e58251.

Cone JJ, Fortin SM, McHenry JA, Stuber GD, McCutcheon JE, Roitman MF (2016). Physiological state gates acquisition and expression of mesolimbic reward prediction signals. *Proc Natl Acad Sci U S A* **113**(7): 1943-1948.

Cone JJ, McCutcheon JE, Roitman MF (2014). Ghrelin acts as an interface between physiological state and phasic dopamine signaling. *J Neurosci* **34**(14): 4905-4913.

Costa RM, Lin SC, Sotnikova TD, Cyr M, Gainetdinov RR, Caron MG*, et al* (2006). Rapid alterations in corticostriatal ensemble coordination during acute dopamine-dependent motor dysfunction. *Neuron* **52**(2): 359-369.

Covey DP, Bunner KD, Schuweiler DR, Cheer JF, Garris PA (2016). Amphetamine elevates nucleus accumbens dopamine via an action potential-dependent mechanism that is modulated by endocannabinoids. *Eur J Neurosci*: in press.

Covey DP, Roitman MF, Garris PA (2014). Illicit dopamine transients: reconciling actions of abused drugs. *Trends Neurosci* **37**(4): 200-210.

Covey DP, Wenzel JM, Cheer JF (2015). Cannabinoid modulation of drug reward and the implications of marijuana legalization. *Brain Res* **1628, Part A**: 233-243.

Cragg SJ, Nicholson C, Kume-Kick J, Tao L, Rice ME (2001). Dopamine-mediated volume transmission in midbrain is regulated by distinct extracellular geometry and uptake. *J Neurophysiol* **85**(4): 1761-1771.

Crocker AD (1997). The regulation of motor control: an evaluation of the role of dopamine receptors in the substantia nigra. *Rev Neurosci* **8**(1): 55-76.

Daberkow DP, Brown HD, Bunner KD, Kraniotis SA, Doellman MA, Ragozzino ME*, et al* (2013). Amphetamine paradoxically augments exocytotic dopamine release and phasic dopamine signals. *J Neurosci* **33**(2): 452-463.

Daigle TL, Ferris MJ, Gainetdinov RR, Sotnikova TD, Urs NM, Jones SR*, et al* (2014). Selective deletion of GRK2 alters psychostimulant-induced behaviors and dopamine neurotransmission. *Neuropsychopharm* **39**(10): 2450-2462.

Davis WM, Smith SG, Khalsa JH (1975). Noradrenergic role in the self-administration of morphine or amphetamine. *Pharmacol Biochem Behav* **3**(3): 477-484.

Daws LC (2009). Unfaithful neurotransmitter transporters: focus on serotonin uptake and implications for antidepressant efficacy. *Pharmacol Ther* **121**(1): 89-99.

Day JJ, Jones JL, Wightman RM, Carelli RM (2010). Phasic nucleus accumbens dopamine release encodes effort- and delay-related costs. *Biol Psychiatry* **68**(3): 306-309.

Day JJ, Roitman MF, Wightman RM, Carelli RM (2007). Associative learning mediates dynamic shifts in dopamine signaling in the nucleus accumbens. *Nat Neurosci* **10**(8): 1020-1028.

Day M, Wang Z, Ding J, An X, Ingham CA, Shering AF*, et al* (2006). Selective elimination of glutamatergic synapses on striatopallidal neurons in Parkinson disease models. *Nat Neurosci* **9**(2): 251-259.

Delfs JM, Zhu Y, Druhan JP, Aston-Jones G (2000). Noradrenaline in the ventral forebrain is critical for opiate withdrawal-induced aversion. *Nature* **403**(6768): 430-434.

Deserno L, Beck A, Huys QJ, Lorenz RC, Buchert R, Buchholz HG*, et al* (2015). Chronic alcohol intake abolishes the relationship between dopamine synthesis capacity and learning signals in the ventral striatum. *Eur J Neurosci* **41**(4): 477-486.

Di Chiara G, Imperato A (1988). Drugs abused by humans preferentially increase synaptic dopamine concentrations in the mesolimbic system of freely moving rats. *Proc Natl Acad Sci U S A* **85**(14): 5274-5278.

Drolet G (ed) (2009). *Progress in Neuro-Psychopharmacology & Biological Psychiatry* Elsevier, Inc: Amsterdam.

Dumont EC, Williams JT (2004). Noradrenaline triggers GABAA inhibition of bed nucleus of the stria terminalis neurons projecting to the ventral tegmental area. *J Neurosci* **24**(38): 8198-8204.

Duvarci S, Bauer EP, Pare D (2009). The bed nucleus of the stria terminalis mediates inter-individual variations in anxiety and fear. *J Neurosci* **29**(33): 10357-10361.

Egli RE, Kash TL, Choo K, Savchenko V, Matthews RT, Blakely RD*, et al* (2004). Norepinephrine Modulates Glutamatergic Transmission in the Bed Nucleus of the Stria Terminalis. *Neuropsychopharm* **30**(4): 657-668.

Ehrich JM, Phillips PE, Chavkin C (2014). Kappa opioid receptor activation potentiates the cocaine-induced increase in evoked dopamine release recorded in vivo in the mouse nucleus accumbens. *Neuropsychopharm* **39**(13): 3036-3048.

Ennis M, Aston-Jones G (1988). Activation of locus coeruleus from nucleus paragigantocellularis: A new excitatory amino acid pathway in brain. *J Neurosci* **8**(10): 3644-3657.

Erb S, Hitchcott PK, Rajabi H, Mueller D, Shaham Y, Stewart J (2000). Alpha-2 adrenergic receptor agonists block stress-induced reinstatement of cocaine seeking. *Neuropsychopharm* **23**(2): 138-150.

Everitt BJ, Robbins TW (2005). Neural systems of reinforcement for drug addiction: from actions to habits to compulsion. *Nat Neurosci* **8**(11): 1481-1489.

Fan Y, Chen P, Li Y, Zhu MY (2013). Effects of chronic social defeat on expression of dopamine beta-hydroxylase in rat brains. *Synapse* **67**(6): 300-312.

Faravelli C, Lo Sauro C, Lelli L, Pietrini F, Lazzeretti L, Godini L*, et al* (2012). The role of life events and HPA axis in anxiety disorders: a review. *Curr Pharm Des* **18**(35): 5663-5674.

Faria MP, Miguel TT, Gomes KS, Nunes-de-Souza RL (2016). Anxiety-like responses induced by nitric oxide within the BNST in mice: Role of CRF1 and NMDA receptors. *Horm Behav* **79**: 74-83.

Fehr C, Sommerlad D, Sander T, Anghelescu I, Dahmen N, Szegedi A*, et al* (2013). Association of VMAT2 gene polymorphisms with alcohol dependence. *J Neural Transm (Vienna)* **120**(8): 1161-1169.

Fendt M, Siegl S, Steiniger-Brach B (2005). Noradrenaline transmission within the ventral bed nucleus of the stria terminalis is critical for fear behavior induced by trimethylthiazoline, a component of fox odor. *J Neurosci* **25**(25): 5998-6004.

Ferris MJ, Calipari ES, Mateo Y, Melchior JR, Roberts DC, Jones SR (2012). Cocaine self-administration produces pharmacodynamic tolerance: differential effects on the potency of dopamine transporter blockers, releasers, and methylphenidate. *Neuropsychopharm* **37**(7): 1708-1716.

Ferris MJ, Calipari ES, Rose JH, Siciliano CA, Sun H, Chen R*, et al* (2015). A Single Amphetamine Infusion Reverses Deficits in Dopamine Nerve-Terminal Function Caused by a History of Cocaine Self-Administration. *Neuropsychopharm* **40**(8): 1826-1836.

Ferris MJ, Mateo Y, Roberts DCS, Jones SR (2011). Cocaine-Insensitive Dopamine Transporters with Intact Substrate Transport Produced by Self-Administration. *Biol Psychiatry* **69**(3): 201-207.

Fieblinger T, Sebastianutto I, Alcacer C, Bimpisidis Z, Maslava N, Sandberg S*, et al* (2014). Mechanisms of dopamine D1 receptor-mediated ERK1/2 activation in the parkinsonian striatum and their modulation by metabotropic glutamate receptor type 5. *J Neurosci* **34**(13): 4728-4740.

Forray MI, Gysling K (2004). Role of noradrenergic projections to the bed nucleus of the stria terminalis in the regulation of the hypothalamic-pituitary-adrenal axis. *Brain Res Brain Res Rev* **47**(1-3): 145-160.

Fortin SM, Chartoff EH, Roitman MF (2016). The Aversive Agent Lithium Chloride Suppresses Phasic Dopamine Release Through Central GLP-1 Receptors. *Neuropsychopharm* **41**(3): 906-915.

Fox ME, Mikhailova MA, Bass CE, Takmakov P, Gainetdinov RR, Budygin EA*, et al* (2016a). Cross-hemispheric dopamine projections have functional significance. *Proc Natl Acad Sci U S A*: In Press.

Fox ME, Rodeberg NT, Wightman RM (2016b). Reciprocal catecholamine changes during opiate intoxication and withdrawal. *Neuropsychopharm*: Under review.

Fox ME, Studebaker RI, Swofford NJ, Wightman RM (2015). Stress and Drug Dependence Differentially Modulate Norepinephrine Signaling in Animals with Varied HPA Axis Function. *Neuropsychopharm* **40**(7): 1752-1761.

Fritschy JM, Grzanna R (1989). Immunohistochemical analysis of the neurotoxic effects of DSP-4 identifies two populations of noradrenergic axon terminals. *Neuroscience* **30**(1): 181-197.

Fuentealba JA, Forray MI, Gysling K (2000). Chronic morphine treatment and withdrawal increase extracellular levels of norepinephrine in the rat bed nucleus of the stria terminalis. *J Neurochem* **75**(2): 741-748.

Garris PA, Christensen JRC, Rebec GV, Wightman RM (1997). Real-time measurement of electrically evoked extracellular dopamine in the striatum of freely moving rats. *J Neurochem* **68**(1): 152-161.

Garris PA, Ciolkowski EL, Pastore P, Wightman RM (1994a). Efflux of dopamine from the synaptic cleft in the nucleus accumbens of the rat brain. *J Neurosci* **14**(10): 6084-6093.

Garris PA, Collins LB, Jones SR, Wightman RM (1993). Evoked extracellular dopamine in vivo in the medial prefrontal cortex. *J Neurochem* **61**(2): 637-647.

Garris PA, Wightman RM (1994b). In vivo voltammetric measurement of evoked extracellular dopamine in the rat basolateral amygdaloid nucleus. *J Physiol* **478 (Pt 2)**: 239-249.

Gasser PJ, Lowry CA, Orchinik M (2006). Corticosterone-sensitive monoamine transport in the rat dorsomedial hypothalamus: potential role for organic cation transporter 3 in stress-induced modulation of monoaminergic neurotransmission. *J Neurosci* **26**(34): 8758-8766.

Gasser PJ, Orchinik M, Raju I, Lowry CA (2009). Distribution of organic cation transporter 3, a corticosterone-sensitive monoamine transporter, in the rat brain. *J Comp Neurol* **512**(4): 529-555.

Geerling JC, Loewy AD (2006). Aldosterone-sensitive neurons in the nucleus of the solitary tract: efferent projections. *J Comp Neurol* **497**(2): 223-250.

Geisler S, Zahm DS (2005). Afferents of the ventral tegmental area in the rat-anatomical substratum for integrative functions. *J Comp Neurol* **490**(3): 270-294.

Geisler S, Zahm DS (2006). Neurotensin afferents of the ventral tegmental area in the rat: [1] re-examination of their origins and [2] responses to acute psychostimulant and antipsychotic drug administration. *Eur J Neurosci* **24**(1): 116-134.

George FR, Goldberg SR (1989). Genetic approaches to the analysis of addiction processes. *Trends Pharmacol Sci* **10**(2): 78-83.

Georges F, Aston-Jones G (2002). Activation of ventral tegmental area cells by the bed nucleus of the stria terminalis: a novel excitatory amino acid input to midbrain dopamine neurons. *J Neurosci* **22**(12): 5173-5187.

Gerfen CR (2000). Molecular effects of dopamine on striatal-projection pathways. *Trends Neurosci* **23, Supplement 1**: S64-S70.

Giros B, Jaber M, Jones SR, Wightman RM, Caron MG (1996). Hyperlocomotion and indifference to cocaine and amphetamine in mice lacking the dopamine transporter. *Nature* **379**(6566): 606-612.

Gompf HS, Budygin EA, Fuller PM, Bass CE (2015). Targeted genetic manipulations of neuronal subtypes using promoter-specific combinatorial AAVs in wild-type animals. *Front Behav Neurosci* **9**: 152.

Graf EN, Wheeler RA, Baker DA, Ebben AL, Hill JE, McReynolds JR*, et al* (2013). Corticosterone acts in the nucleus accumbens to enhance dopamine signaling and potentiate reinstatement of cocaine seeking. *J Neurosci* **33**(29): 11800-11810.

Halfpenny DM, Callado LF, Hopwood SE, Bamigbade TA, Langford RM, Stamford JA (1999). Effects of tramadol stereoisomers on norepinephrine efflux and uptake in the rat locus coeruleus measured by real time voltammetry. *Br J Anaesth* **83**(6): 909-915.

Hamid AA, Pettibone JR, Mabrouk OS, Hetrick VL, Schmidt R, Vander Weele CM*, et al* (2016). Mesolimbic dopamine signals the value of work. *Nat Neurosci* **19**(1): 117-126.

Harris GC, Aston-Jones G (1994). Involvement of D2 dopamine receptors in the nucleus accumbens in the opiate withdrawal syndrome. *Nature* **371**(6493): 155-157.

Harro J, Oreland L, Vasar E, Bradwejn J (1995). Impaired exploratory behaviour after DSP-4 treatment in rats: implications for the increased anxiety after noradrenergic denervation. *Eur Neuropsychopharmacol* **5**(4): 447-455.

Hartung H, Threlfell S, Cragg SJ (2011). Nitric oxide donors enhance the frequency dependence of dopamine release in nucleus accumbens. *Neuropsychopharmacology* **36**(9): 1811-1822.

Harun R, Hare KM, Brough ME, Munoz MJ, Grassi CM, Torres GE*, et al* (2015). Fast-scan cyclic voltammetry demonstrates that L-DOPA produces dose-dependent regionally selective, bimodal effects on striatal dopamine kinetics in vivo. *J Neurochem*: In press.

Heilig M, Egli M (2006). Pharmacological treatment of alcohol dependence: target symptoms and target mechanisms. *Pharmacol Ther* **111**(3): 855-876.

Hemby SE, Martin TJ, Co C, Dworkin SI, Smith JE (1995). The effects of intravenous heroin administration on extracellular nucleus accumbens dopamine concentrations as determined by in vivo microdialysis. *J Pharmacol Exp Ther* **273**(2): 591-598.

Hernandez G, Oleson EB, Gentry RN, Abbas Z, Bernstein DL, Arvanitogiannis A*, et al* (2014). Endocannabinoids promote cocaine-induced impulsivity and its rapid dopaminergic correlates. *Biol Psychiatry* **75**(6): 487-498.

Herr NR, Park J, McElligott ZA, Belle AM, Carelli RM, Wightman RM (2012). In vivo voltammetry monitoring of electrically evoked extracellular norepinephrine in subregions of the bed nucleus of the stria terminalis. *J Neurophysiol* **107**(6): 1731-1737.

Hopwood SE, Owesson CA, Callado LF, McLaughlin DP, Stamford JA (2001). Effects of chronic tramadol on pre- and post-synaptic measures of monoamine function. *J Psychopharmacol* **15**(3): 147-153.

Howard CD, Keefe KA, Garris PA, Daberkow DP (2011). Methamphetamine neurotoxicity decreases phasic, but not tonic, dopaminergic signaling in the rat striatum. *J Neurochem* **118**(4): 668-676.

Howe MW, Tierney PL, Sandberg SG, Phillips PE, Graybiel AM (2013). Prolonged dopamine signalling in striatum signals proximity and value of distant rewards. *Nature* **500**(7464): 575-579.

Hyman SE, Malenka RC, Nestler EJ (2006). Neural mechanisms of addiction: the role of reward-related learning and memory. *Ann Rev Neurosci* **29**: 565-598.

Hyman SM, Hong KI, Chaplin TM, Dabre Z, Comegys AD, Kimmerling A*, et al* (2009). A stress-coping profile of opioid dependent individuals entering naltrexone treatment: a comparison with healthy controls. *Psychol Addict Behav* **23**(4): 613-619.

Itoi K, Sugimoto N, Suzuki S, Sawada K, Das G, Uchida K*, et al* (2011). Targeting of locus ceruleus noradrenergic neurons expressing human interleukin-2 receptor alpha-subunit in transgenic mice by a recombinant immunotoxin anti-Tac(Fv)-PE38: a study for exploring noradrenergic influence upon anxiety-like and depression-like behaviors. *J Neurosci* **31**(16): 6132-6139.

Jaeger CB, Joh TH, Reis DJ (1983). The effect of forebrain lesions in the neonatal rat: survival of midbrain dopaminergic neurons and the crossed nigrostriatal projection. *J Comp Neurol* **218**(1): 74-90.

Janhunen SK, la Fleur SE, Adan RA (2013). Blocking alpha2A adrenoceptors, but not dopamine receptors, augments bupropion-induced hypophagia in rats. *Obesity (Silver Spring)* **21**(12): E700-708.

Jarrard LE (1989). On the use of ibotenic acid to lesion selectively different components of the hippocampal formation. *J Neurosci Methods* **29**(3): 251-259.

Jewell-Motz EA, Liggett SB (1996). G protein-coupled receptor kinase specificity for phosphorylation and desensitization of alpha2-adrenergic receptor subtypes. *J Biol Chem* **271**(30): 18082-18087.

John CE, Budygin EA, Mateo Y, Jones SR (2006). Neurochemical characterization of the release and uptake of dopamine in ventral tegmental area and serotonin in substantia nigra of the mouse. *J Neurochem* **96**(1): 267-282.

Johnson JA, Rodeberg NT, Wightman RM (2016). Failure of Standard Training Sets in the Analysis of Fast-Scan Cyclic Voltammetry Data. *ACS Chem Neurosci* **7**(3): 349-359.

Jones JL, Day JJ, Aragona BJ, Wheeler RA, Wightman RM, Carelli RM (2010). Basolateral amygdala modulates terminal dopamine release in the nucleus accumbens and conditioned responding. *Biol Psychiatry* **67**(8): 737-744.

Jones SR, Gainetdinov RR, Hu XT, Cooper DC, Wightman RM, White FJ*, et al* (1999). Loss of autoreceptor functions in mice lacking the dopamine transporter. *Nat Neurosci* **2**(7): 649-655.

Jones SR, Gainetdinov RR, Jaber M, Giros B, Wightman RM, Caron MG (1998). Profound neuronal plasticity in response to inactivation of the dopamine transporter. *Proc Natl Acad Sci U S A* **95**(7): 4029-4034.

Juarez B, Han M-H (2016). Diversity of Dopaminergic Neural Circuits in Response to Drug Exposure. *Neuropsychopharm*: In press.

Karkhanis AN, Locke JL, McCool BA, Weiner JL, Jones SR (2014). Social isolation rearing increases nucleus accumbens dopamine and norepinephrine responses to acute ethanol in adulthood. *Alcohol Clin Exp Res* **38**(11): 2770-2779.

Kasasbeh A, Lee K, Bieber A, Bennet K, Chang SY (2013). Wireless neurochemical monitoring in humans. *Stereotact Funct Neurosurg* **91**(3): 141-147.

Kash TL, Pleil KE, Marcinkiewcz CA, Lowery-Gionta EG, Crowley N, Mazzone C*, et al* (2015). Neuropeptide regulation of signaling and behavior in the BNST. *Mol Cells* **38**(1): 1-13.

Kashtelyan V, Lichtenberg NT, Chen ML, Cheer JF, Roesch MR (2014). Observation of reward delivery to a conspecific modulates dopamine release in ventral striatum. *Curr Biol* **24**(21): 2564-2568.

Kaufling J, Aston-Jones G (2015). Persistent Adaptations in Afferents to Ventral Tegmental Dopamine Neurons after Opiate Withdrawal. *J Neurosci* **35**(28): 10290-10303.

Keithley RB, Carelli RM, Wightman RM (2010). Rank Estimation and the Multivariate Analysis of in Vivo Fast-Scan Cyclic Voltammetric Data. *Anal Chem* **82**(13): 5541-5551.

Keithley RB, Mark Wightman R, Heien ML (2009). Multivariate concentration determination using principal component regression with residual analysis. *Trends Analyt Chem* **28**(9): 1127-1136.

Kennedy RT, Jones SR, Wightman RM (1992). Dynamic observation of dopamine autoreceptor effects in rat striatal slices. *J Neurochem* **59**(2): 449-455.

Kessler JP, Jean A (1985). Identification of the medullary swallowing regions in the rat. *Exp Brain Res* **57**(2): 256-263.

Kilts CD, Anderson CM (1986). The simultaneous quantification of dopamine, norepinephrine and epinephrine in micropunched rat brain nuclei by on-line trace enrichment HPLC with electrochemical detection: Distribution of catecholamines in the limbic system. *Neurochem Int* **9**(3): 437-445.

Kishida KT, Saez I, Lohrenz T, Witcher MR, Laxton AW, Tatter SB*, et al* (2016). Subsecond dopamine fluctuations in human striatum encode superposed error signals about actual and counterfactual reward. *Proc Natl Acad Sci U S A* **113**(1): 200-205.

Kishida KT, Sandberg SG, Lohrenz T, Comair YG, Saez I, Phillips PE*, et al* (2011). Sub-second dopamine detection in human striatum. *PLoS One* **6**(8): e23291.

Kissinger PT, Hart JB, Adams RN (1973). Voltammetry in brain tissue--a new neurophysiological measurement. *Brain Res* **55**(1): 209-213.

Koob GF (2009). Brain stress systems in the amygdala and addiction. *Brain Res* **1293**: 61-75.

Koob GF, Volkow ND (2010). Neurocircuitry of addiction. *Neuropsychopharm* **35**(1): 217-238.

Kowalczyk WJ, Phillips KA, Jobes ML, Kennedy AP, Ghitza UE, Agage DA*, et al* (2015). Clonidine Maintenance Prolongs Opioid Abstinence and Decouples Stress From Craving in Daily Life: A Randomized Controlled Trial With Ecological Momentary Assessment. *Am J Psychiatry* **172**(8): 760-767.

Lahdesmaki J, Sallinen J, MacDonald E, Kobilka BK, Fagerholm V, Scheinin M (2002). Behavioral and neurochemical characterization of alpha(2A)-adrenergic receptor knockout mice. *Neuroscience* **113**(2): 289-299.

Lapiz MD, Mateo Y, Durkin S, Parker T, Marsden CA (2001). Effects of central noradrenaline depletion by the selective neurotoxin DSP-4 on the behaviour of the isolated rat in the elevated plus maze and water maze. *Psychopharmacology (Berl)* **155**(3): 251-259.

Lee T, Cai LX, Lelyveld VS, Hai A, Jasanoff A (2014). Molecular-level functional magnetic resonance imaging of dopaminergic signaling. *Science* **344**(6183): 533-535.

Leri F, Flores J, Rodaros D, Stewart J (2002). Blockade of stress-induced but not cocaine-induced reinstatement by infusion of noradrenergic antagonists into the bed nucleus of the stria terminalis or the central nucleus of the amygdala. *J Neurosci* **22**(13): 5713-5718.

Loewinger GC, Beckert MV, Tejeda HA, Cheer JF (2012). Methamphetamine-induced dopamine terminal deficits in the nucleus accumbens are exacerbated by reward-associated cues and attenuated by CB1 receptor antagonism. *Neuropharmacology* **62**(7): 2192-2201.

López-Rubalcava C, Lucki I (2000). Strain Differences in the Behavioral Effects of Antidepressant Drugs in the Rat Forced Swimming Test. *Neuropsychopharm* **22**(2): 191-199.

Ma S, Morilak DA (2004). Induction of FOS expression by acute immobilization stress is reduced in locus coeruleus and medial amygdala of Wistar-Kyoto rats compared to Sprague-Dawley rats. *Neuroscience* **124**(4): 963-972.

Maldonado R (1997). Participation of noradrenergic pathways in the expression of opiate withdrawal: biochemical and pharmacological evidence. *Neurosci Biobehav Rev* **21**(1): 91-104.

Mason ST, Iversen SD (1979). Theories of the dorsal bundle extinction effect. *Brain Res* **180**(1): 107-137.

Mateo Y, Lack CM, Morgan D, Roberts DCS, Jones SR (2005). Reduced Dopamine Terminal Function and Insensitivity to Cocaine Following Cocaine Binge Self-Administration and Deprivation. *Neuropsychopharm* **30**(8): 1455-1463.

May LJ, Wightman RM (1989). Heterogeneity of stimulated dopamine overflow within rat striatum as observed with in vivo voltammetry. *Brain Res* **487**(2): 311-320.

Mazei-Robison MS, Nestler EJ (2012). Opiate-Induced Molecular and Cellular Plasticity of Ventral Tegmental Area and Locus Coeruleus Catecholamine Neurons. *Cold Spring Harb Perspect Med* **2**(7).

McCutcheon JE, Beeler JA, Roitman MF (2012). Sucrose-predictive cues evoke greater phasic dopamine release than saccharin-predictive cues. *Synapse* **66**(4): 346-351.

McCutcheon JE, Cone JJ, Sinon CG, Fortin SM, Kantak PA, Witten IB*, et al* (2014). Optical suppression of drug-evoked phasic dopamine release. *Front Neural Circuits* **8**: 114.

McElligott ZA, Fox ME, Walsh PL, Urban DJ, Ferrel MS, Roth BL*, et al* (2013). Noradrenergic Synaptic Function in the Bed Nucleus of the Stria Terminalis Varies in Animal Models of Anxiety and Addiction. *Neuropsychopharm* **38**(9): 1665-1673.

McElligott ZA, Klug JR, Nobis WP, Patel S, Grueter BA, Kash TL*, et al* (2010). Distinct forms of Gq-receptor-dependent plasticity of excitatory transmission in the BNST are differentially affected by stress. *Proc Natl Acad Sci U S A* **107**(5): 2271-2276.

McElligott ZA, Winder DG (2008). Alpha1-adrenergic receptor-induced heterosynaptic long-term depression in the bed nucleus of the stria terminalis is disrupted in mouse models of affective disorders. *Neuropsychopharm* **33**(10): 2313-2323.

McElligott ZA, Winder DG (2009). Modulation of glutamatergic synaptic transmission in the bed nucleus of the stria terminalis. *Prog Neuropsychopharmacol Biol Psych* **33**(8): 1329-1335.

Mebel DM, Wong JC, Dong YJ, Borgland SL (2012). Insulin in the ventral tegmental area reduces hedonic feeding and suppresses dopamine concentration via increased reuptake. *Eur J Neurosci* **36**(3): 2336-2346.

Mefford IN (1981). Application of high performance liquid chromatography with electrochemical detection to neurochemical analysis: measurement of catecholamines, serotonin and metabolites in rat brain. *J Neurosci Methods* **3**(3): 207-224.

Meloni EG, Gerety LP, Knoll AT, Cohen BM, Carlezon WA, Jr. (2006). Behavioral and anatomical interactions between dopamine and corticotropin-releasing factor in the rat. *J Neurosci* **26**(14): 3855-3863.

Miczek KA, Covington Iii HE, Nikulina Jr EM, Hammer RP (2004). Aggression and defeat: persistent effects on cocaine self-administration and gene expression in peptidergic and aminergic mesocorticolimbic circuits. *Neurosci Biobehav Rev* **27**(8): 787-802.

Miles PR, Mundorf ML, Wightman RM (2002). Release and uptake of catecholamines in the bed nucleus of the stria terminalis measured in the mouse brain slice. *Synapse* **44**(3): 188-197.

Mitchell K, Adams RN (1993). Comparison of the effects of voltage-sensitive calcium channel antagonism on the electrically stimulated release of dopamine and norepinephrine in vivo. *Brain Res* **604**(1–2): 349-353.

Montague PR, Hyman SE, Cohen JD (2004). Computational roles for dopamine in behavioural control. *Nature* **431**(7010): 760-767.

Moore RY, Bloom FE (1979). Central catecholamine neuron systems: anatomy and physiology of the norepinephrine and epinephrine systems. *Ann Rev Neurosci* **2**: 113-168.

Moron JA, Brockington A, Wise RA, Rocha BA, Hope BT (2002). Dopamine uptake through the norepinephrine transporter in brain regions with low levels of the dopamine transporter: evidence from knock-out mouse lines. *J Neurosci* **22**(2): 389-395.

Murai T, Yoshida Y, Koide S, Takada K, Misaki T, Koshikawa N*, et al* (1998). Clonidine reduces dopamine and increases GABA in the nucleus accumbens: an in vivo microdialysis study. *Pharmacol Biochem Behav* **60**(3): 695-701.

Nakazato T (1987). Locus coeruleus neurons projecting to the forebrain and the spinal cord in the cat. *Neuroscience* **23**(2): 529-538.

Nauta WJ, Smith GP, Faull RL, Domesick VB (1978). Efferent connections and nigral afferents of the nucleus accumbens septi in the rat. *Neuroscience* **3**(4-5): 385-401.

Near JA, Bigelow JC, Wightman RM (1988). Comparison of uptake of dopamine in rat striatal chopped tissue and synaptosomes. *J Pharmacol Exp Ther* **245**(3): 921-927.

Nedelescu H, Chowdhury TG, Wable GS, Arbuthnott G, Aoki C (2016). Cerebellar sub-divisions differ in exercise-induced plasticity of noradrenergic axons and in their association with resilience to activity-based anorexia. *Brain Struct Funct*: In press.

Nestler EJ (2001). Molecular basis of long-term plasticity underlying addiction. *Nat Rev Neurosci* **2**(2): 119-128.

Nestler EJ, Hyman SE (2010). Animal models of neuropsychiatric disorders. *Nat Neurosci* **13**(10): 1161-1169.

Nieoullon A, Cheramy A, Glowinski J (1977). Interdependence of the nigrostriatal dopaminergic systems on the two sides of the brain in the cat. *Science* **198**(4315): 416-418.

Nobis WP, Kash TL, Silberman Y, Winder DG (2011). beta-Adrenergic receptors enhance excitatory transmission in the bed nucleus of the stria terminalis through a corticotrophin-releasing factor receptor-dependent and cocaine-regulated mechanism. *Biol Psychiatry* **69**(11): 1083-1090.

Oke A, Solnick J, Adams RN (1983). Catecholamine distribution patterns in rat thalamus. *Brain Res* **269**(1): 180-183.

Olds J, Milner P (1954). Positive reinforcement produced by electrical stimulation of septal area and other regions of rat brain. *J Comp Physiol Psychol* **47**(6): 419-427.

Oleson EB, Beckert MV, Morra JT, Lansink CS, Cachope R, Abdullah RA*, et al* (2012). Endocannabinoids shape accumbal encoding of cue-motivated behavior via CB1 receptor activation in the ventral tegmentum. *Neuron* **73**(2): 360-373.

Olson VG, Heusner CL, Bland RJ, During MJ, Weinshenker D, Palmiter RD (2006). Role of noradrenergic signaling by the nucleus tractus solitarius in mediating opiate reward. *Science* **311**(5763): 1017-1020.

Oropeza VC, Page ME, Van Bockstaele EJ (2005). Systemic administration of WIN 55,212-2 increases norepinephrine release in the rat frontal cortex. *Brain Res* **1046**(1-2): 45-54.

Owesson-White C, Belle AM, Herr NR, Peele JL, Gowrishankar P, Carelli RM*, et al* (2016). Cue-evoked dopamine release rapidly modulates D2 neurons in the nucleus accumbens during motivated behavior. *J Neurosci*: in press.

Owesson-White CA, Cheer JF, Beyene M, Carelli RM, Wightman RM (2008). Dynamic changes in accumbens dopamine correlate with learning during intracranial self-stimulation. *Proc Natl Acad Sci U S A* **105**(33): 11957-11962.

Owesson-White CA, Roitman MF, Sombers LA, Belle AM, Keithley RB, Peele JL*, et al* (2012). Sources contributing to the average extracellular concentration of dopamine in the nucleus accumbens. *J Neurochem* **121**(2): 252-262.

Owesson CA, Hopwood SE, Callado LF, Seif I, McLaughlin DP, Stamford JA (2002). Altered presynaptic function in monoaminergic neurons of monoamine oxidase-A knockout mice. *Eur J Neurosci* **15**(9): 1516-1522.

Owesson CA, Seif I, McLaughlin DP, Stamford JA (2003). Different alpha(2) adrenoceptor subtypes control noradrenaline release and cell firing in the locus coeruleus of wildtype and monoamine oxidase-A knockout mice. *Eur J Neurosci* **18**(1): 34-42.

Page ME, Oropeza VC, Sparks SE, Qian Y, Menko AS, Van Bockstaele EJ (2007). Repeated cannabinoid administration increases indices of noradrenergic activity in rats. *Pharmacol Biochem Behav* **86**(1): 162-168.

Palij P, Stamford JA (1992). Real-time monitoring of endogenous noradrenaline release in rat brain slices using fast cyclic voltammetry: 1. Characterisation of evoked noradrenaline efflux and uptake from nerve terminals in the bed nucleus of stria terminalis, pars ventralis. *Brain Res* **587**(1): 137-146.

Palij P, Stamford JA (1993). Real-time monitoring of endogenous noradrenaline release in rat brain slices using fast cyclic voltammetry. 2. Operational characteristics of the

alpha 2 autoreceptor in the bed nucleus of stria terminalis, pars ventralis. *Brain Res* **607**(1-2): 134-140.

Panayi F, Colussi-Mas J, Lambas-Senas L, Renaud B, Scarna H, Berod A (2005). Endogenous neurotensin in the ventral tegmental area contributes to amphetamine behavioral sensitization. *Neuropsychopharm* **30**(5): 871-879.

Papke JB, Moore-Dotson JM, Watson DJ, Wedell CD, French LR, Rendell SR*, et al* (2012). Titration of synaptotagmin I expression differentially regulates release of norepinephrine and neuropeptide Y. *Neuroscience* **218**: 78-88.

Pardon MC, Gould GG, Garcia A, Phillips L, Cook MC, Miller SA*, et al* (2002). Stress reactivity of the brain noradrenergic system in three rat strains differing in their neuroendocrine and behavioral responses to stress: implications for susceptibility to stress-related neuropsychiatric disorders. *Neuroscience* **115**(1): 229-242.

Park J, Aragona BJ, Kile BM, Carelli RM, Wightman RM (2010). In vivo voltammetric monitoring of catecholamine release in subterritories of the nucleus accumbens shell. *Neuroscience* **169**(1): 132-142.

Park J, Bucher ES, Budygin EA, Wightman RM (2015). Norepinephrine and dopamine transmission in 2 limbic regions differentially respond to acute noxious stimulation. *Pain* **156**(2): 318-327.

Park J, Bucher ES, Fontillas K, Owesson-White C, Ariansen JL, Carelli RM*, et al* (2013). Opposing catecholamine changes in the bed nucleus of the stria terminalis during intracranial self-stimulation and its extinction. *Biol Psychiatry* **74**(1): 69-76.

Park J, Kile BM, Wightman RM (2009). In vivo voltammetric monitoring of norepinephrine release in the rat ventral bed nucleus of the stria terminalis and anteroventral thalamic nucleus. *Eur J Neurosci* **30**(11): 2121-2133.

Park J, Takmakov P, Wightman RM (2011). In vivo comparison of norepinephrine and dopamine release in rat brain by simultaneous measurements with fast-scan cyclic voltammetry. *J Neurochem* **119**(5): 932-944.

Park J, Wheeler RA, Fontillas K, Keithley RB, Carelli RM, Wightman RM (2012). Catecholamines in the bed nucleus of the stria terminalis reciprocally respond to reward and aversion. *Biol Psychiatry* **71**(4): 327-334.

Parker JG, Zweifel LS, Clark JJ, Evans SB, Phillips PE, Palmiter RD (2010). Absence of NMDA receptors in dopamine neurons attenuates dopamine release but not conditioned approach during Pavlovian conditioning. *Proc Natl Acad Sci U S A* **107**(30): 13491-13496.

Passerin AM, Cano G, Rabin BS, Delano BA, Napier JL, Sved AF (2000). Role of locus coeruleus in foot shock-evoked Fos expression in rat brain. *Neuroscience* **101**(4): 1071-1082.

Patki G, Atrooz F, Alkadhi I, Solanki N, Salim S (2015). High aggression in rats is associated with elevated stress, anxiety-like behavior, and altered catecholamine content in the brain. *Neurosci Lett* **584**: 308-313.

Pattison LP, McIntosh S, Budygin EA, Hemby SE (2012). Differential regulation of accumbal dopamine transmission in rats following cocaine, heroin and speedball self-administration. *J Neurochem* **122**(1): 138-146.

Paxinos G, Watson C (2007). *The rat brain in stereotaxic coordinates*, 6th edn. Academic Press/Elsevier: Amsterdam ; Boston ; .

Peters JL, Miner LH, Michael AC, Sesack SR (2004). Ultrastructure at carbon fiber microelectrode implantation sites after acute voltammetric measurements in the striatum of anesthetized rats. *J Neurosci Methods* **137**(1): 9-23.

Phillips PE, Stuber GD, Heien ML, Wightman RM, Carelli RM (2003). Subsecond dopamine release promotes cocaine seeking. *Nature* **422**(6932): 614-618.

Phillips PEM, Hancock PJ, Stamford JA (2002). Time window of autoreceptor-mediated inhibition of limbic and striatal dopamine release. *Synapse* **44**(1): 15-22.

Picetti R, Caccavo J, Ho A, Kreek M (2012). Dose escalation and dose preference in extended-access heroin self-administration in Lewis and Fischer rats. *Psychopharmacology* **220**(1): 163-172.

Pothos E, Rada P, Mark GP, Hoebel BG (1991). Dopamine microdialysis in the nucleus accumbens during acute and chronic morphine, naloxone-precipitated withdrawal and clonidine treatment. *Brain Res* **566**(1-2): 348-350.

Raskind MA, Dobie DJ, Kanter ED, Petrie EC, Thompson CE, Peskind ER (2000). The alpha1-adrenergic antagonist prazosin ameliorates combat trauma nightmares in

veterans with posttraumatic stress disorder: a report of 4 cases. *J Clin Psychiatry* **61**(2): 129-133.

Rassnick S, Hoffman GE, Rabin BS, Sved AF (1998). Injection of corticotropin-releasing hormone into the locus coeruleus or foot shock increases neuronal Fos expression. *Neuroscience* **85**(1): 259-268.

Rebec GV, Christensen JR, Guerra C, Bardo MT (1997). Regional and temporal differences in real-time dopamine efflux in the nucleus accumbens during free-choice novelty. *Brain Res* **776**(1-2): 61-67.

Reyes BAS, Van Bockstaele EJ (2006). Divergent projections of catecholaminergic neurons in the nucleus of the solitary tract to limbic forebrain and medullary autonomic brain regions. *Brain research* **1117**(1): 69-79.

Ribeiro Do Couto B, Aguilar MA, Manzanedo C, Rodríguez-Arias M, Armario A, Miñarro J (2006). Social stress is as effective as physical stress in reinstating morphine-induced place preference in mice. *Psychopharmacology* **185**(4): 459-470.

Riday TT, Dankoski EC, Krouse MC, Fish EW, Walsh PL, Han JE*, et al* (2012). Pathway-specific dopaminergic deficits in a mouse model of Angelman syndrome. *J Clin Invest* **122**(12): 4544-4554.

Rittenhouse PA, López-Rubalcava C, Stanwood GD, Lucki I (2002). Amplified behavioral and endocrine responses to forced swim stress in the Wistar–Kyoto rat. *Psychoneuroendocrinology* **27**(3): 303-318.

Robertson SD, Plummer NW, de Marchena J, Jensen P (2013). Developmental origins of central norepinephrine neuron diversity. *Nat Neurosci* **16**(8): 1016-1023.

Robinson DL, Heien ML, Wightman RM (2002). Frequency of dopamine concentration transients increases in dorsal and ventral striatum of male rats during introduction of conspecifics. *J Neurosci* **22**(23): 10477-10486.

Robinson DL, Howard EC, McConnell S, Gonzales RA, Wightman RM (2009). Disparity between tonic and phasic ethanol-induced dopamine increases in the nucleus accumbens of rats. *Alcohol Clin Exp Res* **33**(7): 1187-1196.

Robinson DL, Phillips PE, Budygin EA, Trafton BJ, Garris PA, Wightman RM (2001). Sub-second changes in accumbal dopamine during sexual behavior in male rats. *Neuroreport* **12**(11): 2549-2552.

Robinson DL, Wightman RM (2004). Nomifensine amplifies subsecond dopamine signals in the ventral striatum of freely-moving rats. *J Neurochem* **90**(4): 894-903.

Rodeberg NT, Johnson JA, Cameron CM, Saddoris MP, Carelli RM, Wightman RM (2015). Construction of Training Sets for Valid Calibration of in Vivo Cyclic Voltammetric Data by Principal Component Analysis. *Anal Chem* **87**(22): 11484-11491.

Roitman MF, Stuber GD, Phillips PE, Wightman RM, Carelli RM (2004). Dopamine operates as a subsecond modulator of food seeking. *J Neurosci* **24**(6): 1265-1271.

Roitman MF, Wheeler RA, Wightman RM, Carelli RM (2008). Real-time chemical responses in the nucleus accumbens differentiate rewarding and aversive stimuli. *Nat Neurosci* **11**(12): 1376-1377.

Saddoris MP, Cacciapaglia F, Wightman RM, Carelli RM (2015a). Differential Dopamine Release Dynamics in the Nucleus Accumbens Core and Shell Reveal Complementary Signals for Error Prediction and Incentive Motivation. *J Neurosci* **35**(33): 11572-11582.

Saddoris MP, Sugam JA, Stuber GD, Witten IB, Deisseroth K, Carelli RM (2015b). Mesolimbic dopamine dynamically tracks, and is causally linked to, discrete aspects of value-based decision making. *Biol Psychiatry* **77**(10): 903-911.

Salinas AG, Davis MI, Lovinger DM, Mateo Y (2016). Dopamine dynamics and cocaine sensitivity differ between striosome and matrix compartments of the striatum. *Neuropharmacology*: In press.

Sallinen J, Hoglund I, Engstrom M, Lehtimaki J, Virtanen R, Sirvio J*, et al* (2007). Pharmacological characterization and CNS effects of a novel highly selective alpha2C-adrenoceptor antagonist JP-1302. *Br J Pharmacol* **150**(4): 391-402.

Salvatore MF, Gerhardt GA, Dayton RD, Klein RL, Stanford JA (2009). Bilateral effects of unilateral GDNF administration on dopamine- and GABA-regulating proteins in the rat nigrostriatal system. *Exp Neurol* **219**(1): 197-207.

Sánchez-Cardoso P, Higuera-Matas A, Martín S, del Olmo N, Miguéns M, García-Lecumberri C*, et al* (2007). Modulation of the endogenous opioid system after morphine self-administration and during its extinction: A study in Lewis and Fischer 344 rats. *Neuropharmacology* **52**(3): 931-948.

Schapira AHV (2009). Neurobiology and treatment of Parkinson's disease. *Trends Pharmacol Sci* **30**(1): 41-47.

Scheinin M, Lomasney JW, Hayden-Hixson DM, Schambra UB, Caron MG, Lefkowitz RJ*, et al* (1994). Distribution of α2-adrenergic receptor subtype gene expression in rat brain. *Molecular Brain Research* **21**(1–2): 133-149.

Schindler AG, Soden ME, Zweifel LS, Clark JJ (2016). Reversal of Alcohol-Induced Dysregulation in Dopamine Network Dynamics May Rescue Maladaptive Decision-making. *J Neurosci* **36**(13): 3698-3708.

Schulteis G, Heyser CJ, Koob GF (1999). Differential expression of response-disruptive and somatic indices of opiate withdrawal during the initiation and development of opiate dependence. *Behav Pharmacol* **10**(3): 235-242.

Schultz W (2013). Updating dopamine reward signals. *Curr Opin Neurobiol* **23**(2): 229-238.

Schultz W (2015). Neuronal Reward and Decision Signals: From Theories to Data. *Physiol Rev* **95**(3): 853-951.

Selden NR, Robbins TW, Everitt BJ (1990). Enhanced behavioral conditioning to context and impaired behavioral and neuroendocrine responses to conditioned stimuli following ceruleocortical noradrenergic lesions: support for an attentional hypothesis of central noradrenergic function. *J Neurosci* **10**(2): 531-539.

Shaham Y, Highfield D, Delfs J, Leung S, Stewart J (2000). Clonidine blocks stress-induced reinstatement of heroin seeking in rats: an effect independent of locus coeruleus noradrenergic neurons. *Eur J Neurosci* **12**(1): 292-302.

Shen K, Misic B, Cipollini BN, Bezgin G, Buschkuehl M, Hutchison RM*, et al* (2015). Stable long-range interhemispheric coordination is supported by direct anatomical projections. *Proc Natl Acad Sci U S A* **112**(20): 6473-6478.

Shi W-X, Pun C-L, Zhou Y (2004). Psychostimulants Induce Low-Frequency Oscillations in the Firing Activity of Dopamine Neurons. *Neuropsychopharm* **29**(12): 2160-2167.

Shnitko TA, Kennerly LC, Spear LP, Robinson DL (2014a). Ethanol reduces evoked dopamine release and slows clearance in the rat medial prefrontal cortex. *Alcohol Clin Exp Res* **38**(12): 2969-2977.

Shnitko TA, Robinson DL (2014b). Anatomical and pharmacological characterization of catecholamine transients in the medial prefrontal cortex evoked by ventral tegmental area stimulation. *Synapse* **68**(4): 131-143.

Shnitko TA, Robinson DL (2015a). Regional variation in phasic dopamine release during alcohol and sucrose self-administration in rats. *ACS Chem Neurosci* **6**(1): 147-154.

Shnitko TA, Spear LP, Robinson DL (2015b). Adolescent binge-like alcohol alters sensitivity to acute alcohol effects on dopamine release in the nucleus accumbens of adult rats. *Psychopharmacology (Berl)*.

Silk TJ, Vilgis V, Adamson C, Chen J, Smit L, Vance A*, et al* (2015). Abnormal asymmetry in frontostriatal white matter in children with attention deficit hyperactivity disorder. *Brain Imaging Behav*.

Simpson EH, Morud J, Winiger V, Biezonski D, Zhu JP, Bach ME*, et al* (2014). Genetic variation in COMT activity impacts learning and dopamine release capacity in the striatum. *Learn Mem* **21**(4): 205-214.

Simpson KL, Altman DW, Wang L, Kirifides ML, Lin RC, Waterhouse BD (1997). Lateralization and functional organization of the locus coeruleus projection to the trigeminal somatosensory pathway in rat. *J Comp Neurol* **385**(1): 135-147.

Simpson TL, Saxon AJ, Meredith CW, Malte CA, McBride B, Ferguson LC*, et al* (2009). A pilot trial of the alpha-1 adrenergic antagonist, prazosin, for alcohol dependence. *Alcohol Clin Exp Res* **33**(2): 255-263.

Sinha R (2008). Chronic Stress, Drug Use, and Vulnerability to Addiction. *Ann N Y Acad Sci* **1141**(1): 105-130.

Sloan M, Alegre-Abarrategui J, Potgieter D, Kaufmann AK, Exley R, Deltheil T*, et al* (2016). LRRK2 BAC transgenic rats develop progressive, L-DOPA-responsive motor impairment, and deficits in dopamine circuit function. *Hum Mol Genet* **25**(5): 951-963.

Sombers LA, Beyene M, Carelli RM, Wightman RM (2009). Synaptic overflow of dopamine in the nucleus accumbens arises from neuronal activity in the ventral tegmental area. *J Neurosci* **29**(6): 1735-1742.

Steinberg EE, Boivin JR, Saunders BT, Witten IB, Deisseroth K, Janak PH (2014). Positive reinforcement mediated by midbrain dopamine neurons requires D1 and D2 receptor activation in the nucleus accumbens. *PLoS One* **9**(4): e94771.

Stouffer MA, Woods CA, Patel JC, Lee CR, Witkovsky P, Bao L*, et al* (2015). Insulin enhances striatal dopamine release by activating cholinergic interneurons and thereby signals reward. *Nat Commun* **6**: 8543.

Stuber GD, Wightman RM, Carelli RM (2005). Extinction of cocaine self-administration reveals functionally and temporally distinct dopaminergic signals in the nucleus accumbens. *Neuron* **46**(4): 661-669.

Sugam JA, Day JJ, Wightman RM, Carelli RM (2012). Phasic nucleus accumbens dopamine encodes risk-based decision-making behavior. *Biol Psychiatry* **71**(3): 199-205.

Syed EC, Grima LL, Magill PJ, Bogacz R, Brown P, Walton ME (2016). Action initiation shapes mesolimbic dopamine encoding of future rewards. *Nat Neurosci* **19**(1): 34-36.

Szot P, Miguelez C, White SS, Franklin A, Sikkema C, Wilkinson CW*, et al* (2010). A Comprehensive Analysis of the Effect of DSP4 on the Locus Coeruleus Noradrenergic System in the Rat. *Neuroscience* **166**(1): 279-291.

Takmakov P, McKinney CJ, Carelli RM, Wightman RM (2011). Instrumentation for fast-scan cyclic voltammetry combined with electrophysiology for behavioral experiments in freely moving animals. *Rev Sci Instrum* **82**(7): 074302.

Taylor TN, Potgieter D, Anwar S, Senior SL, Janezic S, Threlfell S*, et al* (2014). Region-specific deficits in dopamine, but not norepinephrine, signaling in a novel A30P alpha-synuclein BAC transgenic mouse. *Neurobiol Dis* **62**: 193-207.

Thiele SL, Chen B, Lo C, Gertler TS, Warre R, Surmeier JD*, et al* (2014). Selective loss of bi-directional synaptic plasticity in the direct and indirect striatal output pathways accompanies generation of parkinsonism and l-DOPA induced dyskinesia in mouse models. *Neurobiol Dis* **71**: 334-344.

Threlfell S, Lalic T, Platt NJ, Jennings KA, Deisseroth K, Cragg SJ (2012). Striatal dopamine release is triggered by synchronized activity in cholinergic interneurons. *Neuron* **75**(1): 58-64.

Trendelenburg AU, Klebroff W, Hein L, Starke K (2001). A study of presynaptic alpha2-autoreceptors in alpha2A/D-, alpha2B- and alpha2C-adrenoceptor-deficient mice. *Naunyn Schmiedebergs Arch Pharmacol* **364**(2): 117-130.

Trescot AM, Datta S, Lee M, Hansen H (2008). Opioid pharmacology. *Pain physician* **11**(2 Suppl): S133-153.

Trout SJ, Kruk ZL (1992). Differences in evoked dopamine efflux in rat caudate putamen, nucleus accumbens and tuberculum olfactorium in the absence of uptake inhibition: influence of autoreceptors. *Br J Pharmacol* **106**(2): 452-458.

Twining RC, Wheeler DS, Ebben AL, Jacobsen AJ, Robble MA, Mantsch JR*, et al* (2015). Aversive stimuli drive drug seeking in a state of low dopamine tone. *Biol Psychiatry* **77**(10): 895-902.

Ungerstedt U (1971). Stereotaxic mapping of the monoamine pathways in the rat brain. *Acta Physiol Scand Suppl* **367**: 1-48.

Van Bockstaele EJ, Valentino RJ (2013). Neuropeptide regulation of the locus coeruleus and opiate-induced plasticity of stress responses. *Adv Pharmacol* **68**: 405-420.

Vander Weele CM, Porter-Stransky KA, Mabrouk OS, Lovic V, Singer BF, Kennedy RT*, et al* (2014). Rapid dopamine transmission within the nucleus accumbens: dramatic difference between morphine and oxycodone delivery. *Eur J Neurosci* **40**(7): 3041-3054.

Venton BJ, Wightman RM (2007). Pharmacologically induced, subsecond dopamine transients in the caudate-putamen of the anesthetized rat. *Synapse* **61**(1): 37-39.

Volgushev M, Chistiakova M, Singer W (1998). Modification of discharge patterns of neocortical neurons by induced oscillations of the membrane potential. *Neuroscience* **83**(1): 15-25.

Volkow ND, Fowler JS, Wang GJ, Swanson JM, Telang F (2007). Dopamine in drug abuse and addiction: results of imaging studies and treatment implications. *Arch Neurol* **64**(11): 1575-1579.

Wakabayashi KT, Bruno MJ, Bass CE, Park J (2016). Application of fast-scan cyclic voltammetry for the in vivo characterization of optically evoked dopamine in the olfactory tubercle of the rat brain. *Analyst*: in press.

Wang X, Cen X, Lu L (2001). Noradrenaline in the bed nucleus of the stria terminalis is critical for stress-induced reactivation of morphine-conditioned place preference in rats. *Eur J Pharmacol* **432**(2–3): 153-161.

Wassum KM, Ostlund SB, Maidment NT (2012). Phasic mesolimbic dopamine signaling precedes and predicts performance of a self-initiated action sequence task. *Biol Psychiatry* **71**(10): 846-854.

Watabe-Uchida M, Zhu L, Ogawa SK, Vamanrao A, Uchida N (2012). Whole-brain mapping of direct inputs to midbrain dopamine neurons. *Neuron* **74**(5): 858-873.

Weinshenker D (2008). Functional consequences of locus coeruleus degeneration in Alzheimer's disease. *Curr Alzheimer Res* **5**(3): 342-345.

Weinshenker D, Schroeder JP (2006). There and Back Again: A Tale of Norepinephrine and Drug Addiction. *Neuropsychopharm* **32**(7): 1433-1451.

Weiss F, Parsons LH, Schulteis G, Hyytia P, Lorang MT, Bloom FE (1996). Ethanol self-administration restores withdrawal-associated deficiencies in accumbal dopamine and 5-hydroxytryptamine release in dependent rats. *J Neurosci* **16**(10): 3474-3485.

Wheeler DS, Robble MA, Hebron EM, Dupont MJ, Ebben AL, Wheeler RA (2015). Drug predictive cues activate aversion-sensitive striatal neurons that encode drug seeking. *J Neurosci* **35**(18): 7215-7225.

Wightman RM, Amatore C, Engstrom RC, Hale PD, Kristensen EW, Kuhr WG*, et al* (1988). Real-time characterization of dopamine overflow and uptake in the rat striatum. *Neuroscience* **25**(2): 513-523.

Wightman RM, Heien MLAV, Wassum KM, Sombers LA, Aragona BJ, Khan AS*, et al* (2007). Dopamine release is heterogeneous within microenvironments of the rat nucleus accumbens. *Eur J Neurosci* **26**(7): 2046-2054.

Willuhn I, Tose A, Wanat MJ, Hart AS, Hollon NG, Phillips PE*, et al* (2014). Phasic dopamine release in the nucleus accumbens in response to pro-social 50 kHz ultrasonic vocalizations in rats. *J Neurosci* **34**(32): 10616-10623.

Witten IB, Steinberg EE, Lee SY, Davidson TJ, Zalocusky KA, Brodsky M*, et al* (2011). Recombinase-driver rat lines: tools, techniques, and optogenetic application to dopamine-mediated reinforcement. *Neuron* **72**(5): 721-733.

Xu F, Gainetdinov RR, Wetsel WC, Jones SR, Bohn LM, Miller GW*, et al* (2000). Mice lacking the norepinephrine transporter are supersensitive to psychostimulants. *Nat Neurosci* **3**(5): 465-471.

Yang J, Sadler TR, Givrad TK, Maarek JM, Holschneider DP (2007). Changes in Brain Functional Activation during Resting and Locomotor States after Unilateral Nigrostriatal Damage in Rats. *NeuroImage* **36**(3): 755-773.

Yorgason JT, Calipari ES, Ferris MJ, Karkhanis AN, Fordahl SC, Weiner JL*, et al* (2016). Social isolation rearing increases dopamine uptake and psychostimulant potency in the striatum. *Neuropharmacology* **101**: 471-479.

Yorgason JT, España RA, Jones SR (2011). Demon Voltammetry and Analysis software: Analysis of cocaine-induced alterations in dopamine signaling using multiple kinetic measures. *J Neurosci Methods* **202**(2): 158-164.

Yoshimoto K, McBride WJ, Lumeng L, Li TK (1992). Alcohol stimulates the release of dopamine and serotonin in the nucleus accumbens. *Alcohol* **9**(1): 17-22.

Zhang S, Qi J, Li X, Wang HL, Britt JP, Hoffman AF*, et al* (2015). Dopaminergic and glutamatergic microdomains in a subset of rodent mesoaccumbens axons. *Nat Neurosci* **18**(3): 386-392.

Zigmond MJ, Abercrombie ED, Berger TW, Grace AA, Stricker EM (1990). Compensations after lesions of central dopaminergic neurons: some clinical and basic implications. *Trends Neurosci* **13**(7): 290-296.

Zigmond MJ, Hastings TG, Abercrombie ED (1992). Neurochemical responses to 6-hydroxydopamine and L-dopa therapy: implications for Parkinson's disease. *Ann N Y Acad Sci* **648**: 71-86.

Zweifel LS, Parker JG, Lobb CJ, Rainwater A, Wall VZ, Fadok JP*, et al* (2009). Disruption of NMDAR-dependent burst firing by dopamine neurons provides selective assessment of phasic dopamine-dependent behavior. *Proc Natl Acad Sci U S A* **106**(18): 7281-7288.